REPORT NO. FRA-OR&D-75-68

ANALYSIS OF RAILROAD CAR TRUCK AND WHEEL FATIGUE
Part I -- Service Load Data and Procedures for the Development of Fatigue Performance Criteria

Milton R. Johnson

MAY 1975
INTERIM REPORT

Prepared for
U.S. DEPARTMENT OF TRANSPORTATION
FEDERAL RAILROAD ADMINISTRATION
Office of Research and Development
Washington DC 20591

NOTICE

This document is disseminated under the sponsorship of the Department of Transportation in the interest of information exchange. The United States Government assumes no liability for its contents or use thereof.

NOTICE

The United States Government does not endorse products or manufacturers. Trade or manufacturers' names appear herein solely because they are considered essential to the object of this report.

TECHNICAL REPORT STANDARD TITLE PAGE

1. Report No.	2. Government Accession No.	3. Recipient's Catalog No.
FRA-OR&D-75-68		PB 244 090

4. Title and Subtitle	5. Report Date
ANALYSIS OF RAILROAD CAR TRUCK AND WHEEL FATIGUE Part I -- Service Load Data and Procedures for the Development of Fatigue Performance Criteria	May 1975 6. Performing Organization Code
7. Author(s) Milton R. Johnson	8. Performing Organization Report No. DOT-TSC-FRA-75-11
9. Performing Organization Name and Address IIT Research Institute* 10 West 35th Street Chicago IL 60616	10. Work Unit No. RR523/R5323 11. Contract or Grant No. DOT-TSC-727
12. Sponsoring Agency Name and Address U.S. Department of Transportation Federal Railroad Administration Office of Research and Development Washington DC 20591	13. Type of Report and Period Covered Interim Report June 1972 - Dec. 1974 14. Sponsoring Agency Code
15. Supplementary Notes *Under contract to:	U.S. Department of Transportation Transportation Systems Center Kendall Square Cambridge MA 02142

16. Abstract

The development of fatigue performance standards for freight car truck components and wheels requires a knowledge of the fluctuating service load environment, and a basis for stating the conservatism of the design with respect to the environment. On this program special emphasis was given to determining the load environment by analyzing data from 53 test runs conducted on the Erie Branch test track of the Bessemer and Lake Erie Railroad. A number of test parameters were varied, such as speed, type of truck, modifications to the suspension system, etc., to determine those parameters having the greatest influence on the severity of the load. Vertical loads were measured at the side-frame-pedestal/roller-bearing-adapter interface and lateral loads were determined at the wheel/rail interface. The cyclic load data are summarized in a series of load spectra. Factors which must be considered in the development of fatigue performance standards from these spectra include reliability goals, the statistical spread of both load and fatigue strength data, and the philosophy followed in the design of the truck itself

17. Key Words	18. Distribution Statement
Fatigue standards Railroad trucks Railroad wheels	DOCUMENT IS AVAILABLE TO THE PUBLIC THROUGH THE NATIONAL TECHNICAL INFORMATION SERVICE, SPRINGFIELD, VIRGINIA 22161 PRICES SUBJECT TO CHANGE

19. Security Classif. (of this report)	20. Security Classif. (of this page)	21. No. of Pages	22. Price PC/MF
Unclassified	Unclassified	140	5.75/2.25

Form DOT F 1700.7 (8-69)

PREFACE

This report presents interim results obtained under the Department of Transportation, Transportation Systems Center (TSC) Contract TSC-727 titled "Analysis of Railroad Car Truck and Wheel Fatigue". This project, which was initiated in June 1972, is being conducted by IIT Research Institute under the direction of Dr. Milton R. Johnson, Project Manager. The work included tests to define the loads acting on freight car trucks in service, which have been conducted by the Bessemer and Lake Erie Railroad (B&LE) under the direction of Mr. Leavitt A. Peterson, Director Applied Research, and Mr. Joseph J. Stark, Assistant Chief Industrial Engineer. Messrs. D. Schlect and R. Davis of B&LE were responsible for the instrumentation and data handling systems. Mr. Roger Steele has served as the TSC technical project officer and his helpful comments and suggestions in guiding the course of the work are gratefully acknowledged.

This report discusses the freight car truck forces which must be recognized in the development of fatigue standards, describes results from the test program, and provides recommendations for establishing fatigue standards on individual freight car truck components and wheels. A subsequent report will present results from the analytical and experimental evaluation of the fatigue strengths of these components.

TABLE OF CONTENTS

TABLE OF CONTENTS (Concl)

LIST OF ILLUSTRATIONS

LIST OF ILLUSTRATIONS (Cont)

LIST OF ILLUSTRATIONS (Cont)

LIST OF ILLUSTRATIONS (Concl)

LIST OF TABLES

1.0 INTRODUCTION

1.1 Objectives and Summary

In the wake of a rising trend in freight train derailments, the Federal Railroad Administration (FRA) has been engaged in the formulation of safety standards covering the design and operation of railroad equipment and facilities. This report is a review of one aspect of railroad safety: the problem of fatigue failures in freight car truck components and wheels, which is one of the major causes of freight train derailments. It also describes a procedure for the development of fatigue design criteria based on performance standards, and presents data for developing such standards.

The overall objective of the program is improvement in the safety and reliability of freight car operations through the definition of fatigue standards for freight car truck components and wheels. These standards would reflect the operating load environment and service life requirements. The scope of the program includes consideration of the principal components of the modern freight car truck, namely, the truck bolster, side frames, bearings, axles, and wheels.

The establishment of fatigue standards requires an adequate understanding of the freight car truck operational load environment, the influence of truck design and operational parameters on this environment, and the establishment of safety margins between the load environment and fatigue strength of truck components. A substantial effort has been devoted to measurement of the nature, magnitude and frequency of forces which are imposed on freight car trucks and wheels within normal service experience. Extensive use has been made of railway truck load data obtained by the Bessemer and Lake Erie Railroad (B&LE) participating as a subcontractor on this project. This railroad has developed extensive facilities for gathering and analyzing freight car truck load

information (Ref. 1).* The nature of the loads, the test methods used to gather load data and the results obtained on the tests are described in Sections 2 through 4 of this report.

A fatigue performance standard describes test procedures for evaluating the fatigue strength of a component. The tests involve subjecting a component to a series of repetitive loads until the part fails following the development of a fatigue crack. The standard requires that the fatigue strength of the component exceeds the fatigue producing properties of the load environment by a given "safety" margin. A number of factors are involved in the choice of a suitable safety margin including:

- statistical distribution of the load environments to which various components are subjected in service
- statistical distribution in the fatigue strengths of components of identical design and construction
- desired reliability of operation
- frequency and quality of inspections
- design philosophy: fail-safe or safe-life

These factors are discussed in Section 5 of this report leading up to the recommendation of procedures for stating fatigue design criteria.

Fatigue performance standards for freight car truck components and wheels can be formulated from the data presented in this report, although it may be advantageous to delay promulgation of such standards until there is a broader understanding of the load environment.

1.2 Background

1.2.1 Truck Design

A freight car truck provides for the transfer of loads from the car structure through the wheels to the rails and also

*References are listed at the end of the report on page 121.

provides isolation of the car from vertical and lateral shock and vibration excitation which originates at the wheel/rail interface.

The principal features of the four-wheel truck are illustrated in Fig. 1.1. The weight of the car is concentrated over the truck by a structural element referred to as the body bolster. This is connected to the truck bolster at the center plate, which provides for the swiveling of the truck to accommodate yawing angular displacements between the truck and the car body. The truck bolster distributes this load from the center plate to the two spring groups, one at each side of the truck, which are supported by the side frames. Two side bearings, one on either side of the center plate provide an alternate means of load transfer between the car body and the truck bolster. These are brought into play by a slight rolling motion of the car body providing lateral stability.

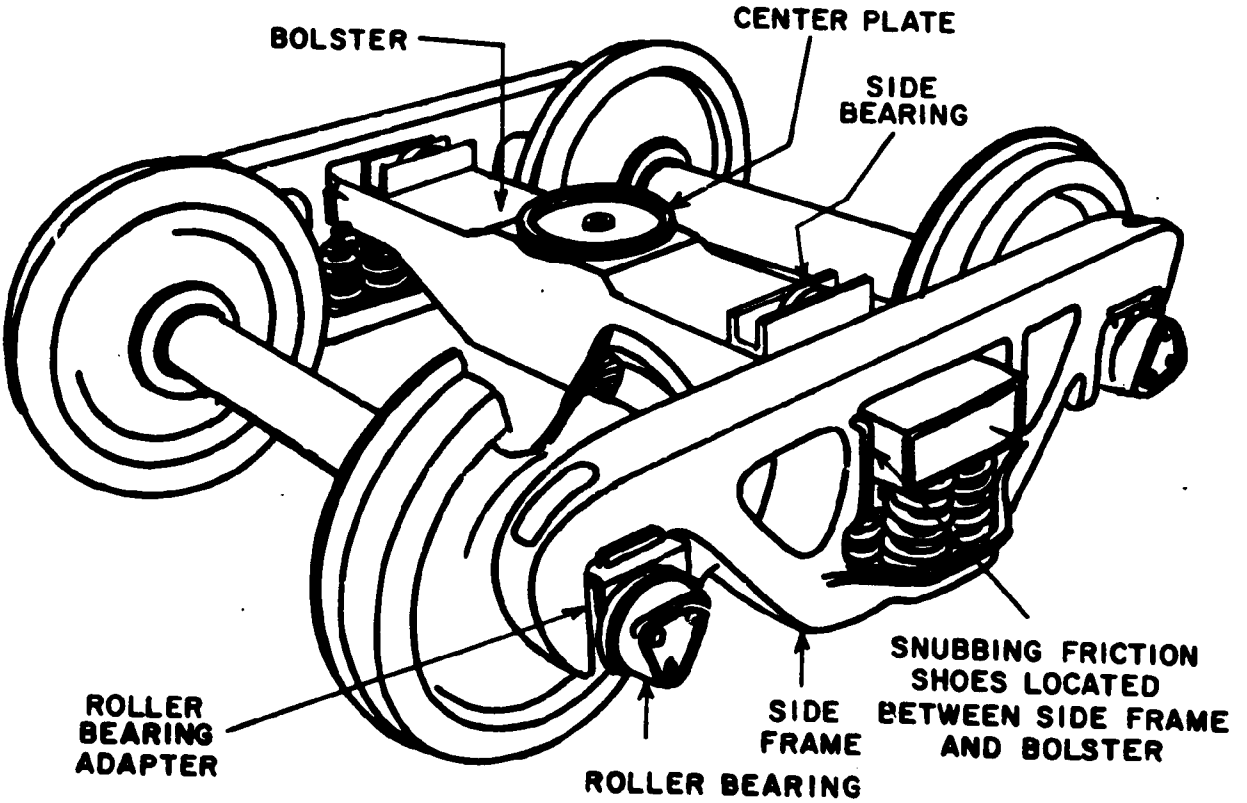

Fig. 1.1 FOUR-WHEEL FREIGHT CAR TRUCK

Conventional freight car truck designs contain only one set of suspension elements, namely, coil springs between the bolster and both the side frames. The side frames distribute the load from the base of the springs to the two axles of the truck. The load is applied to the axles through bearings contained in housings which are independent of the side frame, but effectively connected to it through the jaws or pedestals at the ends of the side frame. The wheels are rigidly mounted to the axles so that a wheel/axle set turns as a unit.

Shock and vibration isolation is accomplished through the relative motion between the bolster and the side frames. The primary freedom for relative movement is in the vertical direction and the total possible motion depends on the choice of the spring group. Freedom for relative motion is also provided in the lateral direction although to a lesser extent. The system must be damped to prevent excessive vertical motions, which would result in bottoming out the springs with accompanying hard solid blows to the bolster. Most trucks are damped by a shoe which provides frictional forces between the bolster and the side frame columns. One popular design (the BARBER S-2 truck) utilizes a friction force that is dependent on the degree of spring travel, another (the RIDE CONTROL truck) a constant frictional force. The spring-loaded friction shoes between the side frames and bolster also offer a resistance to skewing forces which would tend to distort the rectangular array of the truck side frames and axles.

The freight car truck also supports the brake. The air cylinders which initiate the braking forces may be attached to the truck components or the car, but in either case the linkage which transfers the piston rod forces to the brake shoes is connected to the truck components. In this way the truck structure transmits the braking forces from the wheels to the car.

1.2.2 Present Design Standards

Current design standards for freight car truck components and wheels reflect a variety of requirements with regard to

fatigue strength. The only components which must adhere to fatigue requirements are side frames and roller bearings. The side frame test is performed on either of two test machines which apply a pattern of constant amplitude loads (the magnitude of the load depending on the side frame capacity). The load patterns are different for each machine, but generally are substantially above those encountered in normal service. The average of four specimens must exceed 100,000 cycles with a 50,000 cycle minimum (Ref. 2) without the development of a critical crack (defined as a transverse crack which lengthens by 1/4 of an inch). Roller bearings must possess a minimum life expectancy of 500,000 miles with the full rail load acting radially for one-half the mileage. Life expectance is defined as the life at which no more than 10 percent of the bearings require replacement due to fatigue initiated spalling or flaking on the load carrying surfaces (Ref. 3).

Truck bolsters are designed solely on the basis of static load requirements (Ref. 4). Wheel designs must adhere to certain dimensional requirements (Ref. 5). Shot-peening of the plate surfaces is also required. Axle design is specified in terms of dimensional requirements which are based on limitations in stress values (Ref. 6). The allowable stress levels reflect extensive fatigue tests.

2.0 TRUCK COMPONENT LOADS

2.1 Load Characteristics

The establishment of fatigue standards requires an adequate understanding of the freight car truck operational load environment and the influence of truck, car and operational parameters on this environment. The term "load environment" in this context refers to a description of forces on each truck component which are significant with respect to its fatigue strength. This includes the magnitude of the cyclic fluctuations of the load level and the number of cycles at various load levels anticipated during the lifetime of the part. The load environment should be described in such a way to define the force levels on each major component. This requires definition of the load at various interfaces between components such as the wheel/rail interface, the side-frame/spring-group/bolster interface, and the center-plate/side-bearing/truck-bolster interface. Truck and car parameters which influence the environment include the spring travel of the suspension system, the type of damping mechanism, the degree of wheel wear, car truck center distance, height of car center-of-gravity, etc. Operational parameters, such as, the weight of car, train speed, track conditions, etc., will also influence the load environment.

Vertical loads on the structural elements of the truck are characterized by an average value, representing the car weight, and fluctuations about this level due to the dynamic interaction of the suspension system with rail deflections resulting from the nonuniform resilient response of the track substructure, the passage of the truck over track irregularities, such as at crossings and turnouts, and wheel defects, such as a wheel flat spot. A key descriptor of the vertical load environment is the vertical load measured at the side-frame-pedestal/roller-bearing-adapter interface.

Typical records obtained from load cells at opposite sides of an axle at this position are illustrated in Fig. 2.1. The data

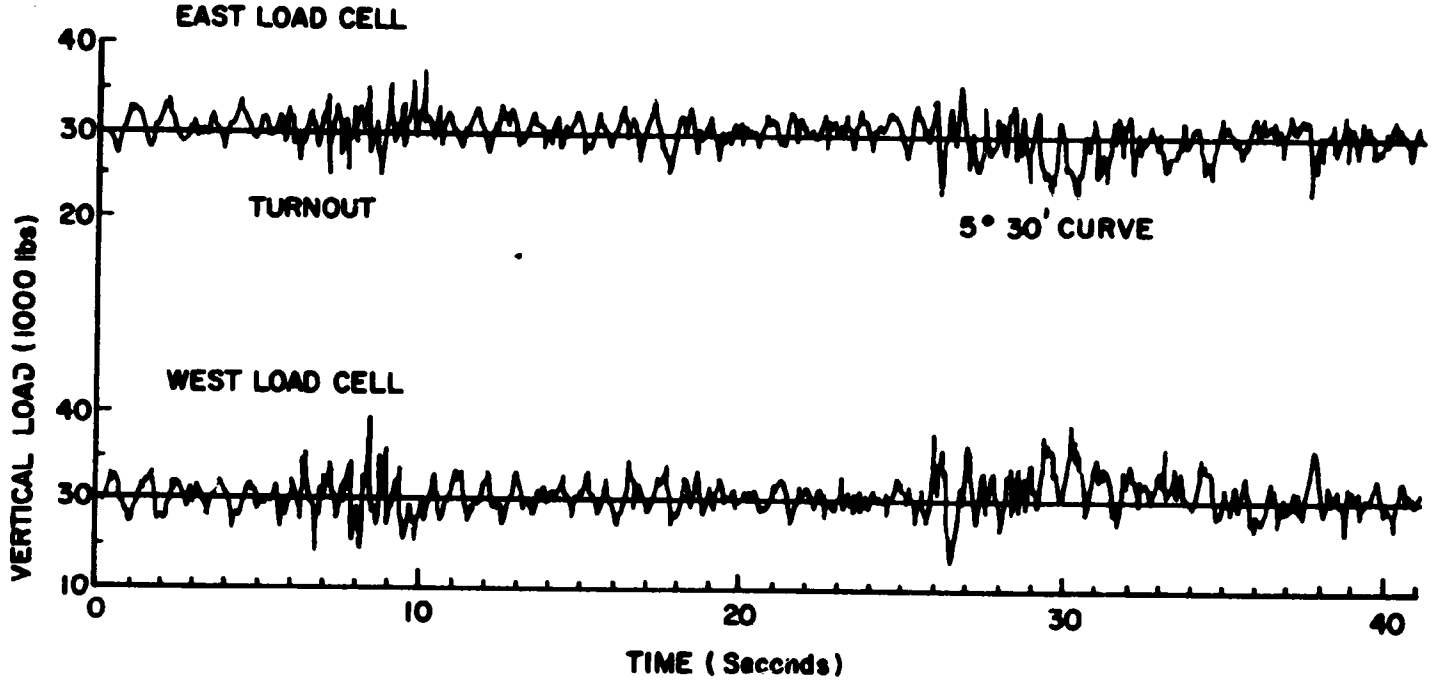

Fig. 2.1 VERTICAL LOAD CELL DATA AT SIDE-FRAME-PEDESTAL/ROLLER-BEARING-ADAPTER INTERFACE

are displayed with reference to a nominal static load at this interface of slightly over 30,000 lbs for a loaded 100 ton (nominal) capacity car. The predominant frequency of the alternating component of load is slightly over 1 Hz representing a rocking motion of the car, which is evident by the 180 degree out-of-phase character of these oscillations. Passage of the car over the turnout initiates a higher-frequency in-phase bouncing motion of the truck which occurs at a frequency of 3 to 5 Hz. Note also the lean of the car to the west when traversing the 5^{o} 30' curve.

A key descriptor of the lateral load on a truck is the lateral load measured at the wheel/rail interface. When operating on tangent track this load is normally characterized by a relatively low-level steady component directed toward the flange and an alternating component. The alternating component is due to the normal side-to-side hunting motion of the wheel/axle set. Larger quasi-steady components of load can be developed by worn wheels where the tread contour causes the wheel/axle set to run toward one of the rails.

The lateral loads at the wheel/rail interfaces are not necessarily equal for the two wheels on a wheel/axle set. This results in a "net lateral" force which is transferred to the other structural elements of the truck.

Significant lateral loads at the wheel/rail interface can be developed during the traversal of curved track. These loads are the result of transfer of force from the car body to the rail, or the result of internal truck forces. Lateral force transfer from the car to the rail is due to coupler angularity on curves, speed not commensurate with superelevation, etc. Internal forces are the result of the yawing slippage of wheel/axle sets.

The forces which act on a railroad car truck on curved track and their relationship to its unique design characteristics (e.g., the rigid interconnection of wheels on the axle, wheel tread profile, flange guidance, etc.) are discussed in works by Porter (Ref. 7), Minchin (Ref. 8), Cain (Ref. 9), and others. These

analyses are concerned with quasi-static, steady-state forces acting on the wheels of the truck due to the combined rolling and slippage of the wheels. When operating on curved track with a tapered wheel, the lateral displacement of the wheel/axle set from the centerline of the track can accommodate some curvature, but a condition of creep or slip must develop to physically maintain the wheel/axle set in the proper orientation if the curvature is above approximately 2 degrees.

A typical set of forces (in a horizontal plane) on a four-wheel truck while traversing curved track is shown in Fig. 2.2. The forces are those acting on the wheels at the rail in the absence of lateral forces from the car. A "rigid" truck is assumed, which implies that the positions of the wheels are maintained in a fixed rectangular array regardless of the forces acting on the truck. Normally the only point where a wheel flange makes contact with the rail is at the outer wheel of the lead axle. Other conditions are possible, such as the flange of the inner wheel of the trailing axle contacting the rail. This can occur when the degree of curvature is high and the track gage clearance is low. Another possibility is the flange of the outer wheel of the trailing axle contacting the rail. This can take place if the rigidity of the truck is not maintained and it undergoes a skewing deformation.

The analysis of the truck forces indicates that the individual wheel/axle sets undergo both a rolling and a slipping motion. The slipping component of the motion can be described by a yawing rotation of the axle about a fixed point. The location of this point is different with each axle, but in each case it lies on a radial line with respect to the curve which is perpendicular to the axis of the truck. Figure 2.3 shows that for the rear axle this point lies at the intersection of the truck axis with the radial line, whereas for the front axle the point is normally located near the inner rail. The forces acting on the basic truck frame (here taken to include the side frames and bolster) as a result of the wheel/rail interaction forces illustrated in Fig. 2.2, are illustrated in Fig. 2.4.

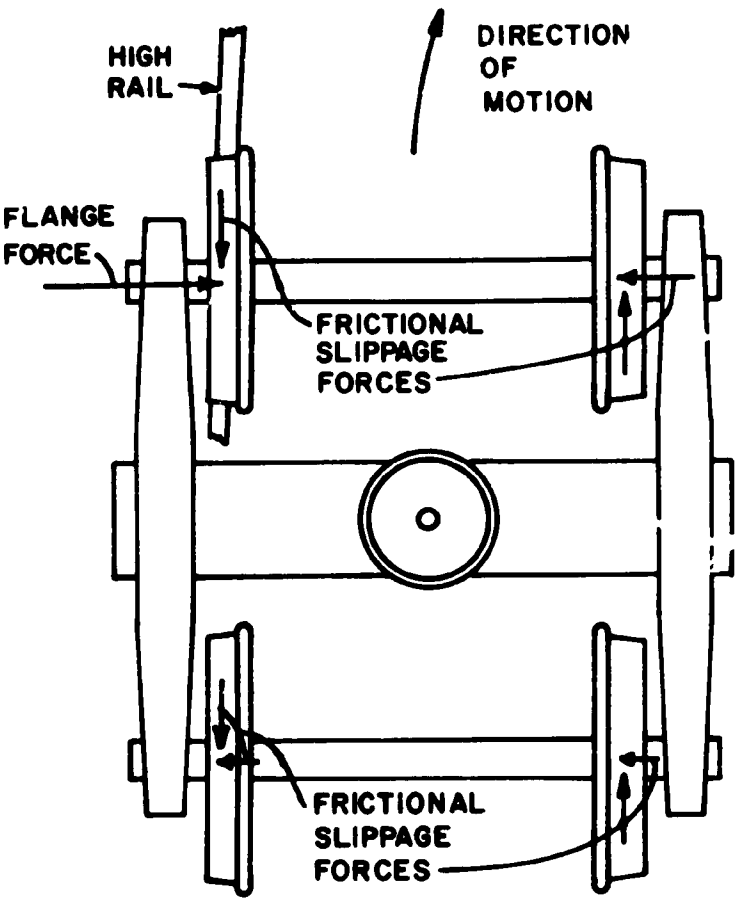

Fig. 2.2 CURVED TRACK FREIGHT CAR TRUCK FORCES AT WHEEL/RAIL INTERFACE

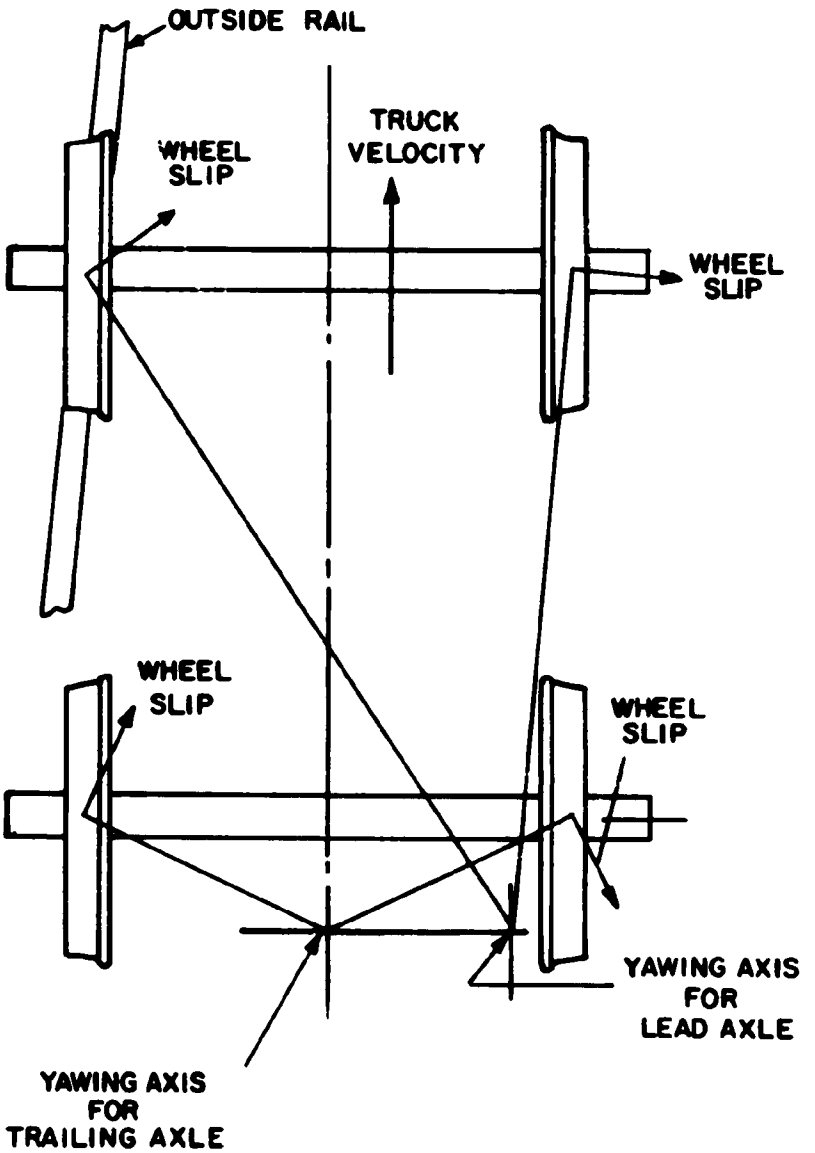

Fig. 2.3 TYPICAL ORIENTATION OF TRUCK ON CURVED TRACK SHOWING AXIS OF ROTATION OF YAWING SLIPPAGE FOR EACH AXLE

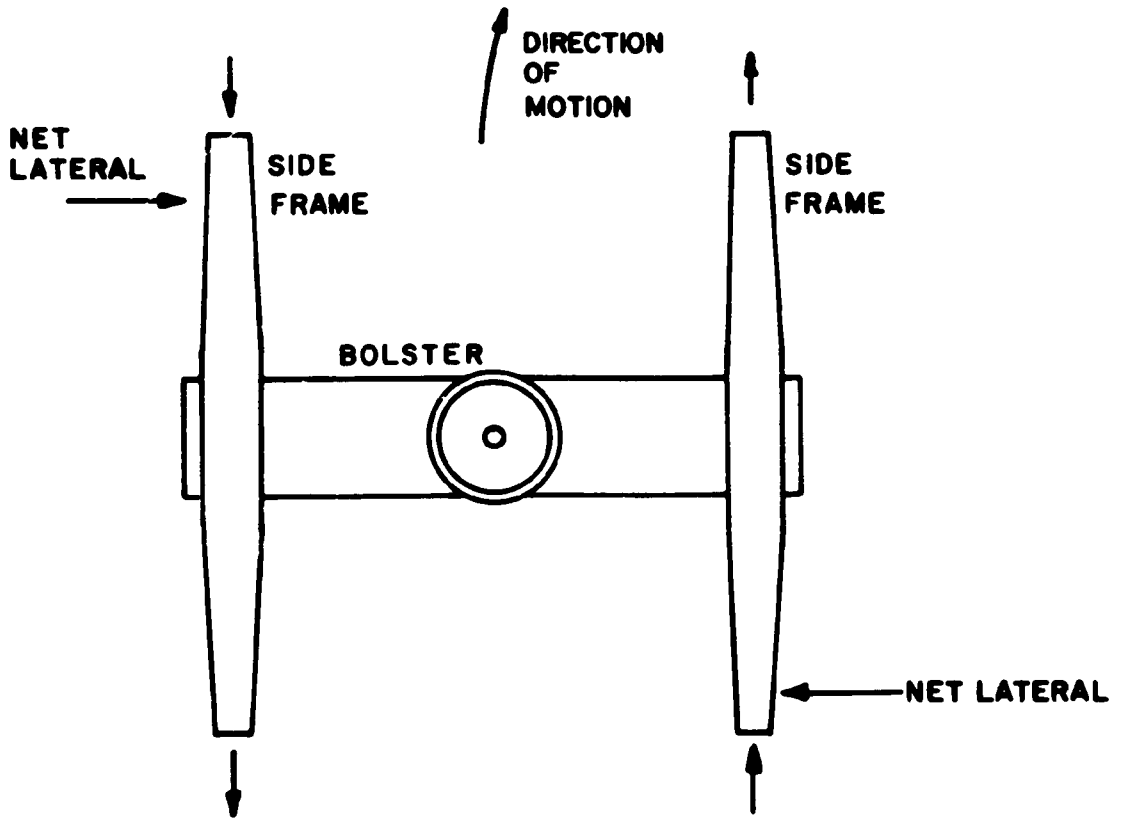

Fig. 2.4 CURVED TRACK FORCES ON TRUCK FRAME

When traversing curved track, the alternating lateral load component is superimposed on a steady component of lateral load which varies with the wheel position in the truck, the wheel on the high rail of the lead axle usually being subjected to the highest loads. This load is directed against the flange. The wheel on the opposite side of the axle is subjected to similar forces directed toward the flange, but of lesser magnitude. The component of steady lateral load on the trailing axle of the truck is usually small in comparison to the lead axle.

Figure 2.5 shows typical lateral wheel load test data. The data are for the lead axle of a truck moving through a reverse curve from a $4^{\circ}54'$ curve to a $6^{\circ}20'$ curve. The figure illustrates the steady and fluctuating components of the load and the larger loads associated with the high rail.

2.2 Load Descriptions

This section describes the loads acting on freight car truck components and wheels which are significant to an evaluation of fatigue damage. The description is subdivided according to the factors leading to the initiation of the load and influencing its magnitude. Although each of these loads fluctuate during normal service operations, not all are of equal significance with respect to fatigue damage.

Directional notation is stated relative to the orientation of the car: the vertical direction is perpendicular to the ground plane, the longitudinal direction is parallel to the central axis of the car, and the lateral direction is in the horizontal plane transverse with respect to the longitudinal direction.

2.2.1 Truck Bolster

Vertical (Fig. 2.6): The vertical load is the principal load acting on the bolster and is due to the weight of the car and lading. Its line-of-action is normally at the center of the bolster, but this can be shifted because of the load transfer to one of the side bearings. Load transfer to the side bearings may become severe on curves or due to car "rock-and-roll" motion, which is generally the result of a high center-of-gravity and a poorly controlled suspension system. The lateral displacement of the line-of-action of the vertical load is illustrated by the record shown in Fig. 2.7. This trace is derived from the vertical load cell data on each side-frame-pedestal/roller-bearing-adapter

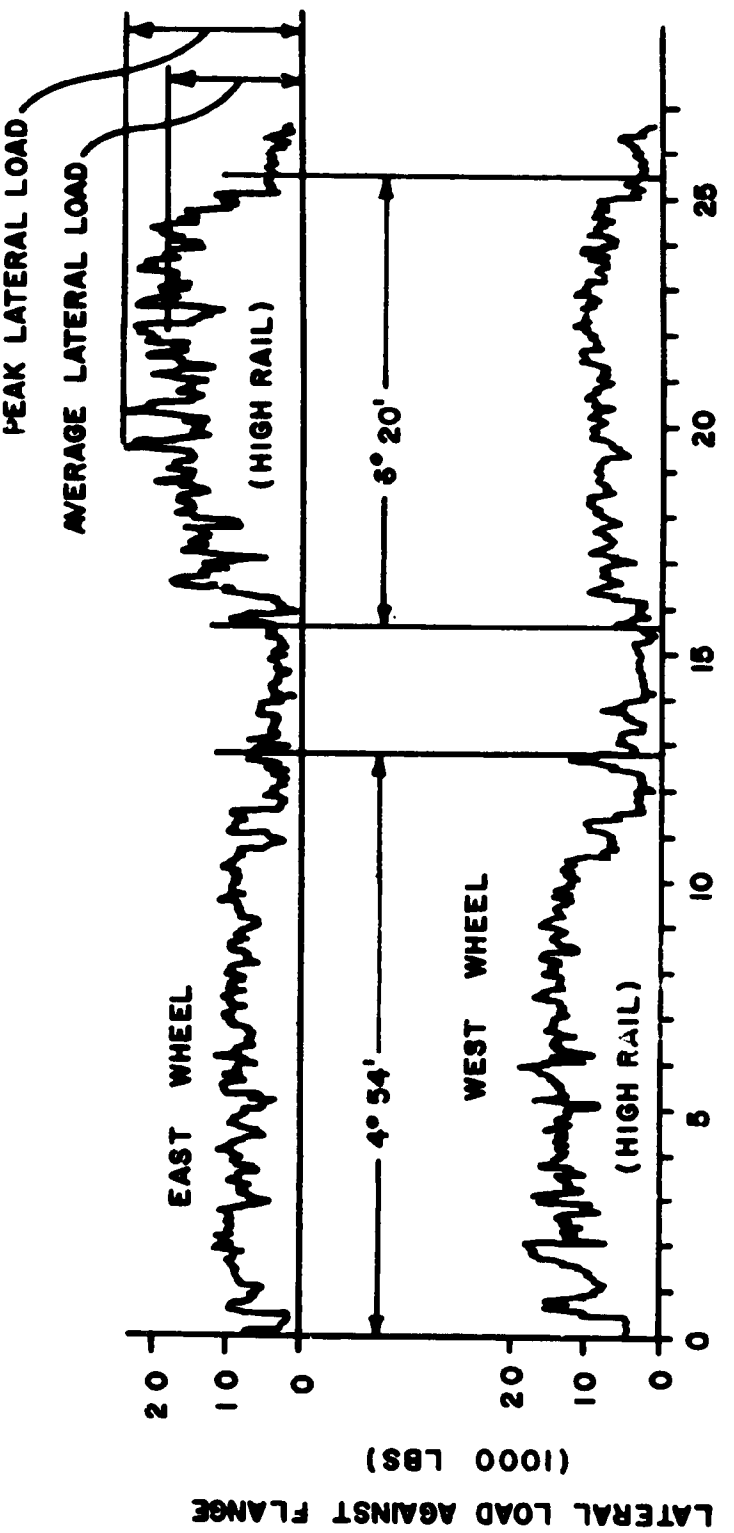

Fig. 2.5 LATERAL WHEEL LOADS ON LEAD AXLE (35 MPH)

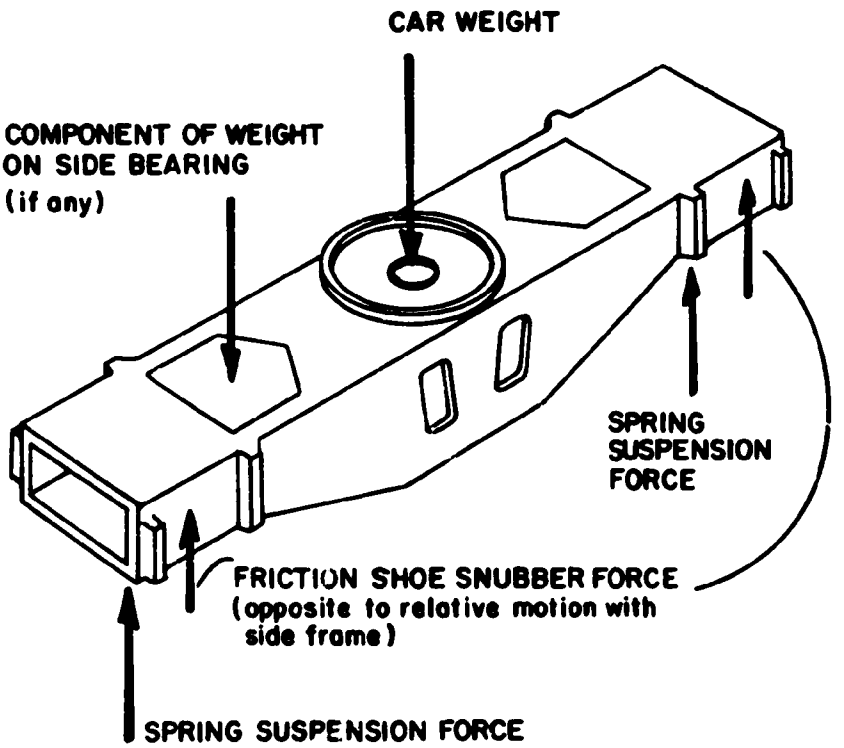

Fig. 2.6 BOLSTER VERTICAL LOADS

interface of a truck and it illustrates the load transfer from a rocking motion of the car at a frequency slightly over 1 Hz.*

*The lateral displacement of the vertical line-of-action was calculated by assuming that the forces on the bolster were in static equilibrium. As illustrated in Fig. 2.7, S_e is the sum of the two vertical load cell records on the east side frame and S_w is the sum of the two vertical load cell records on the west side frame. The displacement of the vertical load is then given by the equation:

$$d = \frac{b(S_w - S_e)}{2(S_w + S_e)}$$

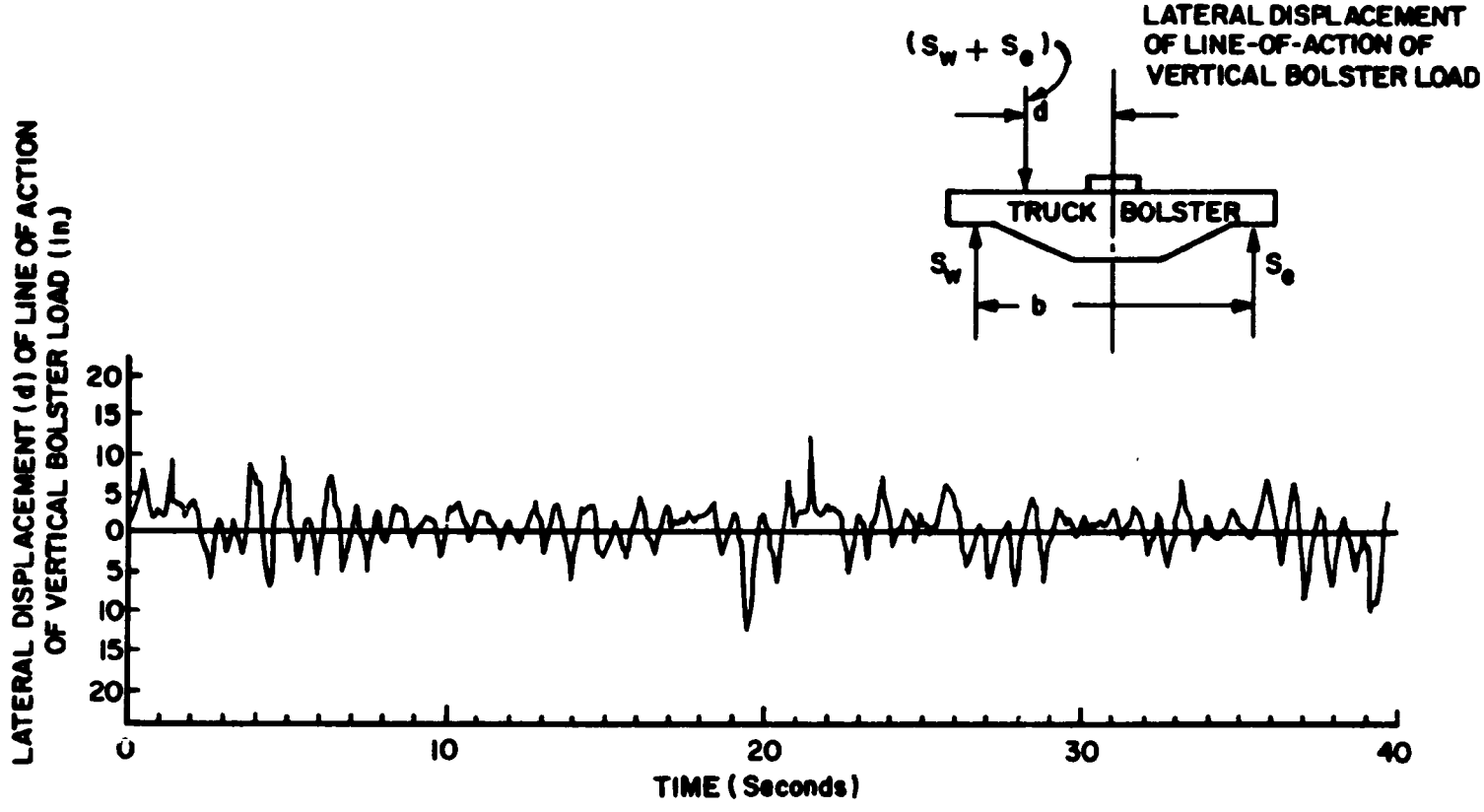

Fig. 2.7 TYPICAL "ROCK" LOAD DATA, TANGENT TRACK, 35 MPH

The most important influence on the vertical load fluctuations is the characteristics of the spring suspension system, a poorly damped system resulting in the most severe oscillations.

Longitudinal (Fig. 2.8): The longitudinal load on the bolster is applied between the truck-bolster/body-bolster center plate nterface and the sides of the bolster mating with the side frame columns. This load is due to braking and inertial forces accompanying acceleration of the truck. The most severe forces occur under car impact conditions when an unloaded car is coupled at high speed into a standing string of cars.

Horizontal Twist (Fig. 2.8): This load refers to the moment applied at the end of the bolster in a horizontal plane. It results from the tendency of the side frame to rotate into an out-of-square position with respect to the bolster during traversal of curved track.

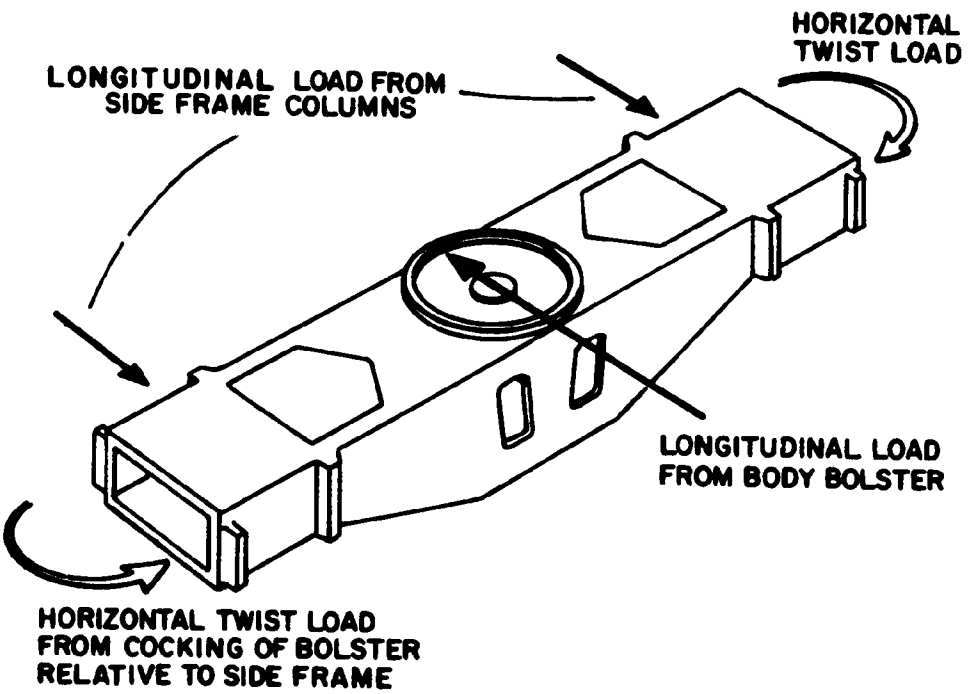

Fig. 2.8 BOLSTER LONGITUDINAL AND HORIZONTAL TWIST LOADS

2.2.2 Side Frame

Vertical (Fig. 2.9): The vertical load is applied between The base of the spring suspension and the roller bearing adapters. The side frame is subjected to higher shock load forces than the bolster, such as those due to crossings or wheel flat spots, because it does not have the benefit of the spring suspension system for the isolation of these loads.

Lateral (Fig. 2.10): The side frame lateral load is applied between the side frame columns and the roller bearing adapters. It is the result of load transfer from the car body, such as would be caused by the angularity of the draft force on the car, or a superelevation of the rail not commensurate with speed. It is also associated with the internal truck forces which maintain the truck in a rectangular configuration while traversing curved track.

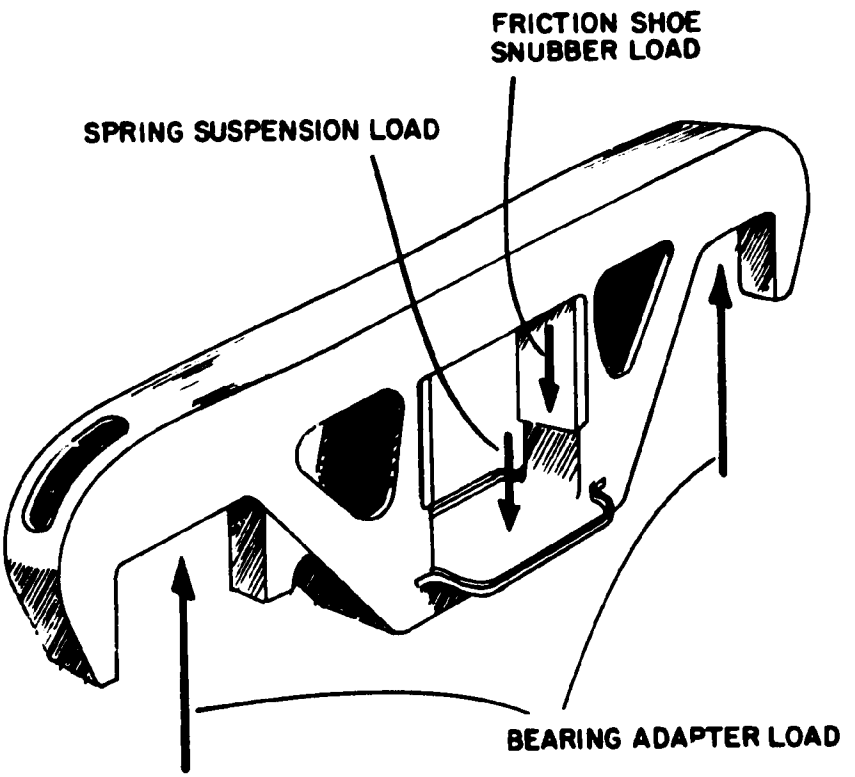

Fig. 2.9 SIDE FRAME VERTICAL LOADS

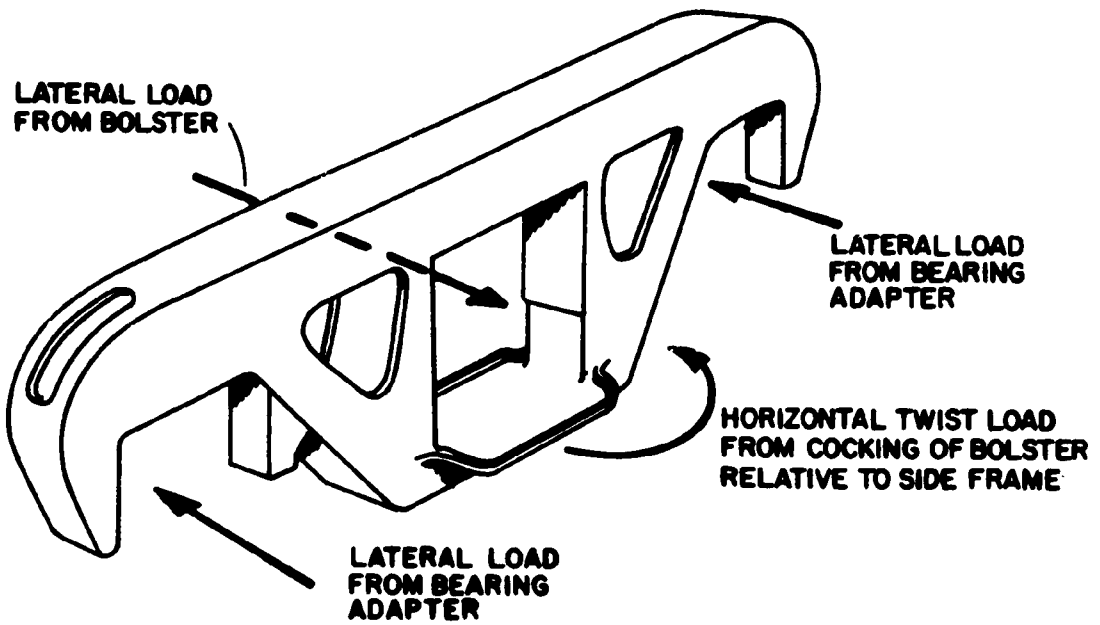

Fig. 2.10 SIDE FRAME LATERAL AND HORIZONTAL TWIST LOADS

Horizontal Twist (Fig. 2.10): The side frame horizontal twist load is the reaction to the bolster horizontal twist load and is manifest as a moment applied from the bolster to the side frame columns. The reaction to this load on the side frame is taken up at the roller bearing adapters.

Longitudinal (Fig. 2.11): Longitudinal loads on the side frame are applied between the side frame column and the pedestal jaw faces. This load is a relatively minor one except under severe shock load conditions, such as high speed car impact.

2.2.3 Roller Bearing Adapters and Bearings

Radial (Fig. 2.12): The principal bearing load is in the radial direction. The major component of this load is in the vertical direction and is due to the weight of the car, although major longitudinal loads can be developed under shock load conditions.

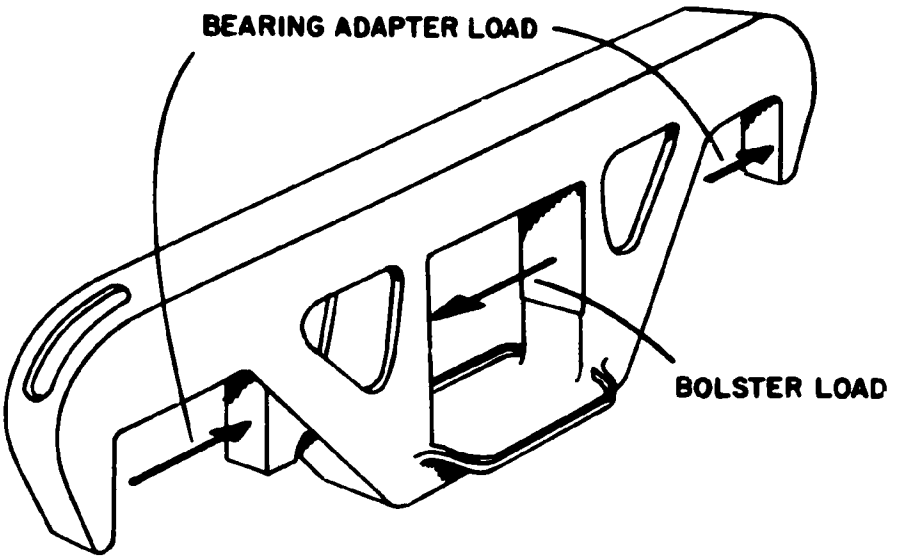

Fig. 2.11 SIDE FRAME LONGITUDINAL LOADS

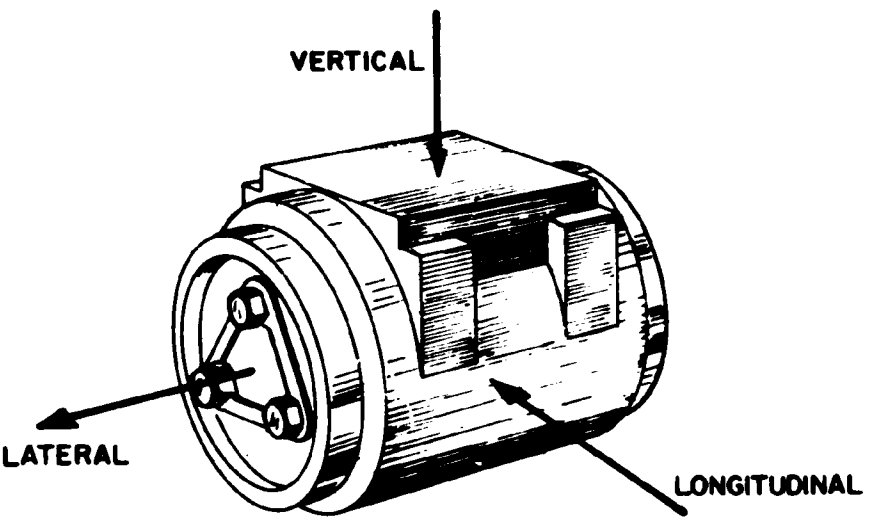

Fig. 2.12 ROLLER BEARING ADAPTER AND BEARING LOADS FROM SIDE FRAME PEDESTAL

Lateral (Fig. 2.12): Lateral bearing load is not present under normal tangent track operations except for random fluctuations associated with truck guidance. When traversing curved track lateral loads can build up to a quasi-steady value.

Longitudinal (Fig. 2.12): Longitudinal bearing loads are developed during the traversal of curved track due to the yawing slippage of the wheel/axle set and under car impact conditions. Under car impact conditions the most damaging effects of the load may be felt by the bearing on the stationary car since the load is initially transferred at one position in the roller/race interface rather than benefiting from the force distribution possible in rotating roller/race components.

2.2.4 Axles

Radial (Fig. 2.13): Radial loads are applied to the axle between the bearings and the wheel seats. These loads result in a bending moment which is carried through the axle. Because of the changing orientation of the axle as the wheel rotates, the radial loads produce a cycle of stress in the axle once per revolution. This becomes the primary consideration in the evaluation of fatigue strength.

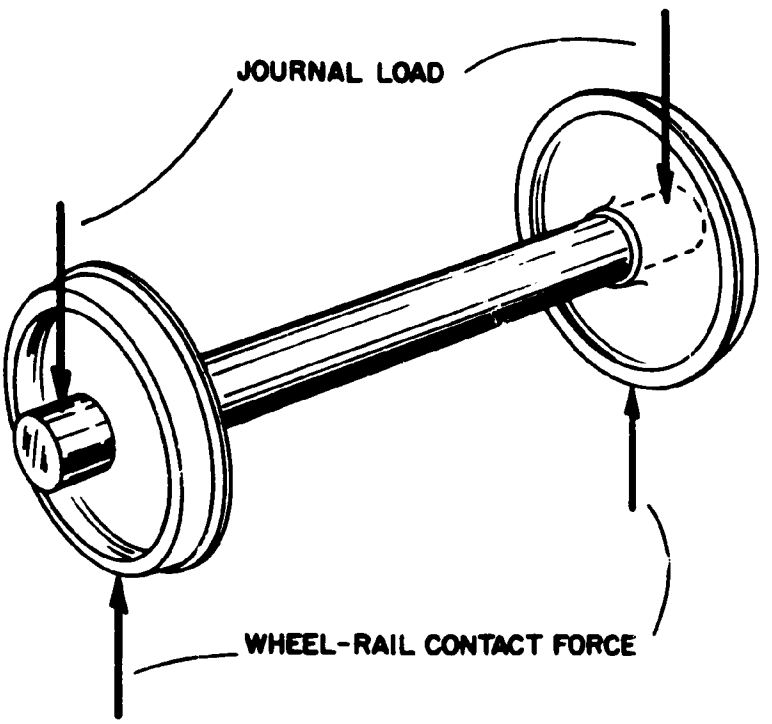

Fig. 2.13 WHEEL-AXLE VERTICAL LOADS

Moment (Fig. 2.14): Lateral load at the wheel/rail interface introduces a moment into the axle at the wheel seat which adds to the moment introduced by the radial loads.

Torque (Fig. 2.14): Torque is applied to the axle from opposing couples due to longitudinal loads at the wheel/rail interface and at the bearing. Axle torque is primarily associated with the yawing slippage of the wheel/axle set when traversing curved track.

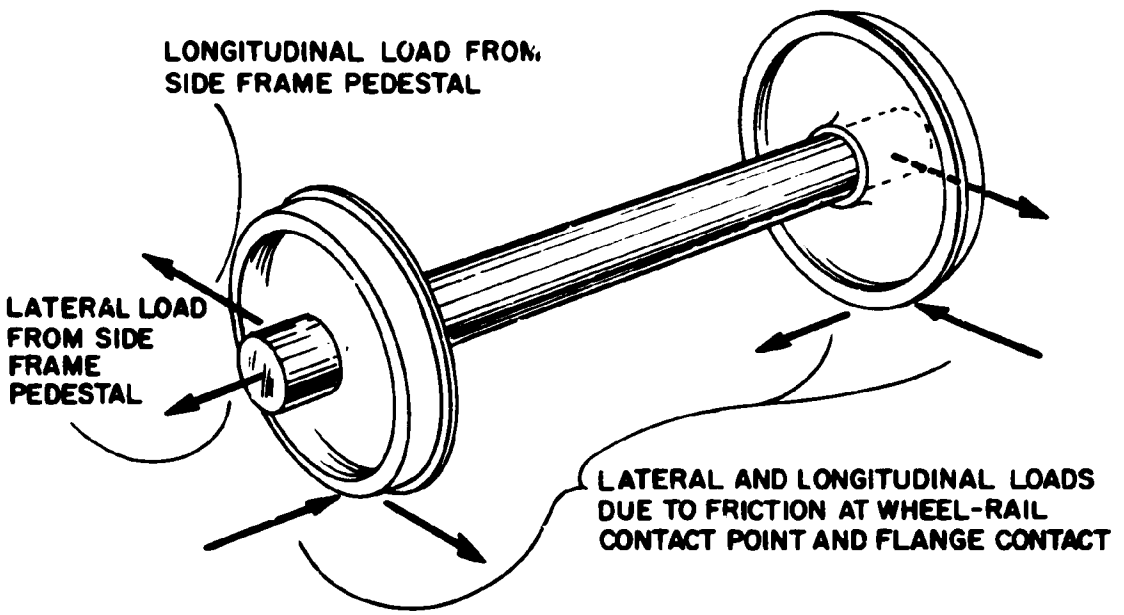

Fig. 2.14 WHEEL-AXLE LATERAL AND LONGITUDINAL LOADS

2.2.5 Wheels

The wheel load environment is the most complex of any of the truck components. Special effects which must be considered are those caused by wheel rotation and tread braking. Both mechanical and thermal loading must be considered in evaluating resistance to fatigue damage.

Vertical (Fig. 2.13): The major load on the wheel is the vertical load which is applied between the wheel/rail contact point on the rim and wheel seat. The magnitude of this load depends on the weight of the car and it is modified by transient factors such as rail irregularities, suspension system oscillations, or wheel flat spots. The major effect of the vertical load is to produce high stresses in the vicinity of the wheel/rail contact point and this high stress pattern is repeated once per wheel revolution. The repeated load phenomena associated with the contact stresses can lead to shattered rim failures. The vertical load also produces fluctuating stresses in the wheel plate as the wheel rotates.

Lateral (Fig. 2.14): Lateral loads are applied between the wheel/rail interface and the wheel seat. This load is due to flange contacts during the normal hunting motion of the wheel/axle set and steady lateral load components which are built up during the traversal of curved track. Lateral loads introduce plate stresses which alternate once per wheel revolution. In most wheel designs this stress pattern is opposite to that caused by the vertical load. In many cases, lateral load stresses are the controlling stresses in the initiation of plate fatigue cracks (Ref. 10).

Thermal: Wheels are also subjected to thermal loading due to the absorption of energy on the tread of the wheel with tread brake systems. The deposition of this energy in the rim leads to high thermal gradients within the wheel. The differential heating causes an expansion and twisting of the rim relative to the plate, which induces steady plate tension stresses as well as steady bending moments in the plate in regions which are highly stressed by lateral loads. The plate becomes more sensitive to fatigue damage at these high stress locations.

The high temperatures reached at the tread can also produce metallurgical changes which affect the ability of the material to resist fatigue damage. Thermal cracking, which refers to a radial crack at the rim of the wheel, is associated with the

thermal load. If the rim is severely heated it expands, producing an inelastic radial deformation of the plate. When the wheel cools the rim shrinks introducing circumferential tensile stresses in the rim, which increases the tendency for crack initiation.

3.0 MEASUREMENT OF LOAD DATA

Since there is only a small amount of published load environmental data on freight car truck components a significant portion of the work on this project was directed at the further analysis of existing unpublished test data and the performance of tests for the measurement of freight car truck forces under various design and operating conditions. The B&LE, a participating subcontractor in the performance of this program, was the source of data. This railroad has developed extensive facilities for gathering and analyzing freight car truck load information (Ref. 1). Some of the data used in this program was obtained during the last several years by the B&LE as part of their efforts to evaluate various truck designs. In addition, a number of test runs were planned and carried out for this program in order to examine the force levels between freight car truck components under conditions which had not been considered in earlier tests.

The basic philosophy of the test program was to determine the combinations of design and operating parameters which lead to severe operating load environments. This involved repeated runs of the test car over a designated track varying one parameter each time.

3.1 Test Track Characteristics

The test area was a seven mile length of track on the Erie branch of the B&LE between Albion and Girard, Pennsylvania. This track contains a wide variety of conditions including turnouts, grade crossings, and curves up to 10 degrees.

A map of the area shown in Fig. 3.1 and the track chart shown in Fig. 3.2 indicate the various features of the test track. Specific features are tabulated:

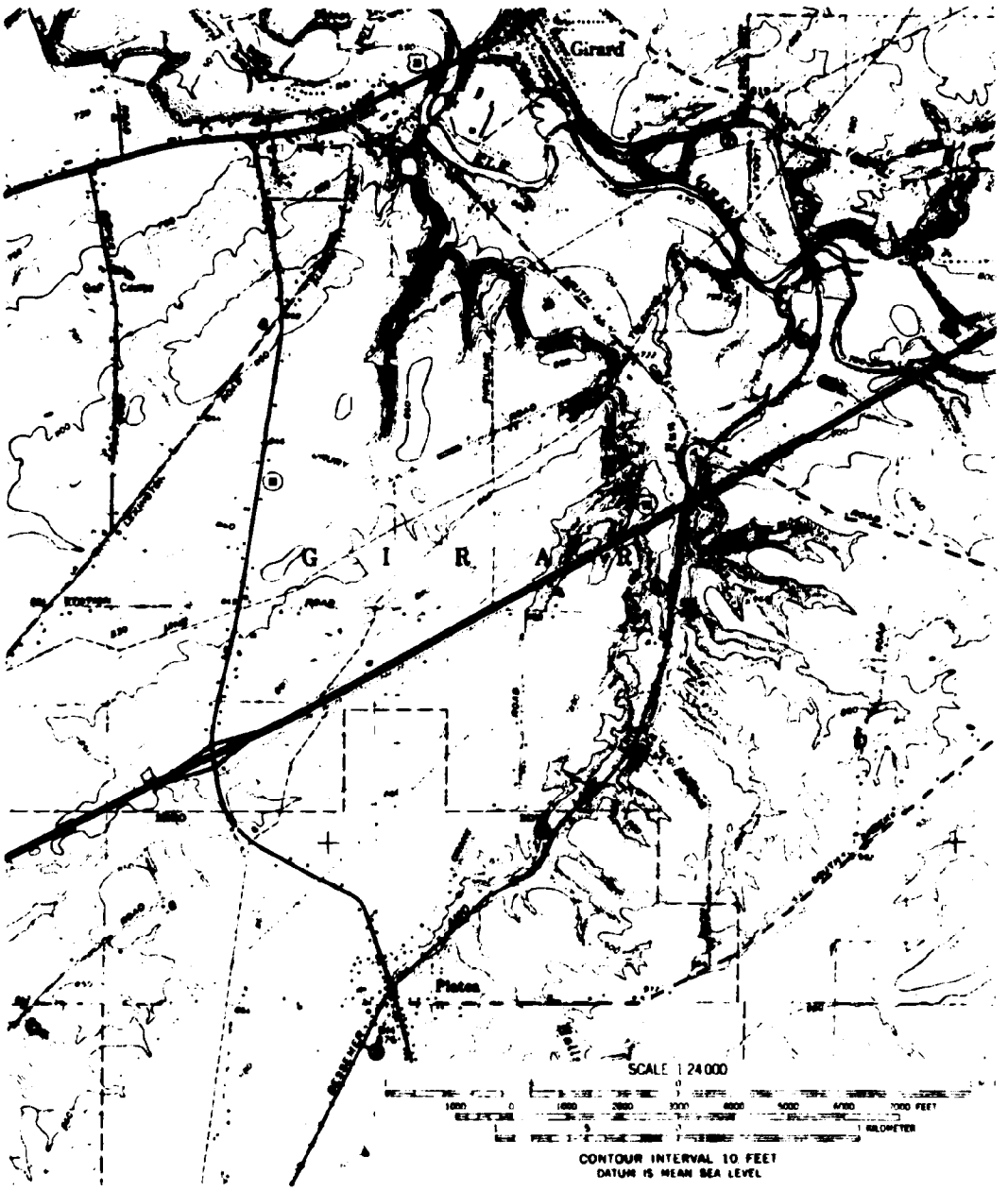

Fig. 3.1 MAP OF B&LE TEST TRACK

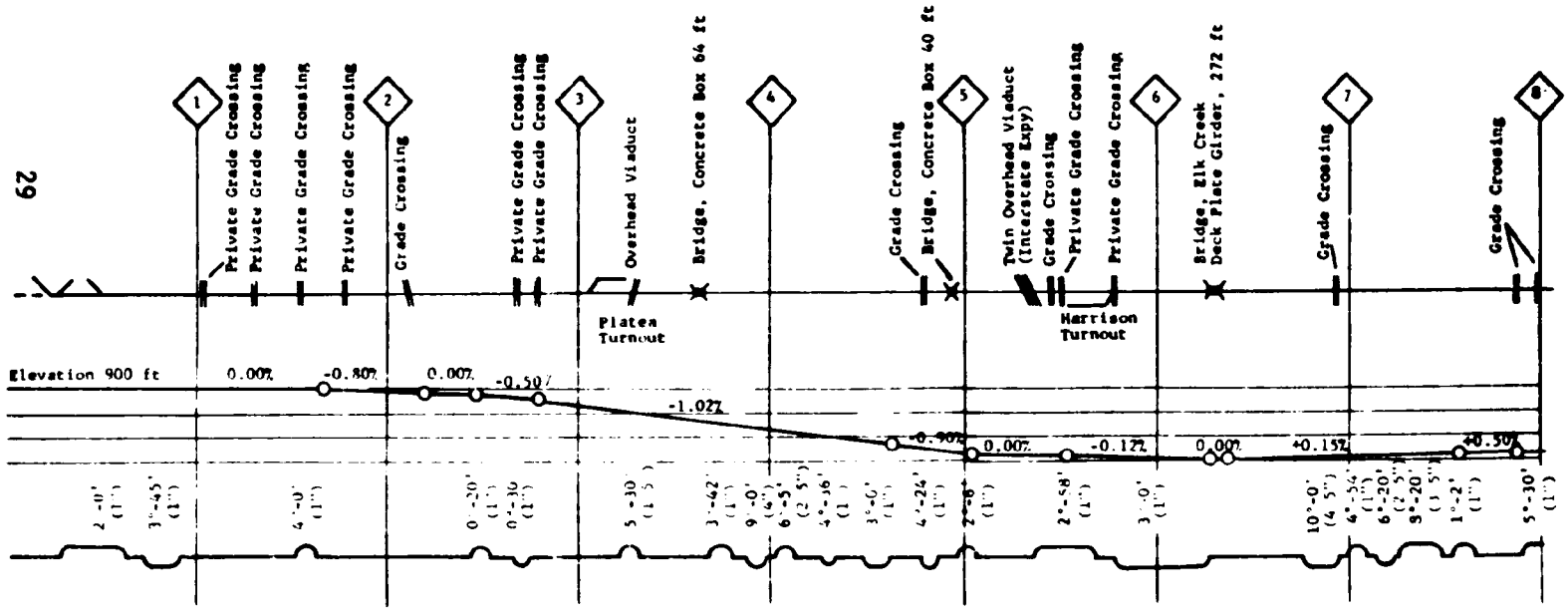

Fig. 3.2 TRACK DIAGRAM FOR B&LE ERIE BRANCH

Grade (+ Northbound)		Miles
0.00%		2.1
-0.01% to -0.50%		1.1
-0.51% to -1.00%		0.9
-1.01% to -1.50%		1.8
+0.01% to +0.50%		1.1
	Total	7.0

Degree of Curvature		Miles
Tangent		4.66
0^{o} 01' - 1^{o} 00'		0.12
2^{o} 01' - 3^{o} 00'		0.99
3^{o} 01' - 4^{o} 00'		0.35
4^{o} 01' - 5^{o} 00'		0.20
5^{o} 01' - 6^{o} 00'		0.07
6^{o} 01' - 7^{o} 00'		0.15
8^{o} 01' - 9^{o} 00'		0.28
9^{o} 01' - 10^{o}00'		0.18
	Total	7.00

The 7.0 mile test section also includes four public grade crossings, eight private grade crossings, three bridges, and two turnouts. The track is constructed of welded rail except for the 10 degree curve. Various features of the test track are illustrated in several photographs. Figure 3.3 shows the 10 degree curve. Figure 3.4 shows the reverse curve from 6^{o} 20' to 4^{o} 54'. One of the longest segments of tangent track is illustrated in Fig. 3.5. One of the two turnouts is shown in Fig. 3.6.

The B&LE has demonstrated through extensive measurements that this track is representative of their entire system. Measurement of this track by the FRA test geometry cars has shown that it is also typical of conditions encountered on other railroads restricted to moderate speed freight operations.

Fig. 3.3 CURVE 10^{o}

Fig. 3.4 REVERSE CURVE $6^{o}20'$ TO $4^{o}54'$

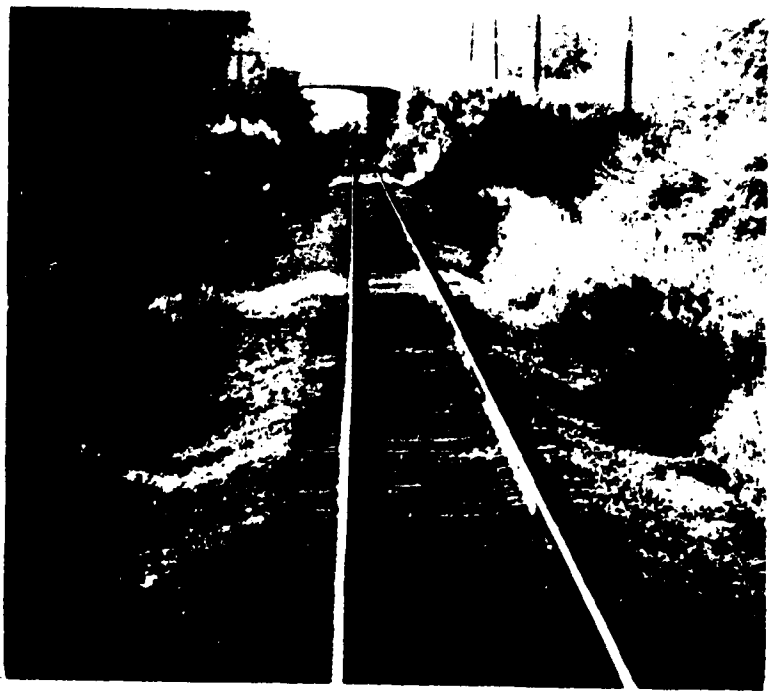

Fig. 3 5 TANGENT TRACK

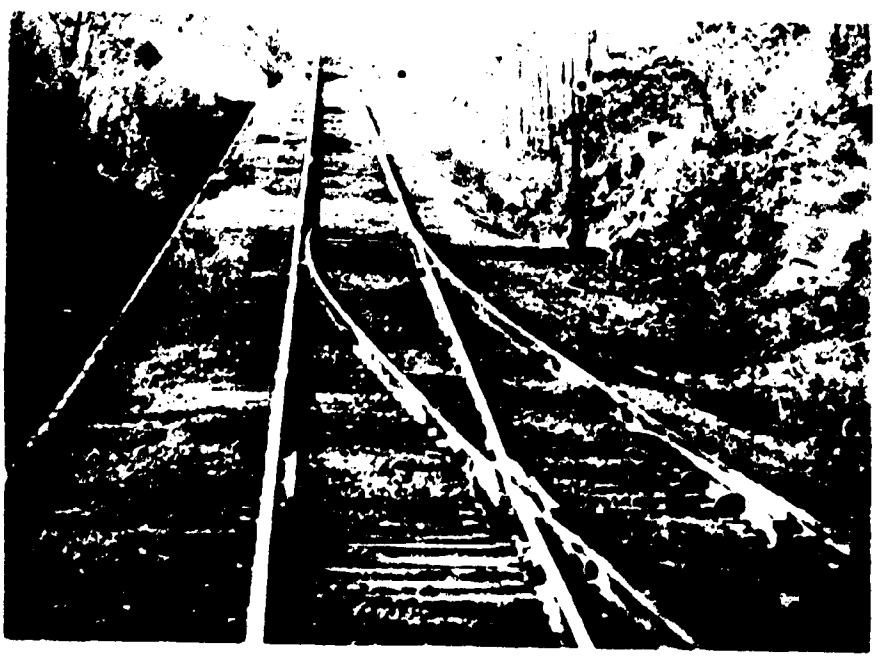

Fig. 3.6 TURNOUT AT PLATEA

3.2 Test Procedures

The principal data obtained on each of the test runs were from the measurement of vertical load at the side-frame-pedestal/roller-bearing-adapter interface and lateral load against the wheel at the wheel/rail interface. The resulting forces acting at other positions in the truck were inferred from these basic measurements. The vertical loads were determined at all four journal positions on the truck from specially constructed load cells placed between the side frame pedestals and roller bearing adapters. One of these load cells is shown in Fig. 3.7.

The lateral loads against each wheel on the truck were calculated utilizing the load cell data and the outputs of strain gage bridges mounted on the axles which were calibrated to give the bending moment in the axle. These data allow the calculation of the equilibrium forces acting on a wheel/axle set from which the lateral force at the wheel/rail interface can be inferred. The calculation of lateral wheel load is provided twice each wheel revolution. (See Appendix A for details of this calculation.)

The principal truck (and car) design parameters which were evaluated during the tests included the truck center distance (20 ft-6 in. to 40 ft-9 in.), design (BARBER S-2, RIDE CONTROL, etc.) spring travel (D-2 and D-5) shock absorbing mechanism (friction shoe snubber, HS-6, etc.), wheel contour (new AAR contour and hollow tread condition at condemning limit) and bearings (roller and plain). Additional tests included examining the loads associated with wheel flat spots and modified suspension systems. A list of the car and truck variables considered is presented in Table 3.1. The principal operating parameters which were investigated included the rail load (empty car or fully loaded car) and speed (10 to 35 mph). Tests were limited to 100-ton capacity cars (6-1/2 by 12 in. journals). Figure 3.8 shows the instrumented truck on the 40 ft-9 in. wheelbase hopper car adjacent to the B&LE instrumentation car. This was the car used in the majority of the tests. Its loaded center-of-gravity was 74 in. above the rail.

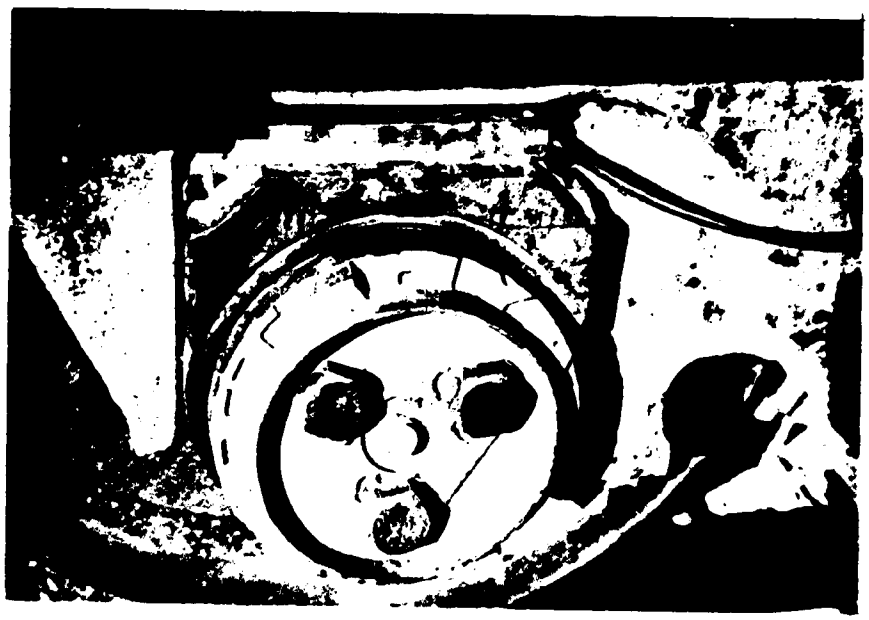

Fig. 3.7 ROLLER BEARING ADAPTER LOAD CELL

TABLE 3.1 SUMMARY OF TEST CASES

Test Run Number	Run Direction North (N) or South (S)	Speed (mph)	Car Designation and Truck Center Distance	Car Loading Condition	Truck Type and Travel of Spring Suspension (in.)	Auxiliary Snubber	Wheel Tread Contour	Special Conditions
1	N	35	Quick Dump Hopper No. 98192 40'-9"	Loaded	RIDE CONTROL 3-11/16	None	New	
2	S					HS-6		
3	N					None	Worn	
4	N					HS-6		
5	N					None	New	
6	N					HS-6		
7	S					None	Worn	
8	N					HS-6		
9	N	20						
10	S							
11	N							
12	N							
13	N							
14	S							
15	N							
16	N	35		Empty (72,300 lb Rail Load)				
17	N							
18	N							
19	N							
20	N	20						
21	N							
22	N							
23	N							
24	N	35		Loaded				
25	S							
26	N							
27	N	20						
28	N							
29	N	35	Quick Damp Hopper No. 98189 40'-9"		BARBER S-2 3-11/16	None	New	
30	N							
31	N							
32	N							
33	S							Frozen Road-bed

TABLE 3.1 SUMMARY OF TEST CASES (Cont.)

Test Run Number	Run Direction North (N) or South (S)	Speed (mph)	Car Designation and Truck Center Distance	Car Loading Condition	Truck Type and Travel of Spring Suspension (in.)	Auxiliary Snubber	Wheel Tread Contour	Special Conditions
34	N	35	Quick Dump Hopper No. 98180 40'-9"	Loaded	BARBER S-2 3-11/16	None	New	Modified Spring Suspension Conditions, see Table 4.2
35	N							
36	N							
37	N							
38	N							
39	N							
40	S							
41	N	27.5						Frozen Roadbed
42	N	20						
43	N							
44	N							Frozen Roadbed
45	N	10						
46	N	35	QCM Hopper 20'-6" No. 4499					
47	N							
48	N							Free Wheeling Truck (Third Axle Bearing)
49	N		Standard Hopper 31'-8" No. 64112		Standard 1-5/8			Plain Bearing
50	N					HS-6		
51	N		Quick Dump Hopper No. 98170 40'-9"		Buckeye Elasto-Cushion Truck 3-11/16	None		Unity Side Bearing Stabilizer
52	N							
53	N				BARBER S-2 3-11/16			Lateral Pads & Conical Centerplate

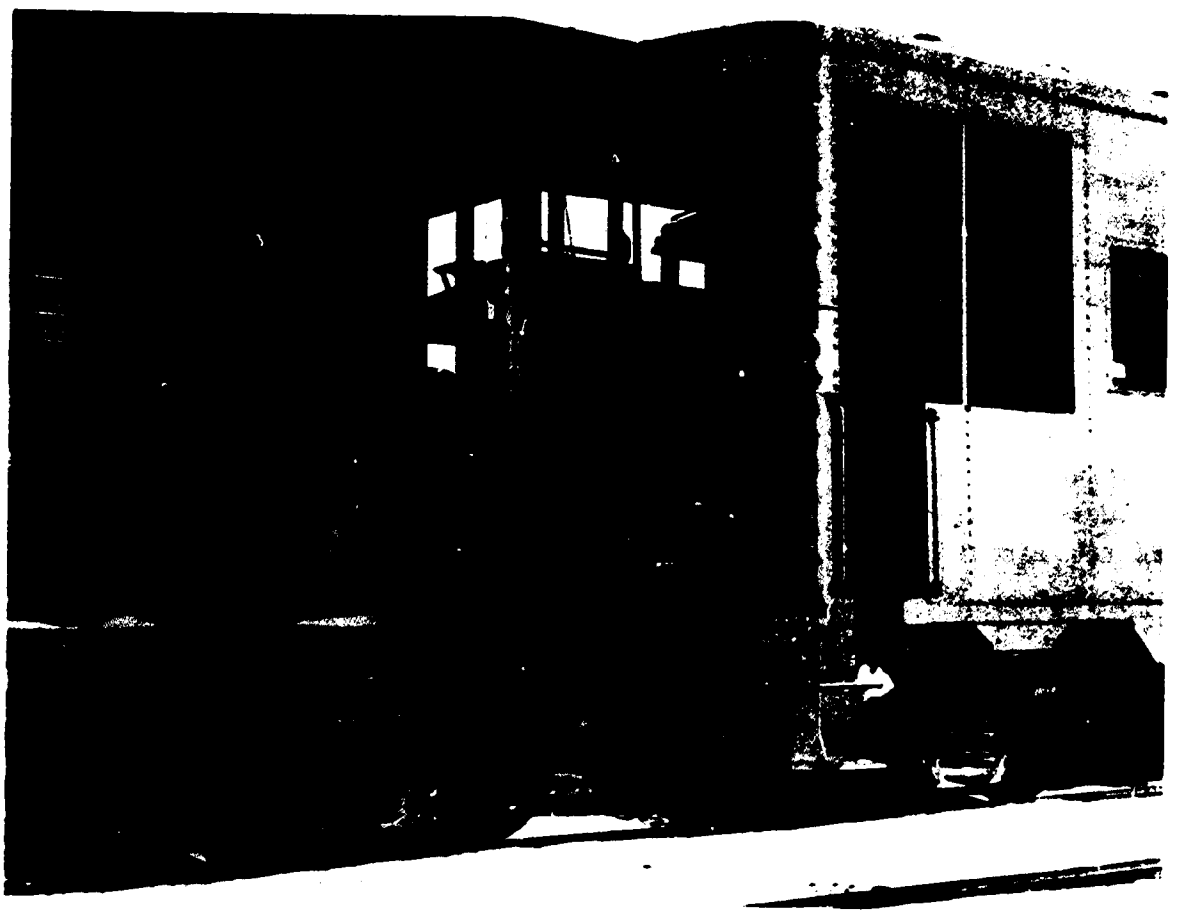

Fig. 3.8 TEST TRUCK AND INSTRUMENTATION CAR

3.3 Analysis of Fluctuating Load Data

The data analysis procedures were geared to identify the aspects of the load environment which are significant to the accumulation of fatigue damage by the various truck components.

This requires information on both the fluctuating load intensity and the frequency of application. A study of test data reveals that the load environment can be characterized by a mean value and a fluctuating component. The mean load may be zero, a value established by the weight of the car, or an operating condition (e.g., the steady component of lateral wheel load on curves).

The test data were recorded in analog form on an FM tape recorder. It was subsequently digitized and played back through a computer for the calculation of certain derived parameters, such as the lateral load against the wheel and the degree of load transfer of vertical load from the centerline of the car.

The data describing the principal load parameters were played back and recorded on a Brush chart for each test run so that the maximum load values could be identified. The test track was divided into 33 segments, reflecting specific track features (e.g., each of the curves, tangent sections between curves, and turnouts) for more detailed analysis. In the case of vertical load cell data this analysis involved counting the number and intensity of fluctuating loads between crossings of the mean load level. This was done automatically through the use of a specially developed computer program. Similar analysis of the test data was performed for the lateral wheel load data.

Many techniques are available for summarizing fluctuating load data. We have adopted the widely used procedure of counting the peak loads between crossings of the mean level as illustrated in Fig. 3.9. This format accurately summarizes the load environment and it can be readily used for the specification of fatigue performance tests. The mean-level-crossing-peak data are displayed on a "load spectrum", which is a plot of the peak levels (both

positive and negative) of the alternating component of the load versus the number of times the load level is exceeded in a given counting interval.

The spectrum is developed by counting the number of times the load exceeds given incremental values from the mean static load over the course of a test run. Both positive and negative peaks are counted and the total counts at each level are reduced to a per mile basis for presentation. This format is used extensively in the next section for summarizing and describing the fluctuating load environment.

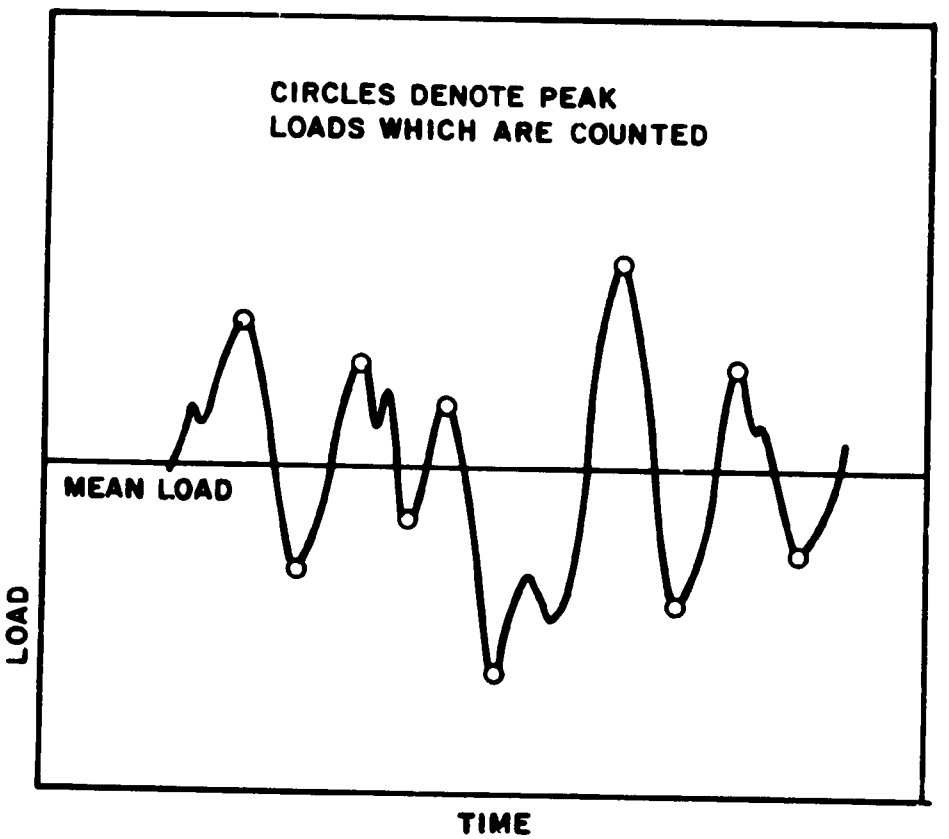

Fig. 3.9 ILLUSTRATION OF PEAK LOAD COUNT BETWEEN MEAN LEVEL CROSSINGS

4.0 SERVICE LOAD DATA

The freight car truck load environment is described in this section. The data are based on results from the analysis of B&LE test records and can be used to formulate load spectra for fatigue performance testing of freight car truck components. All data are presented with reference to a loaded* 100-ton capacity car (263,000 lbs rail load). Load data for cars of lower capacity may be estimated by assuming that the forces are proportional to the rail load.

4.1 Side-Frame-Pedestal/Roller-Bearing-Adapter (SF/BA) Interface Vertical Load Data

The data presented in this section describe the vertical fluctuating loads at the interface between the side-frame-pedestals and the roller-bearing-adapters. Most of the spectra used to describe these loads are shown with reference to the number of load cycles per mile, but for rotating components it is necessary to develop a load spectrum with reference to wheel revolutions per mile. Load spectra defined in terms of the number of cycles per mile are relevant to side frame and bolster fatigue as described in the following paragraphs.

Side Frame

The SF/BA spectrum represents one-half of the vertical load acting on the side frame. Test results show that the two SF/BA loads on a side frame are almost always in phase and of the same magnitude so that there is a negligible difference between the spectra for the two positions. It has also been shown that the SF/BA spectra are of negligible difference for side frames on opposite sides of the truck, although the instantaneous loads are not necessarily the same magnitude or in phase.

*Data from empty car test runs indicated load levels substantially below loaded car conditions.

Bolster

The SF/BA spectrum represents one-fourth the total bolster load if the car and truck are in the bounce mode of oscillation. The data obtained on the B&LE tests indicated that the primary mode of oscillation for the car is a roll motion. This implies that the principal bolster loading is one of the movement of the vertical-force line-of-action from one side of the bolster to the other. When this movement is large it involves load transfer to the side bearings. Therefore the SF/BA spectra can be used to designate out-of-phase symmetrical loads applied at either end of the bolster (see Section 4.3). In Section 4.5 the possibility is described that bounce modes of oscillation may become predominant at speeds above 50 mph. This phenomena would affect the SF/BA spectra as it applies to both the side frame and bolster, but since it was not possible to conduct tests in this speed range the effect is not included in the data presented in this section.

When dealing with the rotating parts on the truck, the wheels, axles and bearings, one must consider that cyclic stresses are developed in these components during their rotation even though there is only a steady load acting on the component. Thus, for these components the loads should be defined by a spectrum showing the number of revolutions given load levels are exceeded. A vertical load spectrum with reference to revolutions per mile (designated SF/BA_r) may then be used for these components as follows.

Bearings

The SF/BA_r spectrum represents the variation in the vertical loads acting on the bearing.

Wheels

The true vertical wheel load is influenced by the instantaneous value of each of the two journal loads. Since these loads are not necessarily identical the vertical wheel load can vary from the indicated spectrum. If the spectrum is influenced

primarily by the truck bounce mode of oscillation, the vertical wheel load spectrum will be approximately the same as the SF/BA_r spectrum. On the other hand, if the spectrum is influenced primarily by the rocking action of the car, the vertical wheel load spectrum may be as much as 35 percent more severe (from a load intensity standpoint) than the SF/BA_r spectrum.

Axle

The SF/BA_r spectrum can be used to evaluate bending moment fluctuations within the axle. The axle bending moment is caused by the offset between the bearing and wheel loads. Note that additional moments would be introduced by lateral loads at the wheel/rail interface. The SF/BA_r spectrum would have to be combined with a spectrum for lateral wheel load to provide an adequate representation of fluctuating axle bending moments.

4.1.1 Average Data

An average load spectrum derived from the analysis of the BARBER S-2 and RIDE CONTROL truck test runs at 35 mph is presented in Fig. 4.1. This spectrum and the ones which follow are drawn with reference to a nominal journal load of 30,000 lbs for a loaded 100-ton capacity car.

Figure 4.1 was developed from test data where there was no reason to expect major variations in the character of the SF/BA loads. The data were obtained with test trucks having 3-11/16 in. spring travel installed on a hopper car with 40 ft-9 in. truck centers. The spectrum was developed by averaging 68 load cell records from 18 test runs.* The variations in these data are indicated by the plus and minus one standard deviation curves shown in the figure. Note that the low frequency end of the lower curve would be influenced by the frequency with which the car is unloaded.

---

*See Appendix B for further details on the method of deriving load spectra of the vertical SF/BA load.

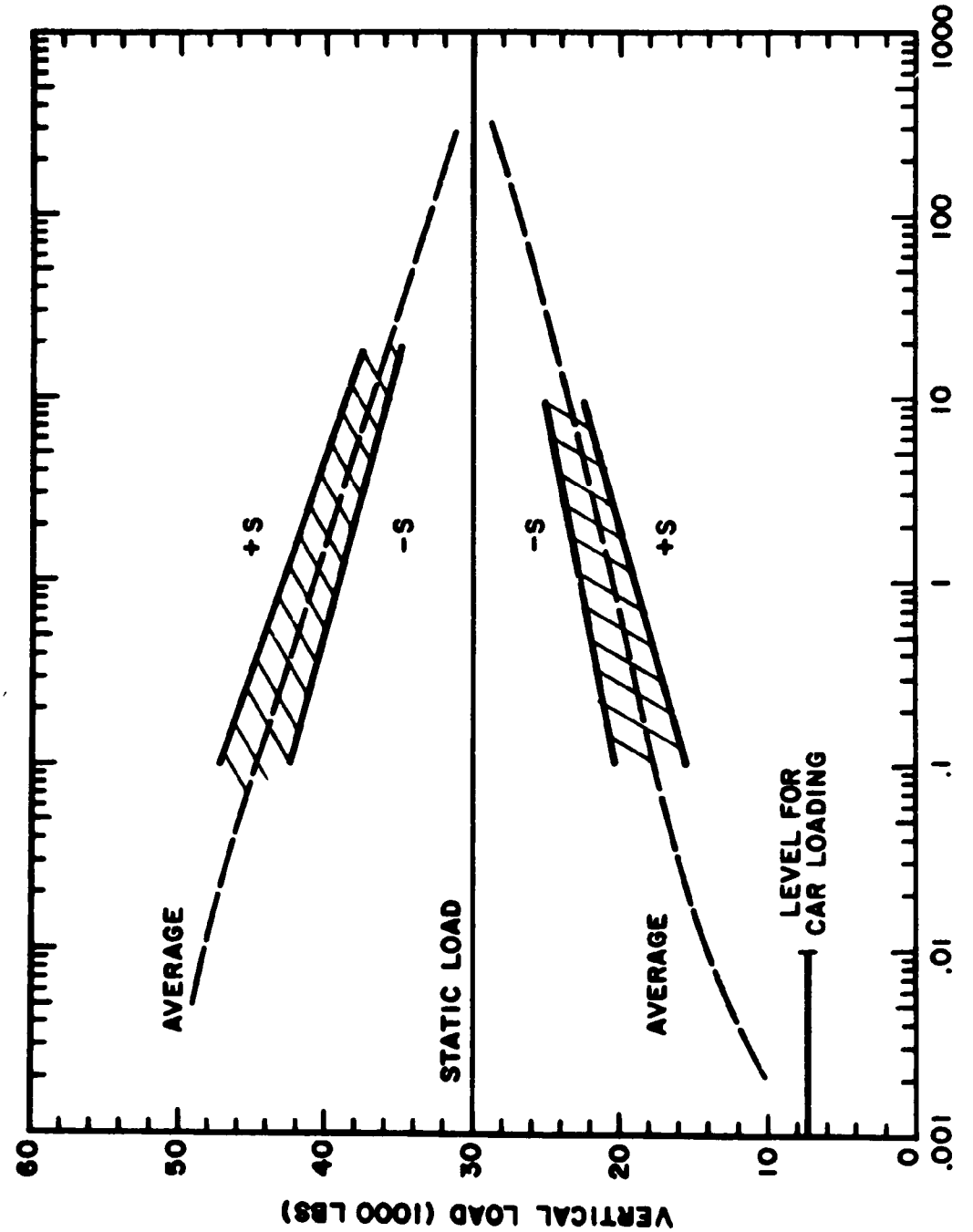

Fig. 4.1 AVERAGE VERTICAL SF/BA LOAD SPECTRUM AT 35 MPH

4.1.2 Comparison of BARBER S-2 and RIDE CONTROL Truck Data

Figure 4.2 shows the results of grouping data from the RIDE CONTROL truck runs and the BARBER S-2 truck runs. A slight difference in the resulting spectra is indicated. The BARBER S-2 truck data are based on 42 load cell records from 11 test runs and the RIDE CONTROL truck data are based on 26 load cell records from seven test runs. The spread of the data is also indicated by showing the plus and minus one standard deviation curves. These curves are presented to show that small, but statistically significant differences, are obtained on tests with different trucks. It does not necessarily follow that one truck is superior to the other because the spectra represent data over a rather narrow range of conditions and were obtained from tests of only one truck of each type.

4.1.3 D-2 Spring Group Data

Figure 4.3 compares the average load spectrum curve (Fig. 4.1) with data obtained from a car equipped with plain bearings and a D-2 spring suspension (1-5/8 in. spring travel). Two spectra are shown. One represents the unsnubbed spring condition (based on two load cell records). It indicates a level of cyclic load substantially above the average curve and represents the most severe environment measured on any of the tests. The other spectrum (based on two load cell records) shows the results of adding an HS-6 snubber to the spring group which moderates the cyclic load environment.

4.1.4 Spring and Snubbing Variations

A number of test runs were made with variations in the main spring suspension system of the truck. The results showed no significant variations in the SF/BA load spectra when these changes were made. This is demonstrated by the following comparisons.

The RIDE CONTROL truck was tested with normal spring suspension conditions and with the substitution of a snubber for one of the main suspension springs. There were no significant differences

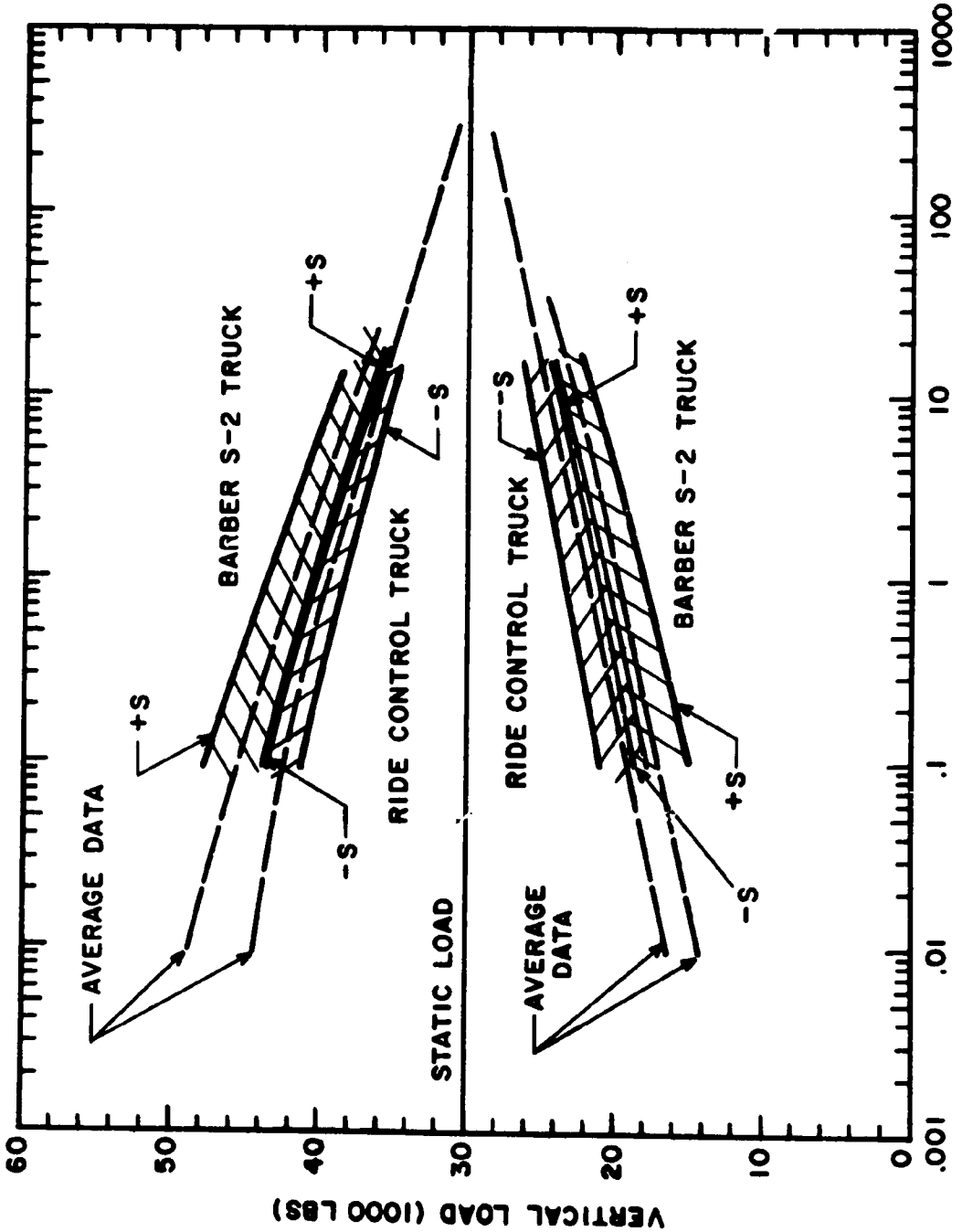

Fig. 4.2 COMPARISON OF VERTICAL SF/BA LOAD SPECTRA FOR BARBER S-2 AND RIDE CONTROL TRUCKS AT 35 MPH

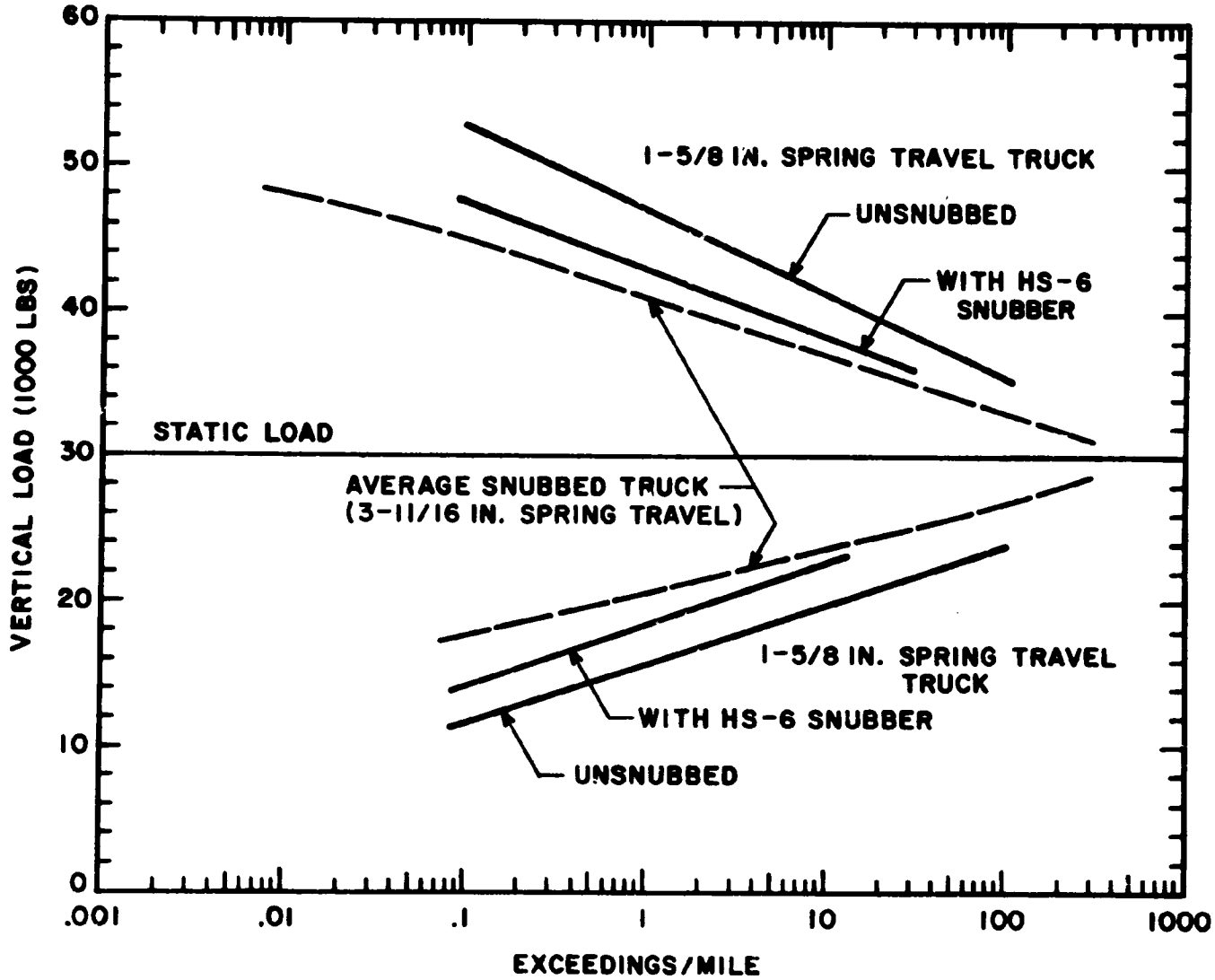

Fig. 4.3 COMPARISON OF VERTICAL SF/BA LOAD SPECTRA FOR TRUCK EQUIPPED WITH 1-5/8 INCH TRAVEL SPRING SUSPENSION AND PLAIN BEARINGS WITH AVERAGE SPECTRUM AT 35 MPH

in these test results. This is shown in Table 4.1 which compares the load spectra by indicating the maximum cyclic load registered in a 4.1 mile length of the test run and the number of cyclic loads exceeding plus or minus 7500 lbs. The comparison shows that the average results are within the range of the standard deviation of the test data.

The BARBER S-2 truck was tested under normal and modified springing conditions. Table 4.2 shows the variations in spring suspension and indicates that both the number of main suspension springs and the springs loading the friction shoes, which provide snubbing to suspension system oscillations, were varied. Table 4.3 compares the load spectra data for the BARBER S-2 truck tested under these springing variations with normal conditions. The modified springing tests are lumped together in this comparison, since there were no significant differences among the individual test runs. The comparison is again based on the maximum cyclic loads in 4.1 miles and the number of cyclic loads exceedings plus and minus 7500 lbs. Average data from the two test groups are within the range of the standard deviation indicating that there is no significant difference in the test data.

4.1.5 Wheel Tread Condition

Tests were conducted on a RIDE CONTROL truck equipped with wheels where the tread was worn close to the condemning limit (see Appendix C for tread contours). The tests showed that there were no significant differences in the SF/BA load spectra when compared with tests with a new wheel tread contour. Table 4.4 compares the average maximum loads in 4.1 miles of the test run and the number of cyclic loads exceeding plus and minus 7500 lbs. Note that the standard deviation of the data in each of the two test groups exceeds the differences in the overall averages.

4.1.6 Frozen Roadbed

Tests were conducted with the BARBER S-2 truck on both normal roadbed and frozen roadbed. The frozen roadbed tests were conducted in January 1974 following a 2 week period when the

TABLE 4.1 COMPARISON OF VERTICAL LOAD SPECTRA DATA FOR RIDE CONTROL TRUCK WITH AND WITHOUT AUXILIARY SNUBBER

Comparison Basis	New Wheel and Worn Wheel Tests, Standard Springing Conditions data from 18 load cell records (from 5 test runs)	New Wheel and Worn Wheel Tests, with Snubber in Main Spring Group data from 8 load cell records (from 2 test runs)
Average Minimum Load in 4.1 miles (lbs)	-9,730	-8,480
Standard Deviation (lbs)	1,800	670
Average Maximum Load: in 4.1 miles (lbs)	+11,480	+11,940
Standard Deviation (lbs)	1,370	1,080
Average Number of Negative Peaks per Mile Exceeding -7500 lbs	2.1	1.1
Standard Deviation	1.6	.3
Average Number of Positive Peaks per Mile Exceeding +7500 lbs	4.3	4.7
Standard Deviation	1.8	1.8

TABLE 4.2 SPRING GROUP ARRANGEMENTS FOR REDUCED SPRINGING AND SNUBBING TEST RUNS WITH BARBER S-2 TRUCK

Test No.	Spring Group East Side				Spring Group West Side			
	Number of Outer Springs (D-5)	Number of Inner Springs (D-5)	Number of Outer Friction Shoe Control Springs	Number of Inner Friction Shoe Control Springs	Number of Outer Springs (D-5)	Number of Inner Springs (D-5)	Number of Outer Friction Shoe Control Springs	Number of Inner Friction Shoe Control Springs
34	7	6	2	0	7	6	2	2
36	7	6	2	2	6	6	2	2
37	6	6	2	2	6	6	2	2
38	6	6	2	1	6	6	2	1
39	7	6	2	0	7	6	2	0
40	7	6	2	0	7	6	2	0
Normal Arrangement	7	6	2	2	7	6	2	2

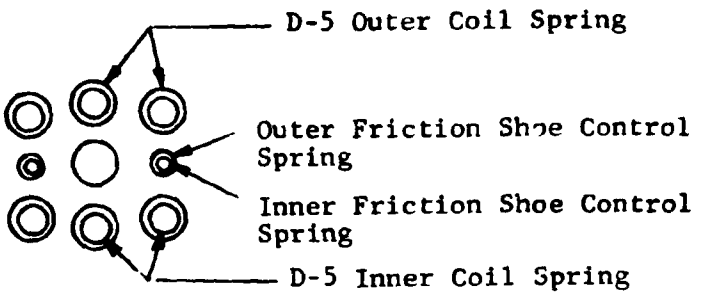

Plan View of Spring Group

TABLE 4.3 COMPARISON OF VERTICAL LOAD SPECTRA DATA FOR BARBER S-2 TRUCK WITH NORMAL SPRINGING AND MODIFIED SPRINGING*

Comparison Basis	Normal Springing, Normal and Frozen Roadbed data from 20 load cell records (from 5 test runs)	Reduced Springing, Normal and Frozen Roadbed data from 22 load cell records (from 6 test runs)
Average Minimum Load in 4.1 miles (lbs)	-12,150	-11,980
Standard Deviation (lbs)	2,150	1,720
Average Maximum Load in 4.1 miles (lbs)	+14,690	+14,340
Standard Deviation (lbs)	1,690	2,200
Average Number of Negative Peaks per Mile Exceeding -7500 lbs	6.3	4.9
Standard Deviation	3.6	2.2
Average Number of Positive Peaks per Mile Exceeding +7500 lbs	9.8	9.6
Standard Deviation	3.8	4.3

*See Table 4.2.

TABLE 4.4 COMPARISON OF VERTICAL LOAD SPECTRA DATA FOR RIDE CONTROL TRUCK WITH NEW WHEEL TREAD CONTOURS AND WORN WHEELS

Comparison Basis	New Wheel Tread Contour data from 12 load cell records (from 3 test runs)	Worn Wheel Tread Contour data from 14 load cell records (from 4 test runs)
Average Minimum Load in 4.1 miles (lbs)	-8,990	-9,650
Standard Deviation (lbs)	1,870	1,400
Average Maximum Load in 4.1 miles (lbs)	11,780	11,480
Standard Deviation (lbs)	1,380	1,240
Average Number of Negative Peaks per Mile Exceeding -7500 lbs	1.2	2.3
Standard Deviation	.6	1.8
Average Number of Positive Peaks per Mile Exceeding +7500 lbs	4.6	4.3
Standard Deviation	1.8	1.9

temperature remained below freezing. Comparison of the test data shows that there were no significant differences in the SF/BA load spectra. Table 4.5 compares the average maximum loads in 4.1 miles of the test run and the number of cyclic loads exceeding plus and minus 7500 lbs. Note that the standard deviation of the data in each of the two test groups exceeds the differences in the overall averages.

4.1.7 Speed

Figures 4.4 and 4.5 show the effects of speed on the SF/BA load spectra. Figure 4.4 compares data from test runs on the BARBER S-2 truck at speeds of 10, 20 and 27.5 mph with the average BARBER S-2 truck curve developed for 35 mph. The data indicate that at 27.5 mph there is essentially no change from the 35 mph curve, but that there is a significant reduction in intensity of the load spectra for the 10 and 20 mph tests. In making this comparison it must be recognized that only limited data were obtained at speeds other than 35 mph. The 10 and 27.5 mph curves represent the results of one test run each and the 20 mph curve represents the results of two test runs. Figure 4.5 shows a comparison between RIDE CONTROL truck average data at 35 mph and two test runs at 20 mph. This comparison shows no substantial difference between the data.

4.1.8 Wheel Flats

Several tests runs were made with a wheel/axle set having 2-in.-long flat spots on the wheel tread. This condition introduces severe vertical transient loads into the truck. The load from a wheel flat occurs once per wheel revolution as illustrated in Figs. 4.6 and 4.7. The magnitude of the transient load is not constant but varies from one revolution of the wheel to the next. The normal hunting action of the wheel/axle set will vary the manner in which the flat spot contacts the rail from one revolution to the next. The maximum load is developed only when the flat spot hits squarely on the rail.

TABLE 4.5 COMPARISON OF VERTICAL LOAD SPECTRA DATA FOR BARBER S-2 TRUCK ON NORMAL AND FROZEN ROADBED

Comparison Basis	Normal Roadbed, data from 26 load cell records (from 7 test runs)	Frozen Roadbed, data from 16 load cell records (from 4 test runs)
Average Minimum Load in 4.1 miles (lbs)	-11,650	-12,710
Standard Deviation (lbs)	1,890	1,810
Average Maximum Load in 4.1 miles (lbs)	+14,770	+14,070
Standard Deviation (lbs)	2,060	1,750
Average Number of Negative Peaks per Mile Exceeding -7500 lbs	4.9	6.8
Standard Deviation	1.9	4.0
Average Number of Positive Peaks per Mile Exceeding +7500 lbs	10.7	8.0
Standard Deviation	4.1	3.4

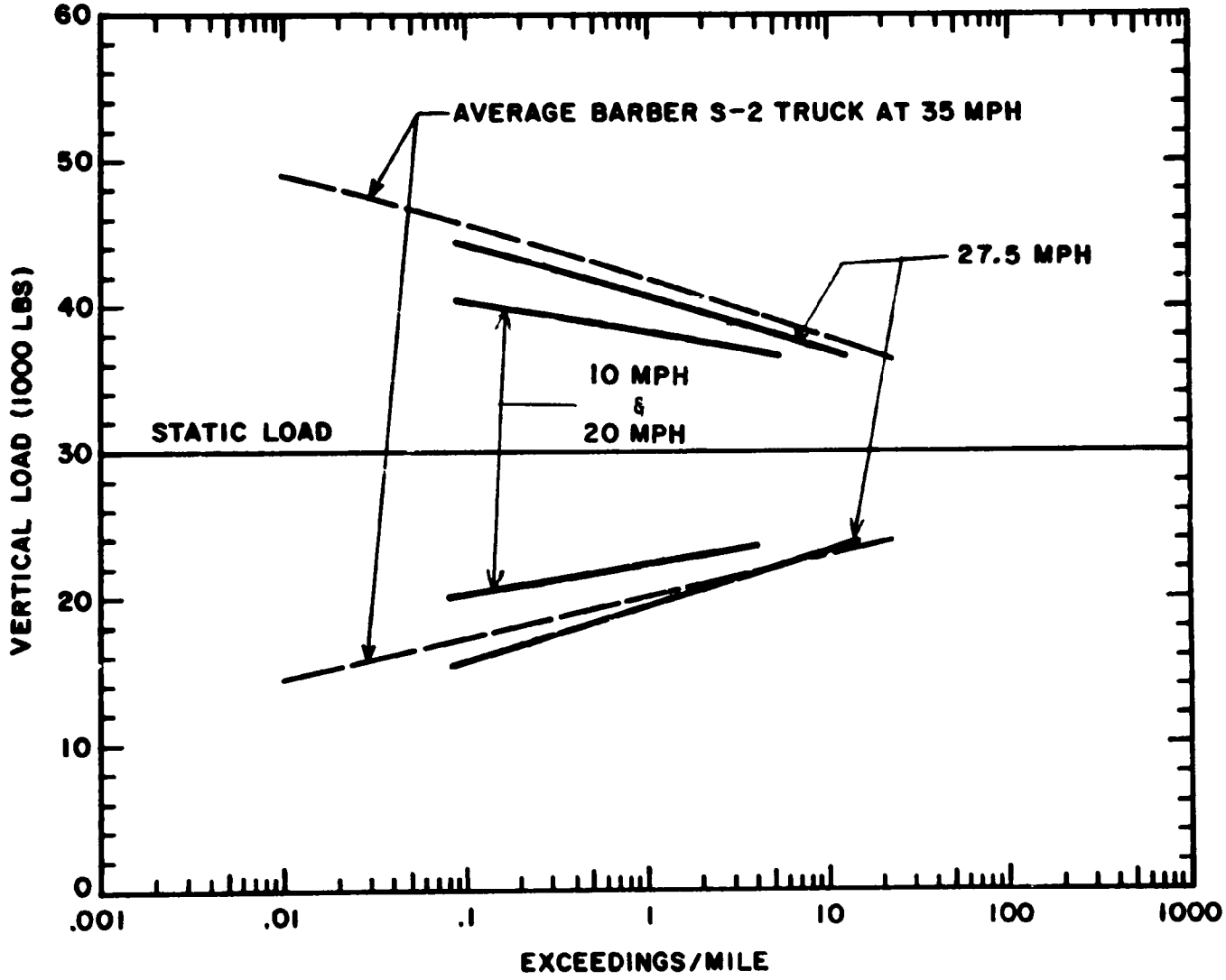

Fig. 4.4 COMPARISON OF BARBER S-2 TRUCK 10, 20 AND 27.5 MPH DATA WITH AVERAGE VERTICAL SF/BA LOAD SPECTRUM FOR BARBER S-2 TRUCK AT 35 MPH

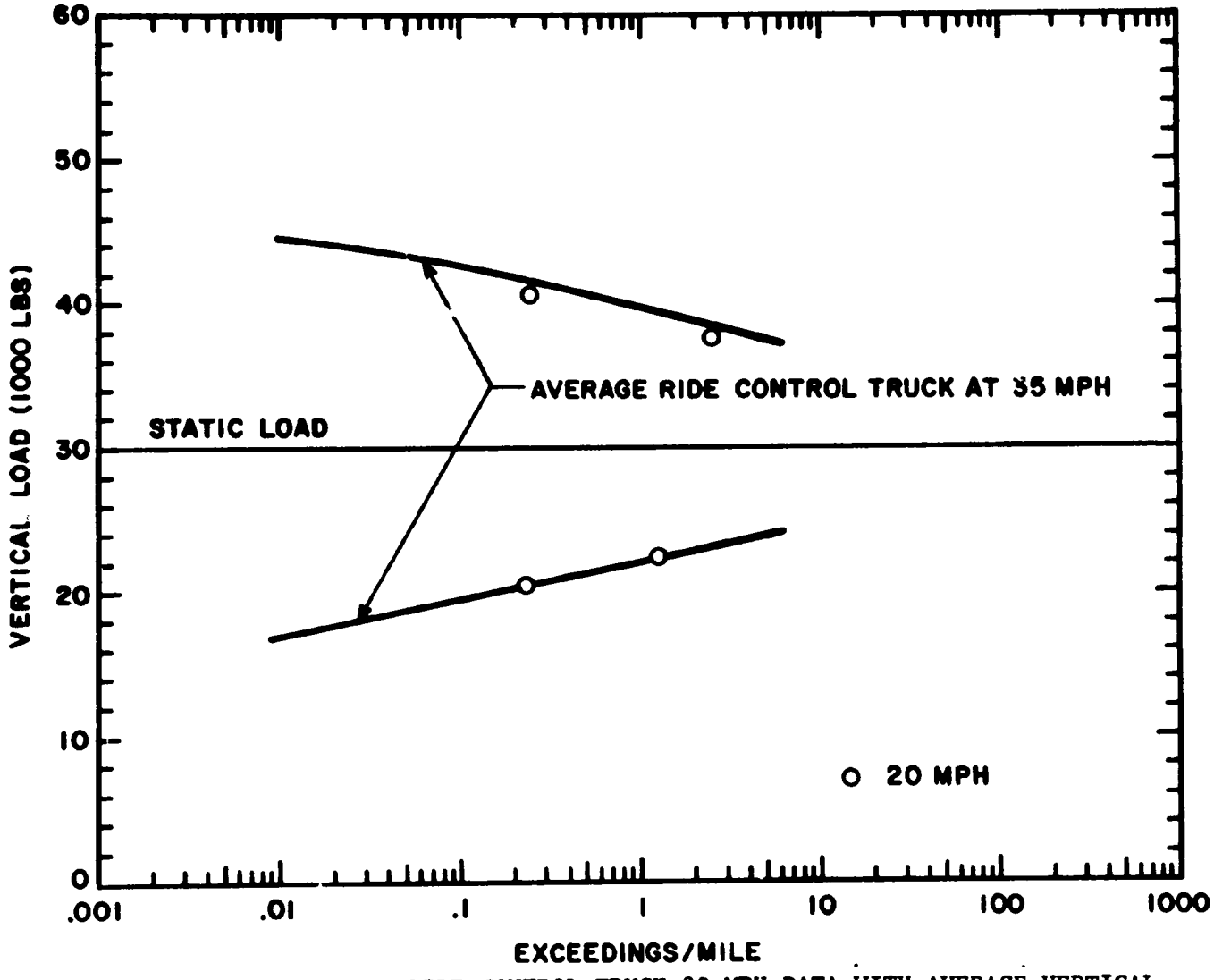

Fig. 4.3 COMPARISON OF RIDE CONTROL TRUCK 20 MPH DATA WITH AVERAGE VERTICAL SF/BA LOAD SPECTRUM FOR RIDE CONTROL TRUCK AT 35 MPH

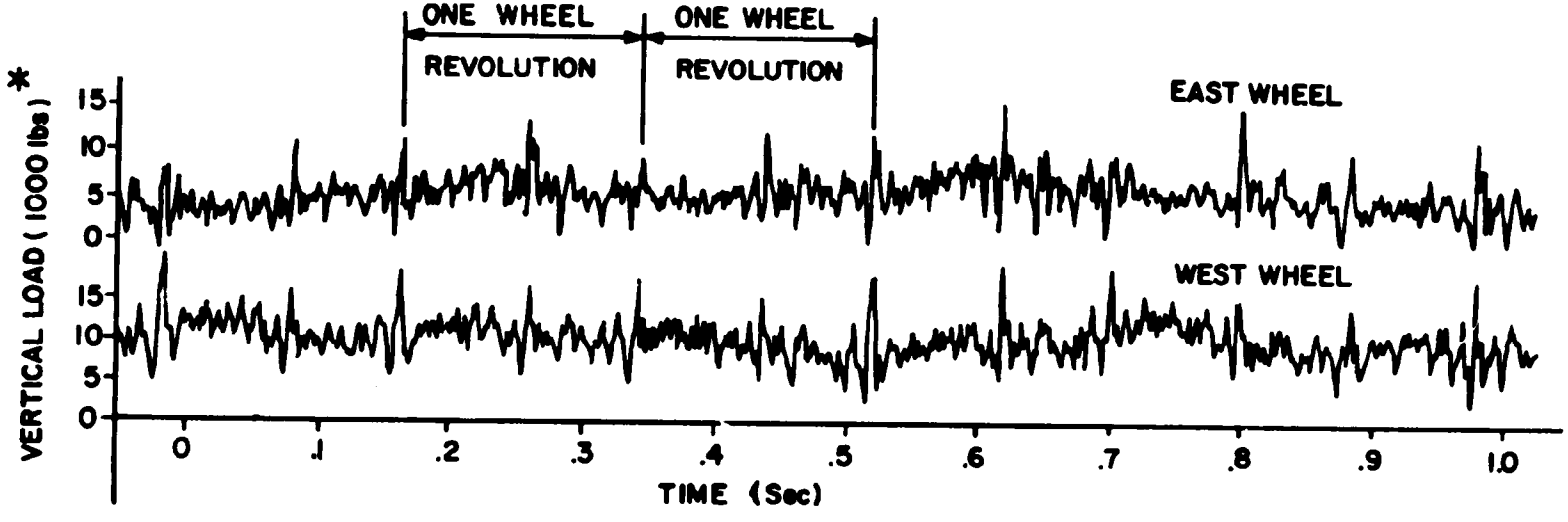

Fig. 4.6 TYPICAL VERTICAL LOAD RECORDS AT SF/BA INTERFACE FOR WHEELS WITH 2 INCH FLAT SPOTS AT 35 MPH (*Note: Arbitrary reference for vertical load scales)

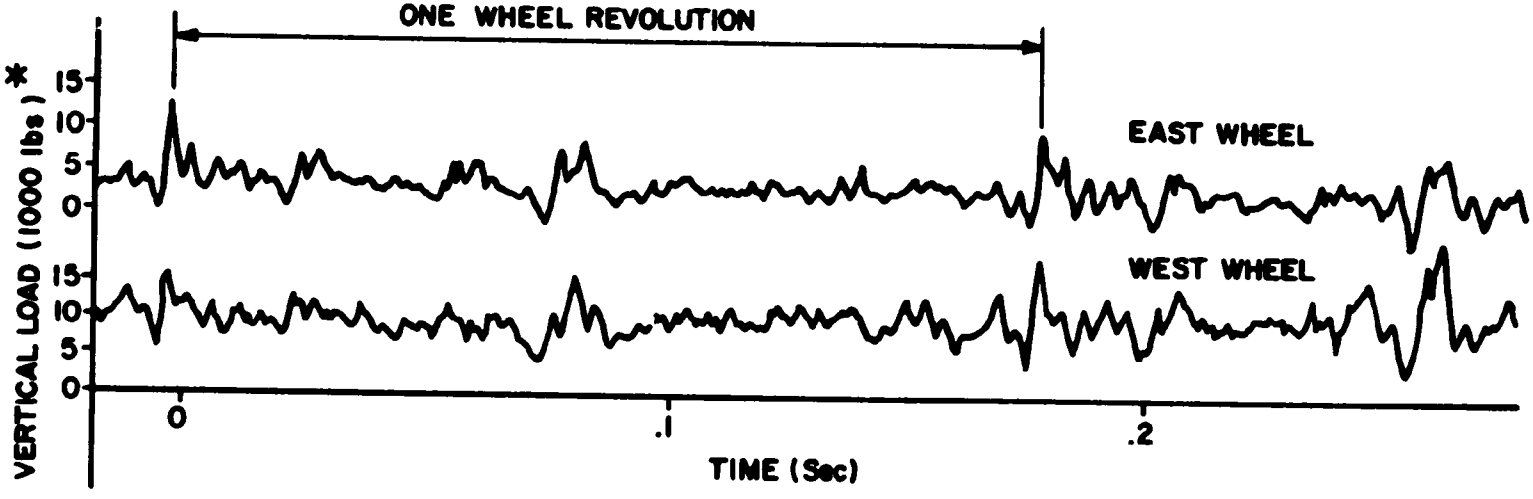

Fig. 4.7 TYPICAL VERTICAL LOAD RECORDS AT SF/BA INTERFACE FOR WHEELS WITH 2 INCH FLAT SPOTS AT 35 MPH (*Note: Arbitrary reference for vertical load scales)

Test runs were made at both 35 and 20 mph with the flat wheels. Table 4.6 shows the frequency of transient load levels referenced to the average running load. At 35 mph 1 percent of the peak transient loads exceed 10,000 lbs over the normal running load and 10 percent of the peak loads exceed 8000 lbs, etc. At 20 mph the intensity of the peak load is somewhat less. One percent of the peak transient loads exceed 8600 lbs and 10 percent of the peak loads exceed 6600 lbs, etc. Modified load spectra curves including the flat wheel data are shown in Figs. 4.8 and 4.9. Figure 4.3 shows the modification of the SF/BA average load spectra curve for 35 mph and Fig. 4.9 shows the modification of the SF/BA curve for the RIDE CONTROL truck at 20 mph. These curves are not directly calculated from the data, but were established by modifying the average vertical spectra data (Fig. 4.1 for both BARBER S-2 and RIDE CONTROL truck data at 35 mph, and Fig. 4.5 for RIDE CONTROL truck data at 20 mph). The modification involved adding the incremental load levels shown in Table 4.6 at the indicated frequencies of occurrence.

TABLE 4.6 FREQUENCY OF LOAD LEVELS DUE TO 2 INCH WHEEL FLATS, LOAD OCCURRING ONCE PER WHEEL REVOLUTION

	20 mph	35 mph
1 percent exceed	8,600 lbs	10,000 lbs
10 percent exceed	6,600	8,000
40 percent exceed	5,000	6,000
75 percent exceed	3,000	4,000
90 percent exceed	1,400	2,000

4.1.9 Track Characteristics

Figure 4.10 compares spectra for operations over a 10 degree curve and tangent track with the average spectra. The increased load associated with the curve traversal is due to the excitation of car body roll motions. The spread of this data indicates the extreme of variations of spectra with track characteristics.

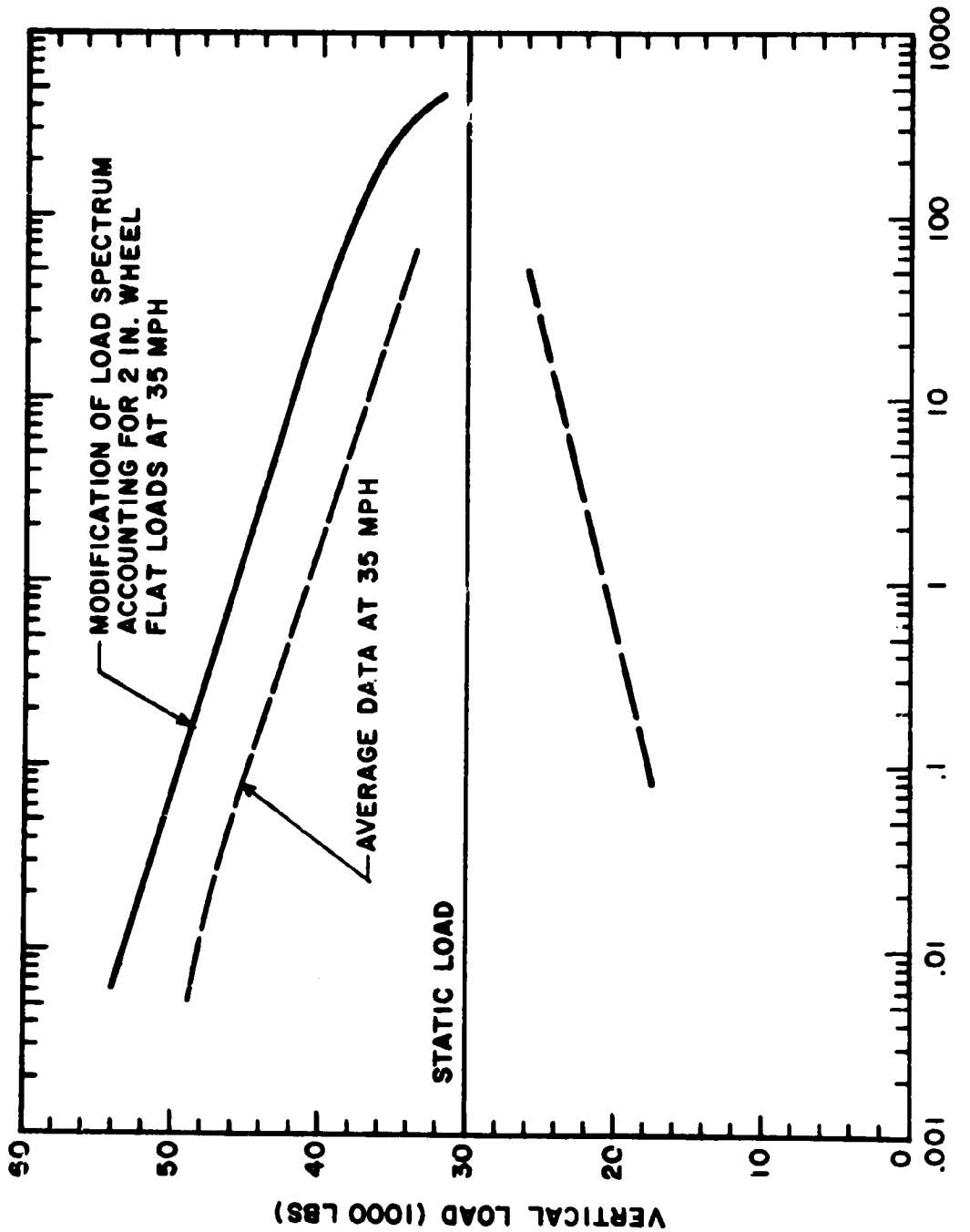

Fig. 4.8 COMPARISON OF VERTICAL SF/BA LOAD SPECTRA WITH AND WITHOUT WHEEL FLAT LOADS AT 35 MPH

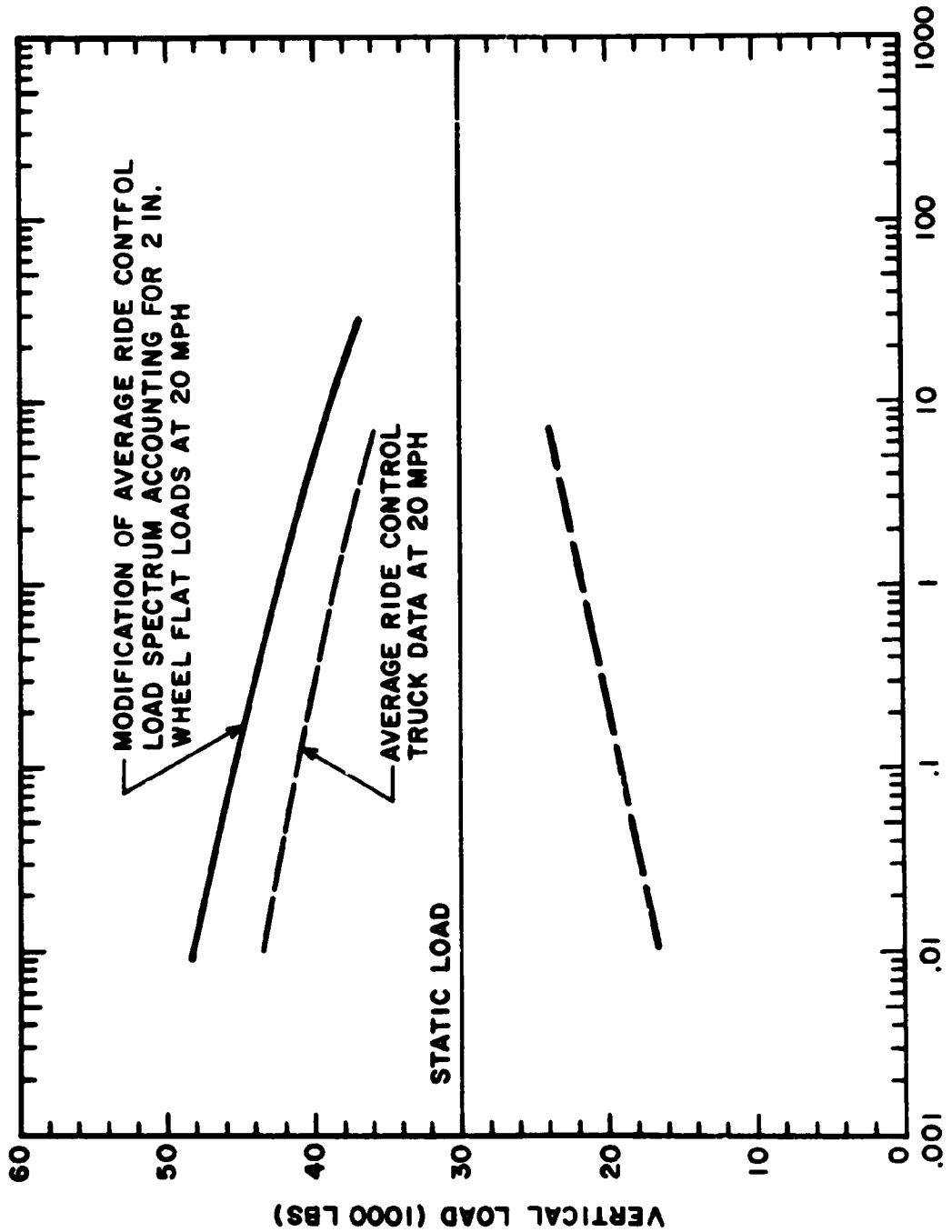

Fig. 4.9 COMPARISON OF VERTICAL SF/BA LOAD SPECTRA WITH AND WITHOUT WHEEL FLAT LOADS AT 20 MPH

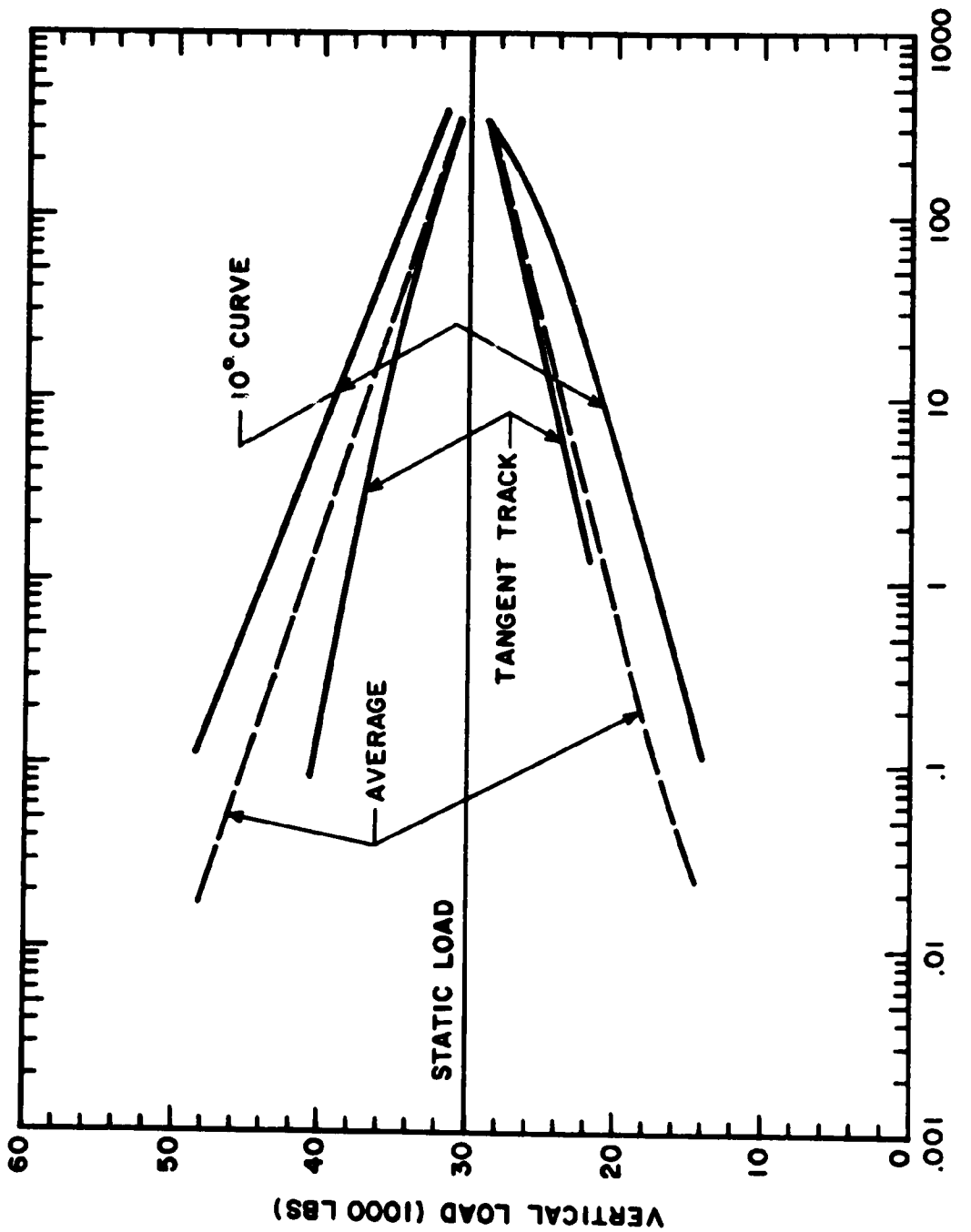

Fig. 4.10 COMPARISON OF TANGENT TRACK AND 10^{o} CURVE VERTICAL SF/BA LOAD SPECTRA WITH AVERAGE SPECTRUM AT 35 MPH

Traversal of a turnout also leads to the exitation of significant cyclic loads. This is indicated in Fig. 4.11 where a load spectrum curve is developed on the basis of cyclic loads per traversal of a turnout. The data are based on 68 load cell records from 34 test runs traversing the Platea turnout. The dashed line on this figure indicates the expected spectrum for the length of track included in the turnout segment (370 ft) based upon the average data for the entire test run (Fig. 4.1).

4.1.10 Short Wheelbase Car

The SF/BA load spectrum developed for a short wheelbase car (20 ft-6 in. truck centers) equipped with BARBER S-2 trucks is illustrated in Fig. 4.12. It shows that this car had a vertical spectrum less severe than the average. The data are based on four load cell records from a single test run.

4.1.11 Roll Control Device

Figure 4.13 compares the average SF/BA load spectrum with the results from eight load cell records obtained on two test runs of a BUCKEYE truck equipped with a car-body roll control device. The data indicate that the use of this device reduces the intensity of the vertical load spectrum. This would be expected in view of the reduced car-body roll motions.

4.1.12 Elastomeric Pads

Figure 4.14 shows a comparison of the average SF/BA load spectrum with results from a truck equipped with elastomeric pads providing flexibility for lateral motion between the side frame pedestals and the roller bearing adapters. The spectrum represents results from a single test run (four load cell records) and indicates a substantial reduction in load intensity. This test was conducted at 35 mph and does not give a clear indication of the performance of the device at other speeds. There have been reports that the use of these elastomeric pads provides beneficial results only in the lower speed ranges since the increased flexibility allows the development of severe lateral oscillations at higher speeds.

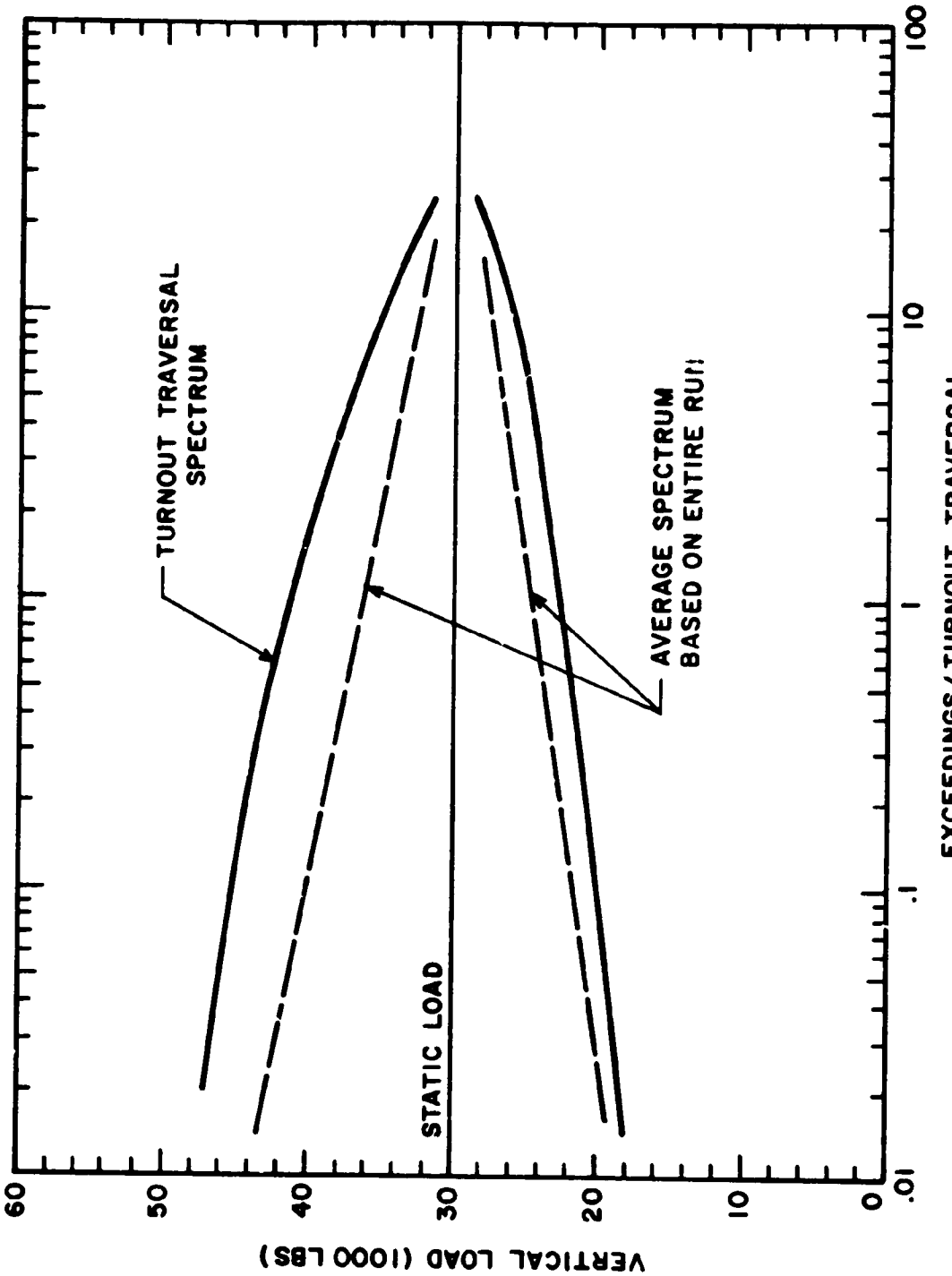

Fig. 4.11 AVERAGE VERTICAL SF/BA LOAD SPECTRUM FOR TRAVERSAL OF TURNOUT

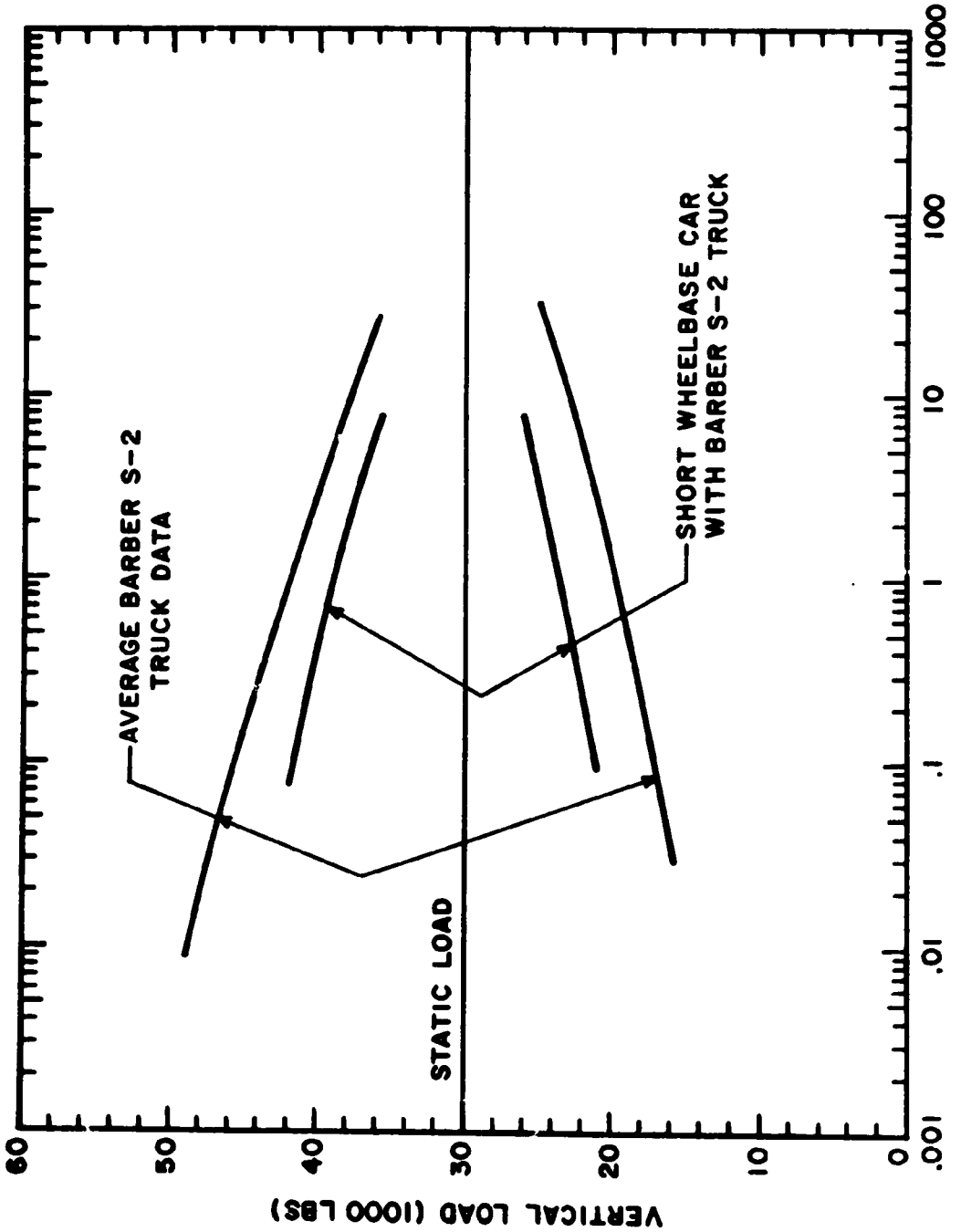

Fig. 4.12 COMPARISON OF VERTICAL SF/BA LOAD SPECTRUM FOR CAR WITH 20 FT-6 INCH TRUCK CENTERS WITH AVERAGE SPECTRUM AT 35 MPH

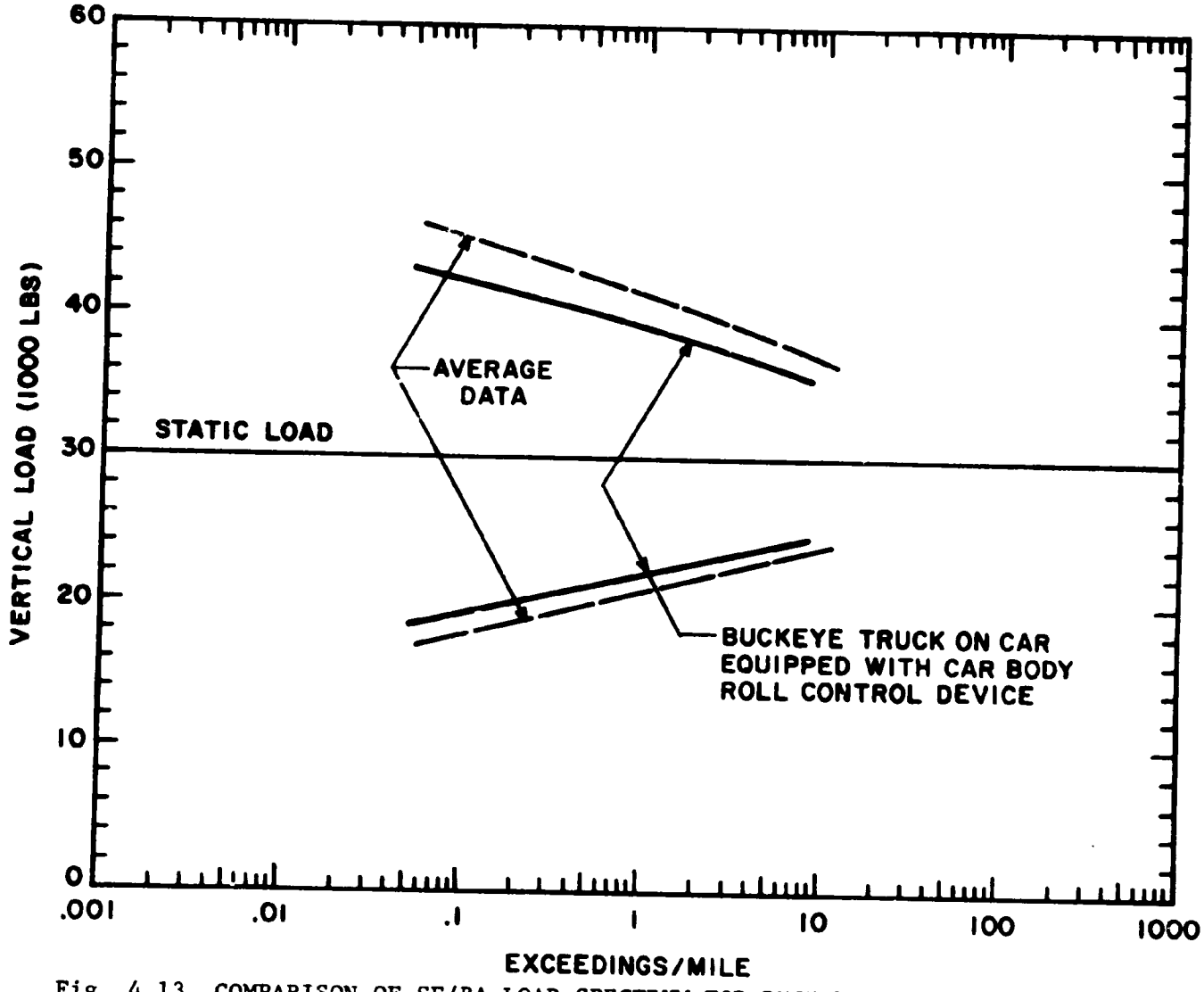

Fig. 4.13 COMPARISON OF SF/BA LOAD SPECTRUM FOR BUCKEYE TRUCK EQUIPPED WITH ROLL CONTROL DEVICE WITH AVERAGE SPECTRUM AT 35 MPH

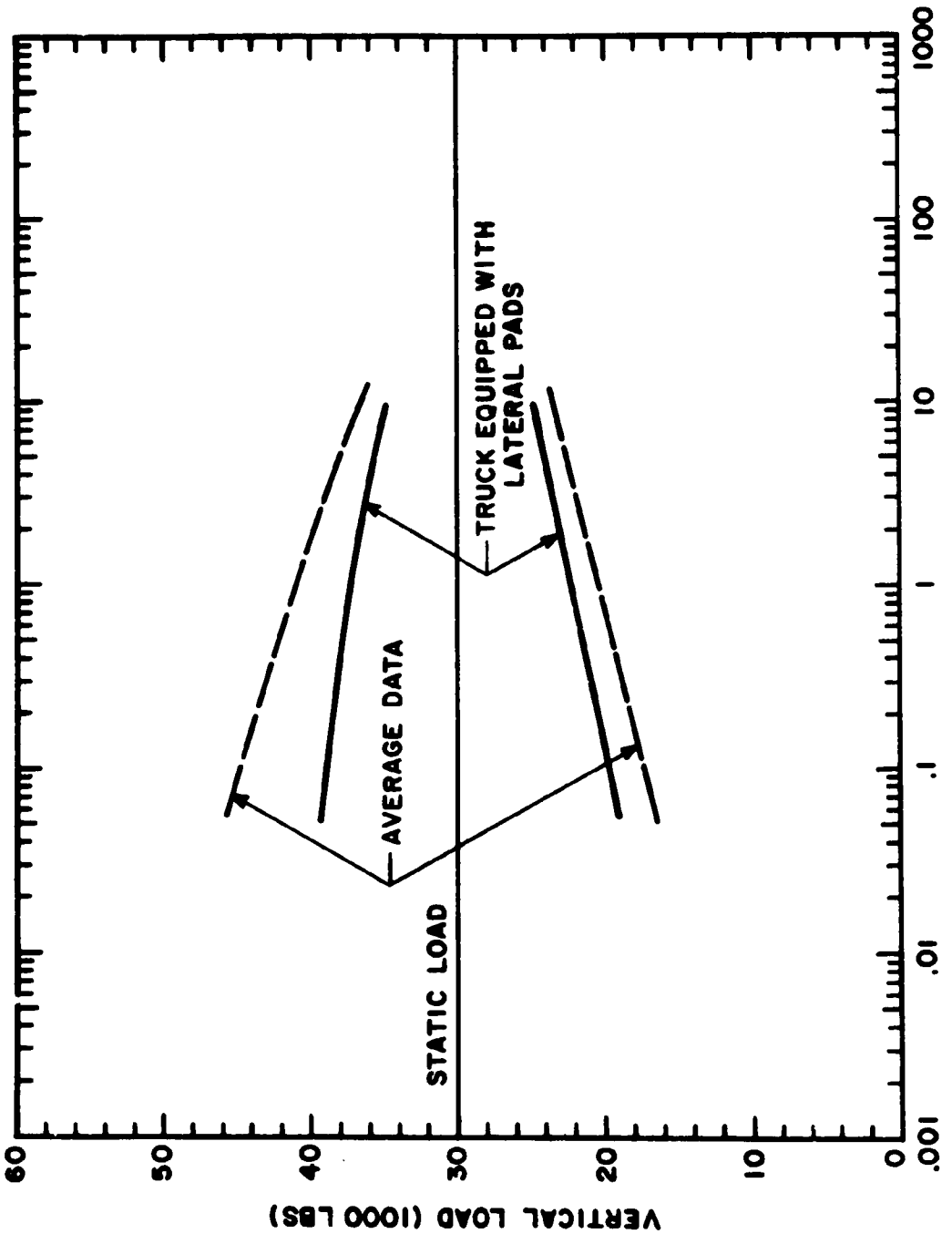

Fig. 4.14 COMPARISON OF SF/BA LOAD SPECTRUM FOR TRUCK EQUIPPED WITH LATERAL ELASTOMERIC PADS WITH AVERAGE SPECTRUM AT 35 MPH

4.1.13 Spectra for Rotating Components

As previously indicated it is necessary to develop a load spectrum for components, such as the bearings, wheels and axles, which presents the load intensity as a function of the number of revolutions for which various load levels are exceeded. For these components the number of revolutions of operation at an elevated load are more important in determining fatigue life than the number of times an elevated load is attained. The relationship between the spectra on an exceeding/mile basis and that on a revolution/mile basis can be visualized by considering the occurrence of four pulses each 1/4-wheel revolution in duration exceeding a specified load in a one-mile section. These four pulses would be recorded as four exceedings/mile but as only one revolution/mile. The average curve (Fig. 4.1) for the SF/BA_r load spectrum presented in this format is shown in Fig. 4.15.

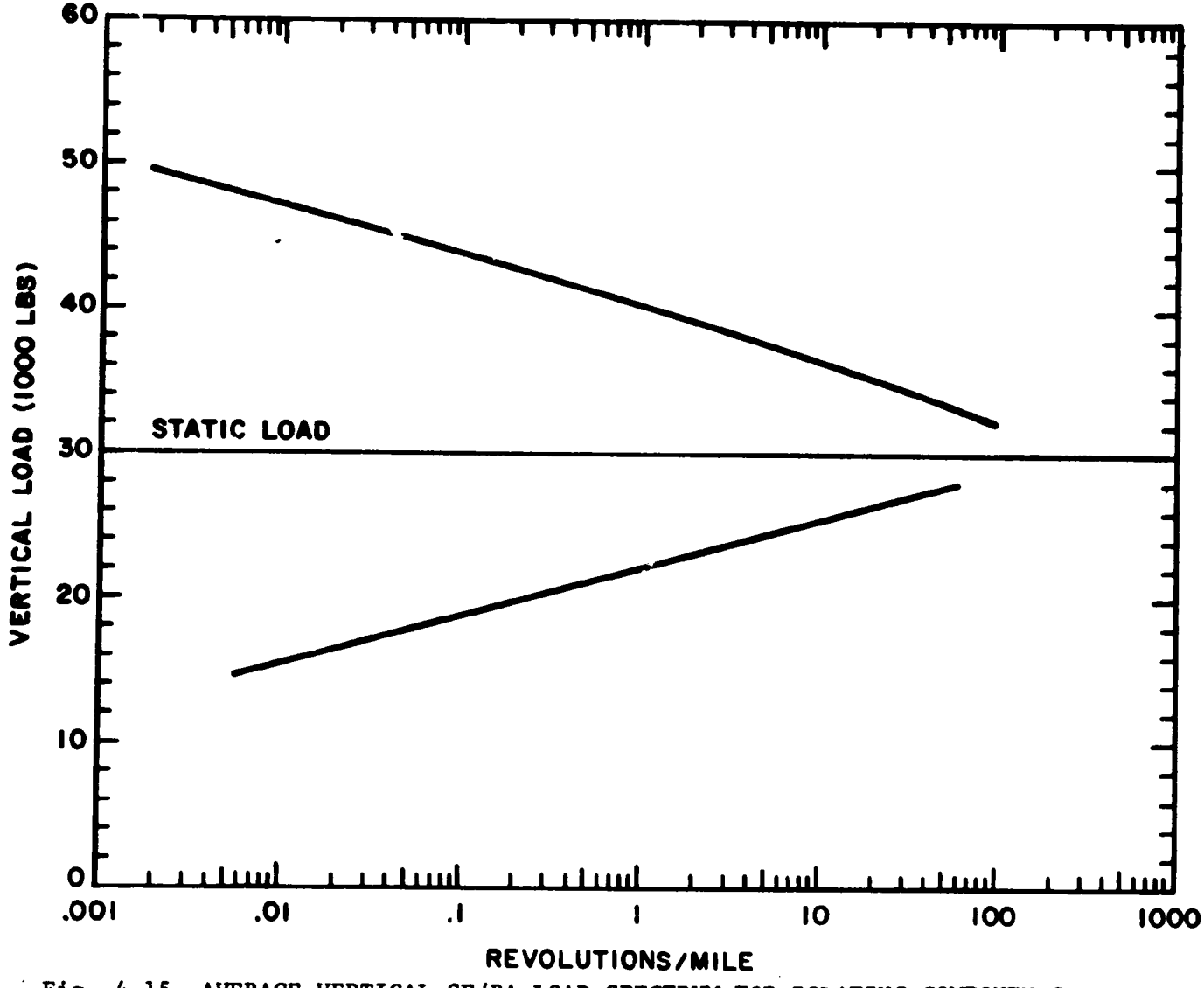

Fig. 4.15 AVERAGE VERTICAL SF/BA LOAD SPECTRUM FOR ROTATING COMPONENTS WITH REFERENCE TO NUMBER OF REVOLUTIONS LOAD LEVEL IS EXCEEDED

4.2 Lateral Loads at the Wheel/Rail Interface

Lateral loads at the wheel/rail interface lead to alternating stresses in the wheel plate and, together with the vertical loads, produce alternating stresses in the axle. Net lateral loads on a wheel/axle set result in lateral bearing loads and tend to distort the rectangular configuration of the truck. This causes lateral loads on the side frame and twist loads on the bolster and side frame (net lateral load data are presented in Section 4.4).

4.2.1 Tangent Track Operation

When operating on tangent track the lateral load at the wheel/rail interface is characterized by an alternating load with the major loads directed toward the flange, but with some transient loads directed away from the flange. This is due to the normal side-to-side hunting motion of the wheel/axle set. In addition the lateral wheel load data indicate a steady component of load acting toward the flange on tangent track depending on the particular operating conditions existing at the time of the test. The analysis of 54 wheel load records, for example, indicates an overall average of 2000 lbs acting toward the flange. The data also indicate considerable variability in this load as shown by a 4100 lbs standard deviation about the average value. Tests made with worn wheels indicated both a larger average load, 3800 lbs, as well as a greater spread in the data, as shown by a standard deviation of 6500 lbs. The worn wheel data are the result of the analysis of 14 wheel load records.

4.2.2 Curved Track

Test results show that the steady component of lateral load acting toward the flange at the wheel/rail interface is a function of the degree of curvature. Figures 4.16 through 4.19 show the average loads acting toward the flange at the four wheel positions on the truck as a function of the degree of curvature for a car with 40 ft-9 in. truck centers. These data were obtained using both BARBER S-2 and RIDE CONTROL trucks on 13 test runs where there were no unusual factors influencing the lateral wheel load environment. The spread of the data is indicated by a plot of the plus

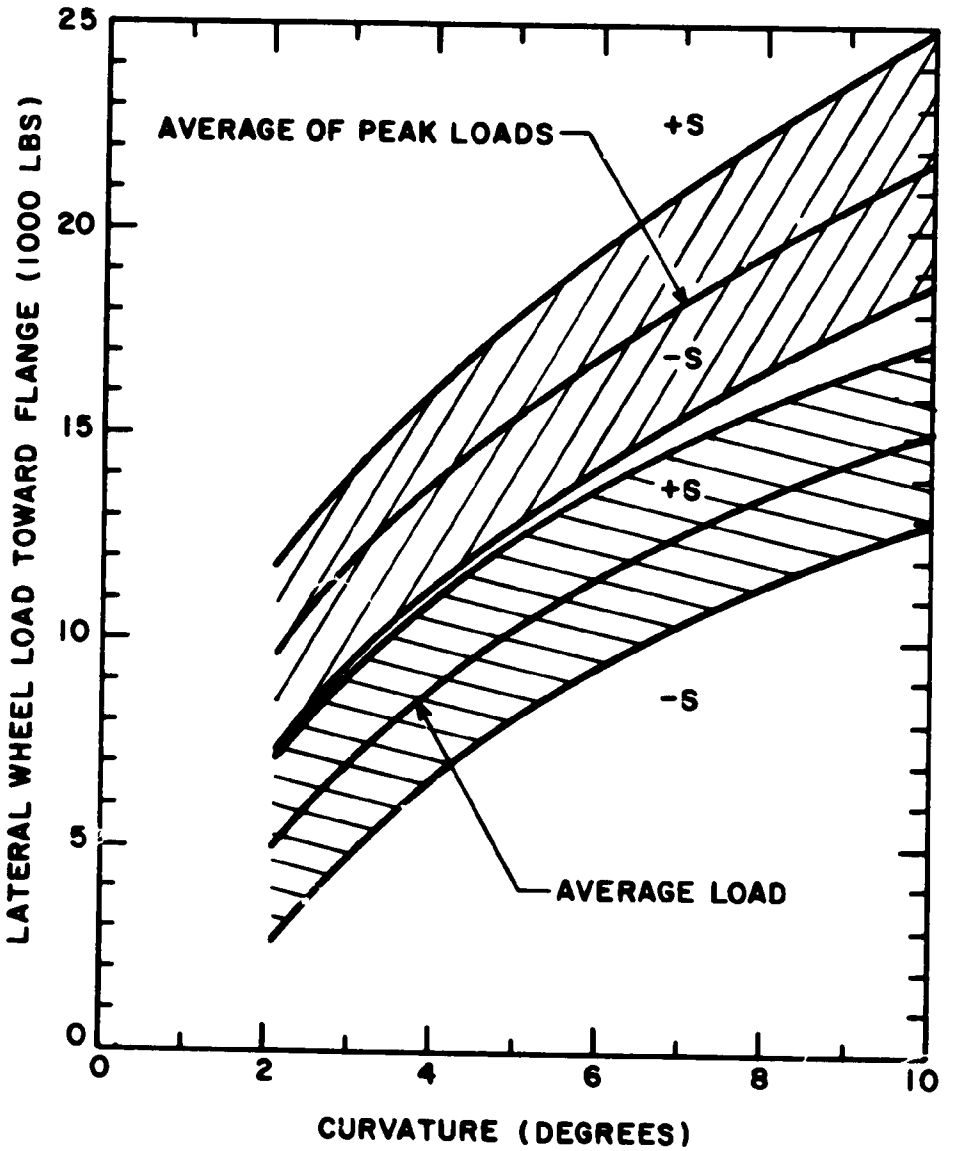

Fig. 4.16 LATERAL WHEEL LOADS ON LEAD AXLE, HIGH RAIL WITH NORMAL TRUCK CONDITIONS AT 35 MPH

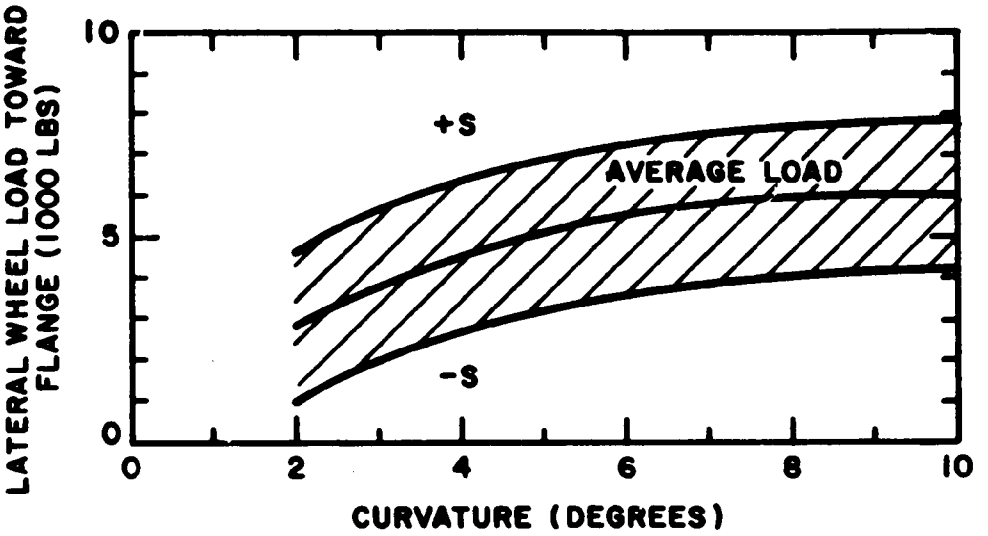

Fig. 4.17 AVERAGE LATERAL WHEEL LOADS ON LEAD AXLE, LOW RAIL WITH NORMAL TRUCK CONDITIONS AT 35 MPH

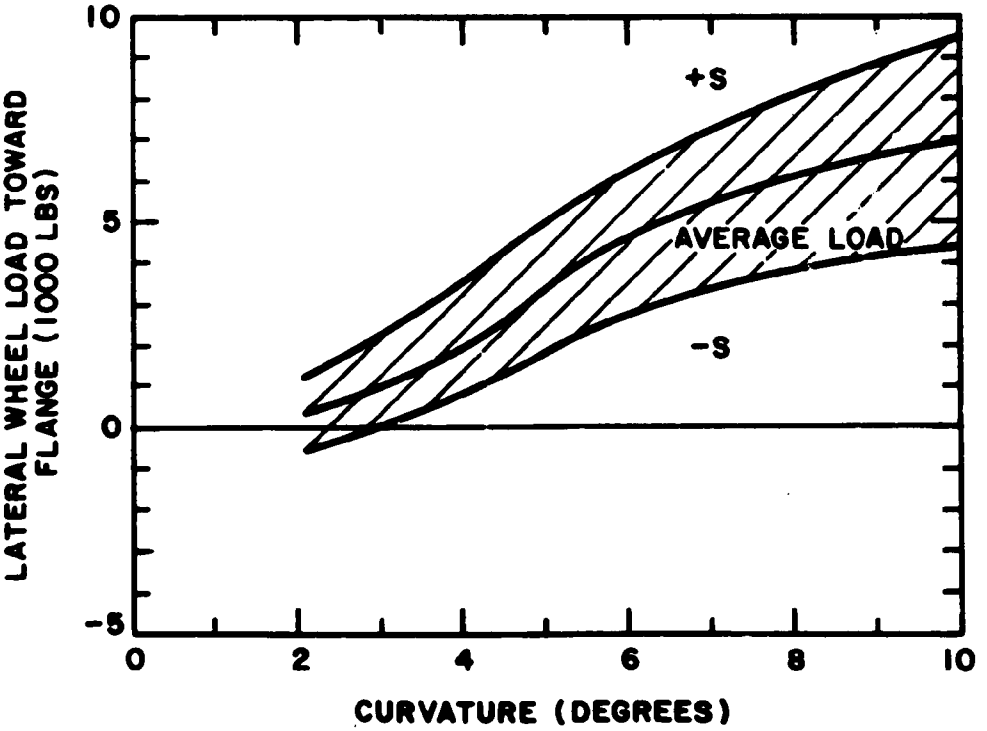

Fig. 4.18 AVERAGE LATERAL WHEEL LOADS ON TRAIL AXLE, HIGH RAIL WITH NORMAL TRUCK CONDITIONS AT 35 MPH

and minus one standard deviation curves. The highest loads were measured on the lead axle at the high rail. The average peak lateral load as well as its plus and minus one standard deviation curves are shown in Fig. 4.16 for this position. (For a definition of the peak and average load while traversing curve track see Fig. 2.5.) The lateral wheel load at the low rail of the lead axle increases with curvature, but the rate of increase decreases with increasing curvature. The lateral wheel load at the high rail of the trail axle is at a low level for curves of less than 4 degrees, increases in the range from 4 to 6 degrees, and remains almost constant above 6 degrees. This shows the tendency of the trailing axle to run against the high rail when the curvature exceeds approximately 4 degrees. The lateral wheel load at the low rail of the trail axle is maintained at a relatively low force level independent of curvature. These data are developed for a speed of 35 mph which is slightly over the equilibrium speed for the superelevation of these curves.

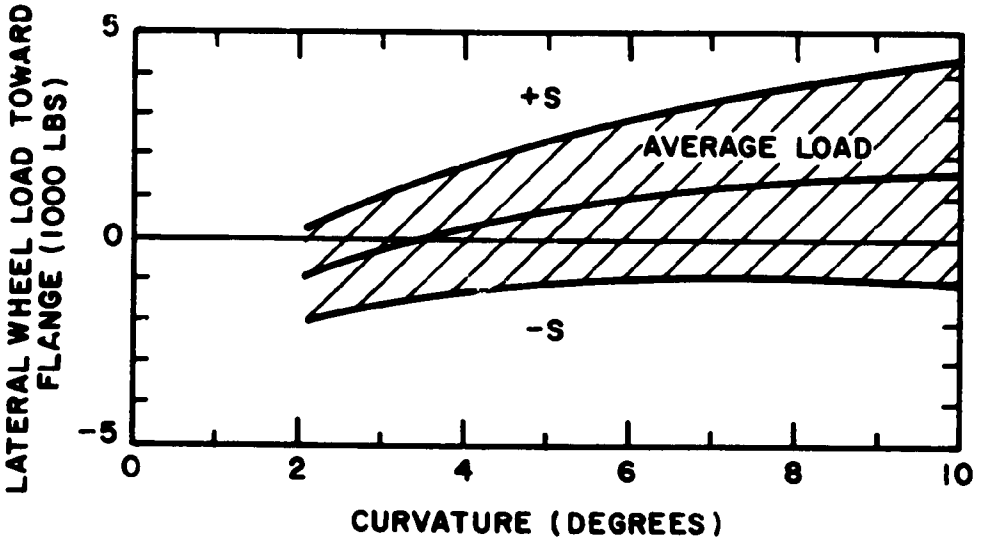

Fig. 4.19 AVERAGE LATERAL WHEEL LOADS ON TRAIL AXLE, LOW RAIL WITH NORMAL TRUCK CONDITIONS AT 35 MPH

The effect of speed on the lateral wheel load is indicated by Figs. 4.20 through 4.22. Figure 4.20 shows the average lateral wheel loads at the four wheel positions as a function of curvature for a speed of 20 mph and the average peak load at the high rail position on the lead axle. Although there is considerable scatter in the data the same trends indicated for 35 mph are shown except that force levels are lower, particularly for the sharper curves. These data are based on analysis of wheel loads on three test runs. Figure 4.21 shows data from one run at a speed of 27.5 mph. The lateral wheel load relationship with curvature is approximately the same as for the 35 mph data. Figure 4.22 shows data from one run at a speed of 10 mph. The force data again generally indicate an increasing trend with curvature, but in this case the low rail loads are generally higher than the high rail loads. This is due to the traversal of the curve at less than the equilibrium speed for the superelevation of the high rail so that the truck tends to run against the low rail.

The lateral wheel load data from tests with worn wheels (see Appendix C) show greater scatter than the tests with new wheel contours. Figure 4.23 shows the lateral wheel load data obtained in four test runs and indicates a trend of increasing load with curvature as previously noted for new wheel contours.

Car length is a major parameter influercing lateral loads at the wheel/rail interface, the lateral loads increasing with the truck center distance. This is evident from Fig. 4.24 which shows lateral wheel load data for a 20 ft-6 in. truck center distance car.

The use of a "free-wheeling" wheel/axle set, where the wheels are free to rotate independently of each other, results in lower lateral wheel load forces when traversing curved track. The data from one test run is presented in Table 4.7. It indicates lead axle average force levels varying from 5,000 lbs toward the flange to 6,000 lbs away from the flange, peak loads toward the

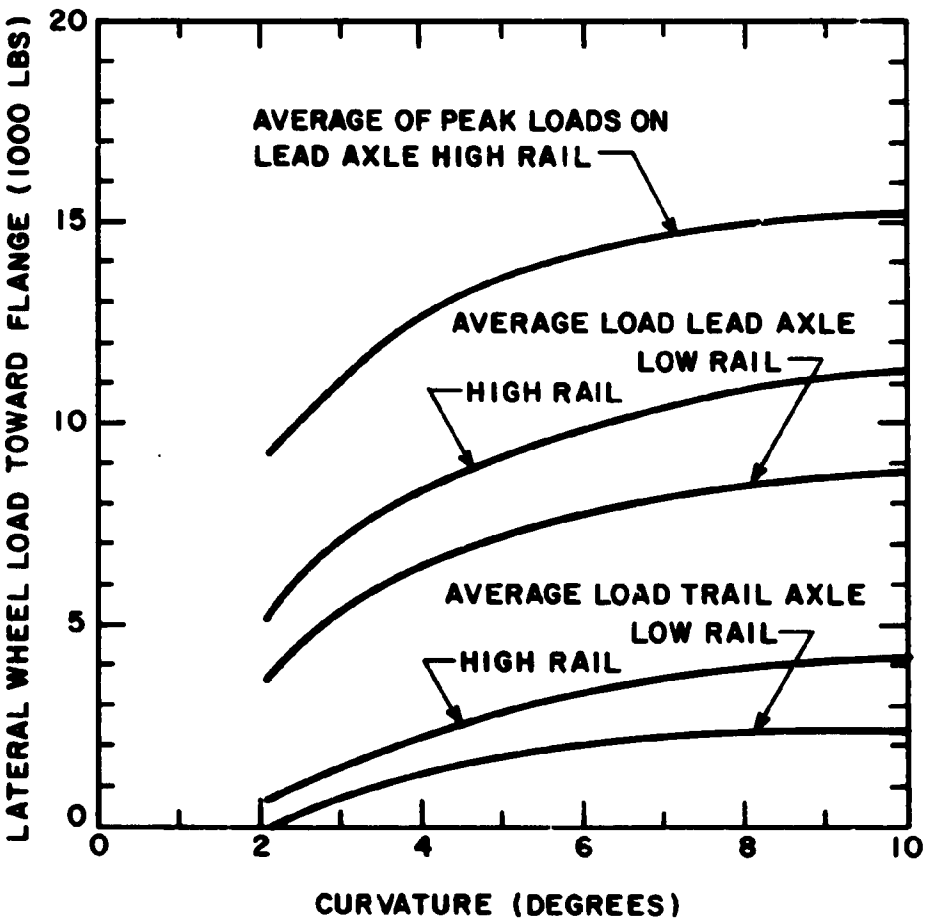

Fig. 4.20 LATERAL WHEEL LOADS AT 20 MPH

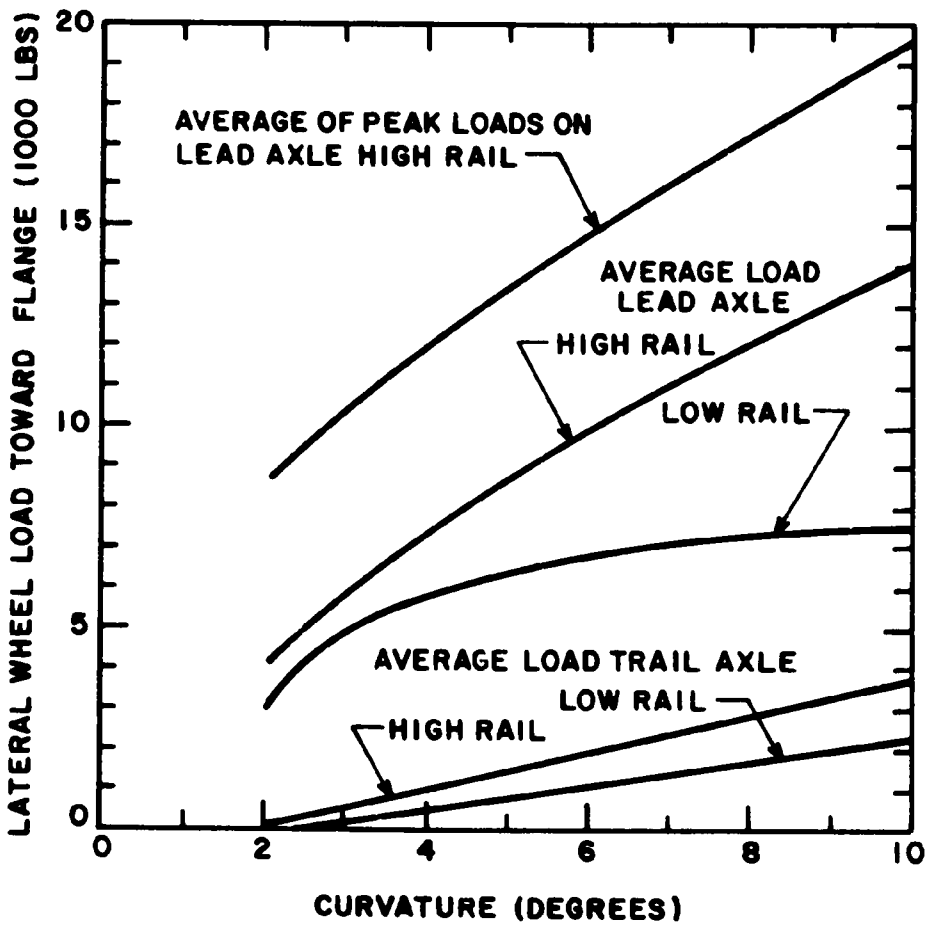

Fig. 4.21 LATERAL WHEEL LOADS AT 27.5 MPH

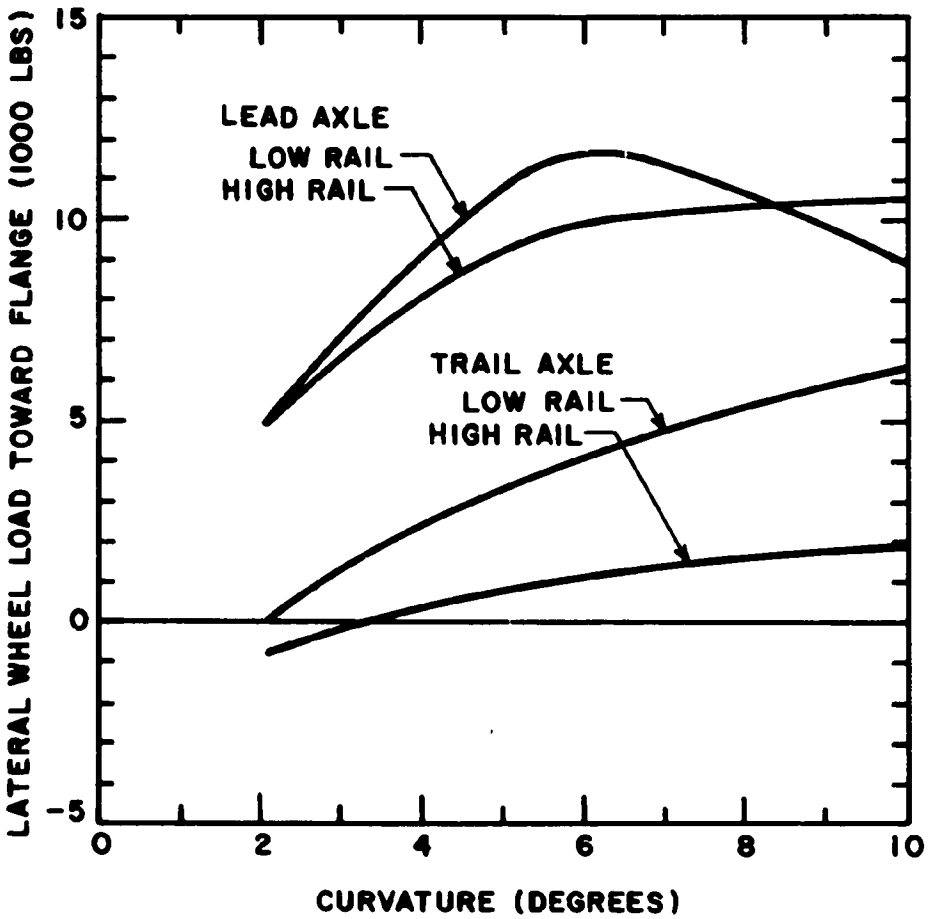

Fig. 4.22 AVERAGE LATERAL WHEEL LOADS AT 10 MPH

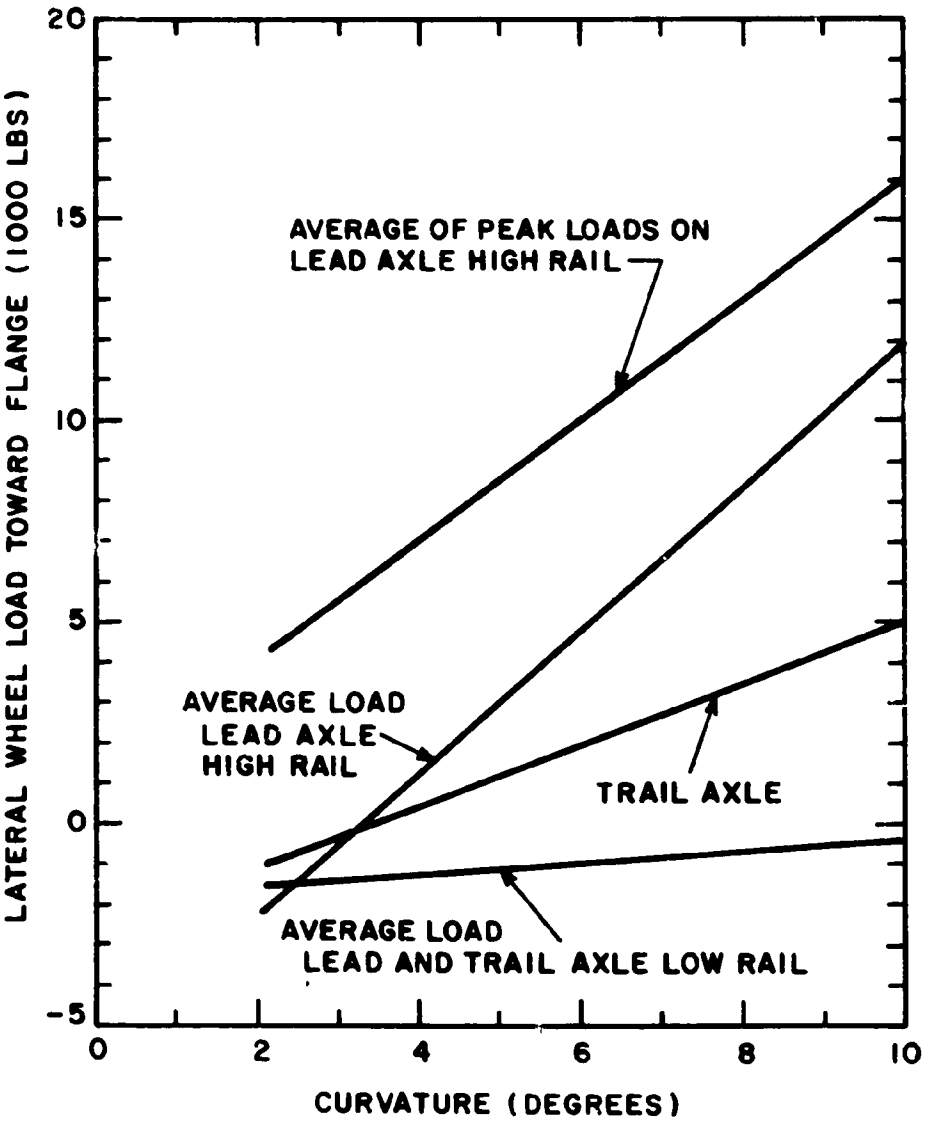

Fig. 4.23 LATERAL WHEEL LOADS WITH WORN WHEELS AT 35 MPH

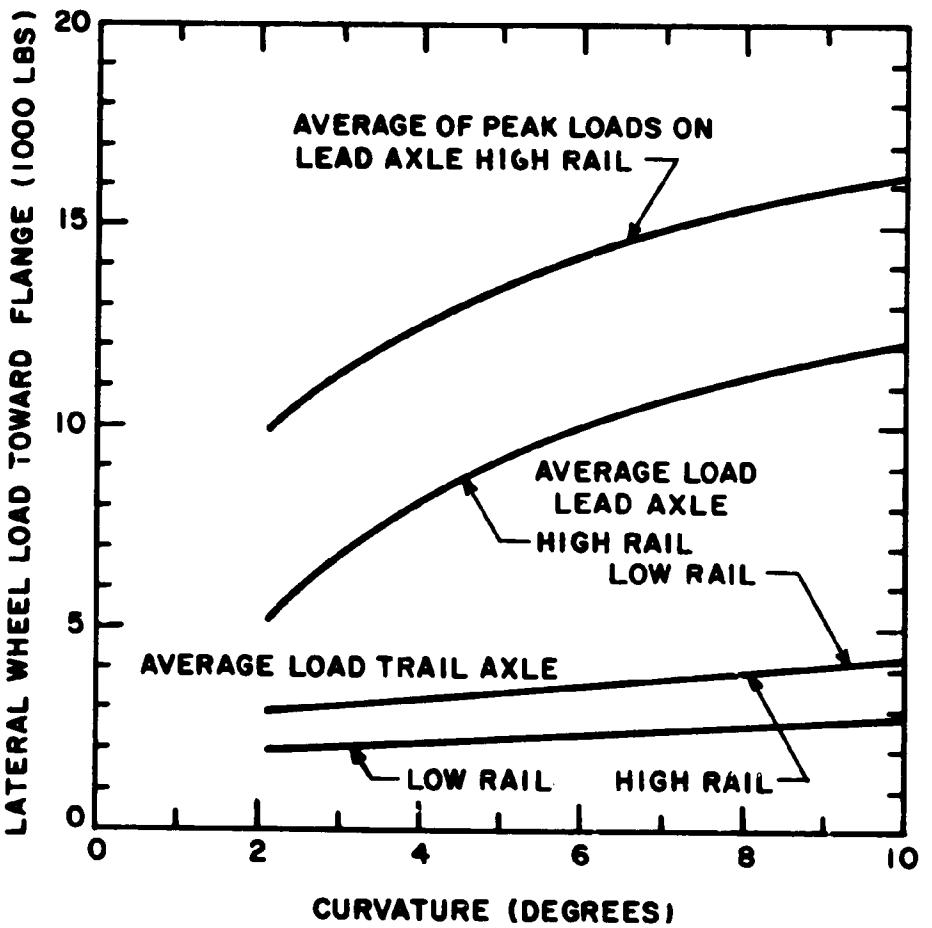

Fig. 4.24 LATERAL WHEEL LOADS WITH SHORT WHEELBASE CAR (20 FT-6 INCH TRUCK CENTERS) AT 35 MPH

TABLE 4.7 LATERAL WHEEL LOAD FOR FREE-WHEELING TRUCK

Curvature	Lateral Wheel Load Directed Toward Flange (1000 lbs), (Negative Load Direction Away from Flange)				
	Average Load*				Peak Load* Lead Axle High Rail
	Lead Axle		Trail Axle		
	High Rail	Low Rail	High Rail	Low Rail	
2°6'	4	2	1	0	7
2°58'	4	3	0	0	11
3°	-6	-6	0	1	3
3°	-6	-6	0	0	-2
3°42'	-2	-2	1	0	4
4°24'	-6	-6	0	1	4
4°36'	-6	-4	1	0	3
5°30'	3	1	2	0	8
6°5'	0	3	0	1	5
9°	4	5	1	1	8
10°	-4	-5	2	-2	6

*Note: Lateral loads are given with reference to the average lateral load on tangent track. These average loads were 11,000 lbs directed toward the flange on both wheels of the lead axle and 3,000 lbs directed toward the flange on both wheels of the trail axle.

flange reaching 11,000 lbs. However, there is no correlation of these force levels with curvature such as shown for other truck conditions. The wheels used in these tests had a new wheel contour. Forces on the wheels on the trailing axle were less than 2,000 lbs. When this truck was operating on tangent track the lateral wheel loads acting on the lead axle varied over a range of $\pm$ 4,000 lbs about the mean value indicating a tendency for the truck to run alternately against one rail or the other.

The use of an auxiliary car-body roll control device can lead to severe lateral wheel loads when traversing curved track. This is shown by plots of average data from two test runs in Fig. 4.25. The high loads would be expected in view of the nature of the device which offered greater resistance to truck swiveling while damping the roll motion of the car.

4.2.3 Lateral Wheel Load Spectra

The lateral wheel load data can be utilized to develop a load spectra with reference to wheel plate fatigue recognizing that a steady lateral load will produce one cycle of stress in the wheel per wheel revolution. The spectra* are presented as a function of "revolutions/mile" and therefore the plotted curve denotes, the number of wheel revolutions per mile that a given lateral wheel load is exceeded. The spectra presented in this section are developed from an analysis of selected lead-axle test run data over the B&LE test track and therefore represent the effects of the distribution of tangent and curved track segments found in this section of track. Figure 4.26 shows the average spectrum from 10 test runs where there were no special conditions influencing the lateral wheel load. The wheel tread conformed to the standard AAR contour for these cases. The spread of the data making up the average curve is illustrated by showing plus and minus one standard deviation.

---

*See Appendix B for further details on the method of deriving load spectra of the lateral wheel/rail load.

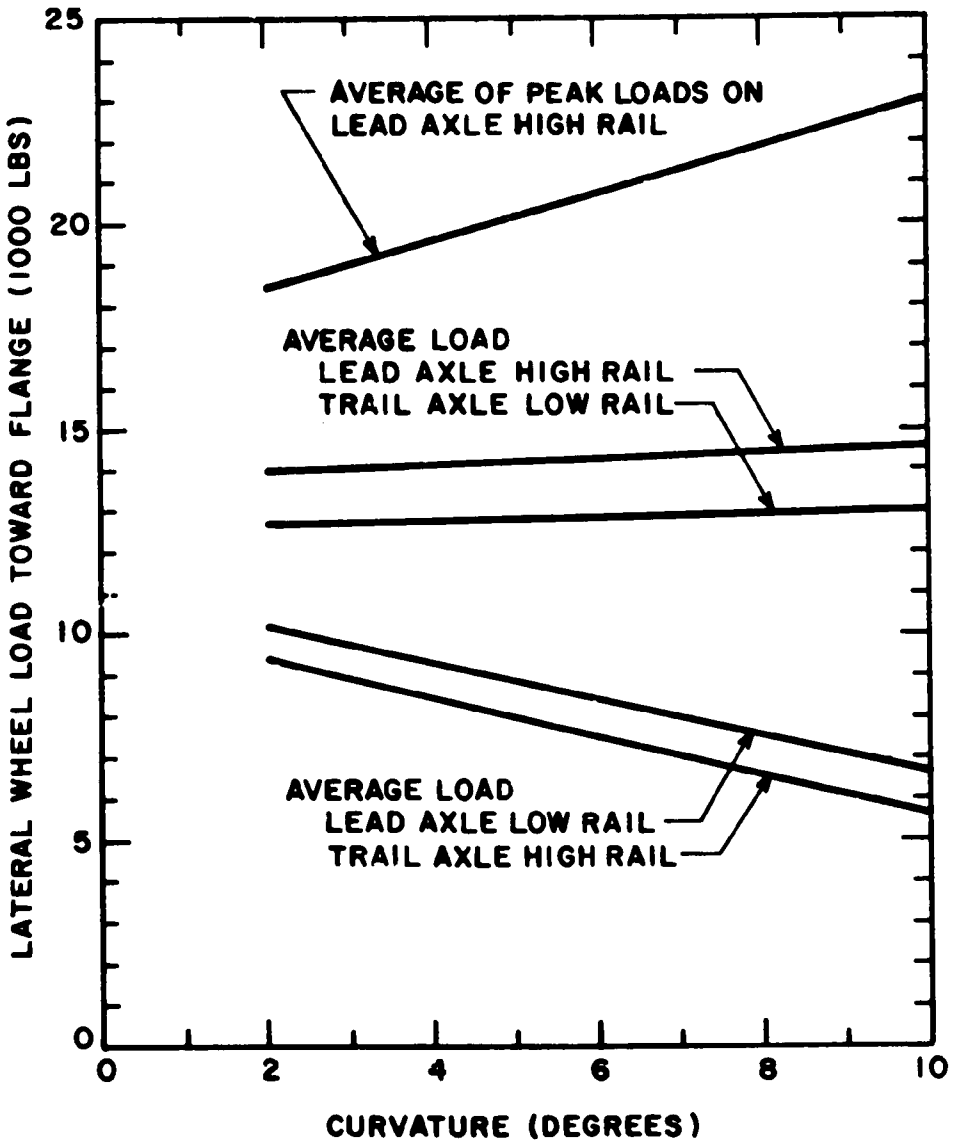

Fig. 4.25 LATERAL WHEEL LOADS WITH AUXILIARY CAR BODY ROLL CONTROL DEVICE AT 35 MPH

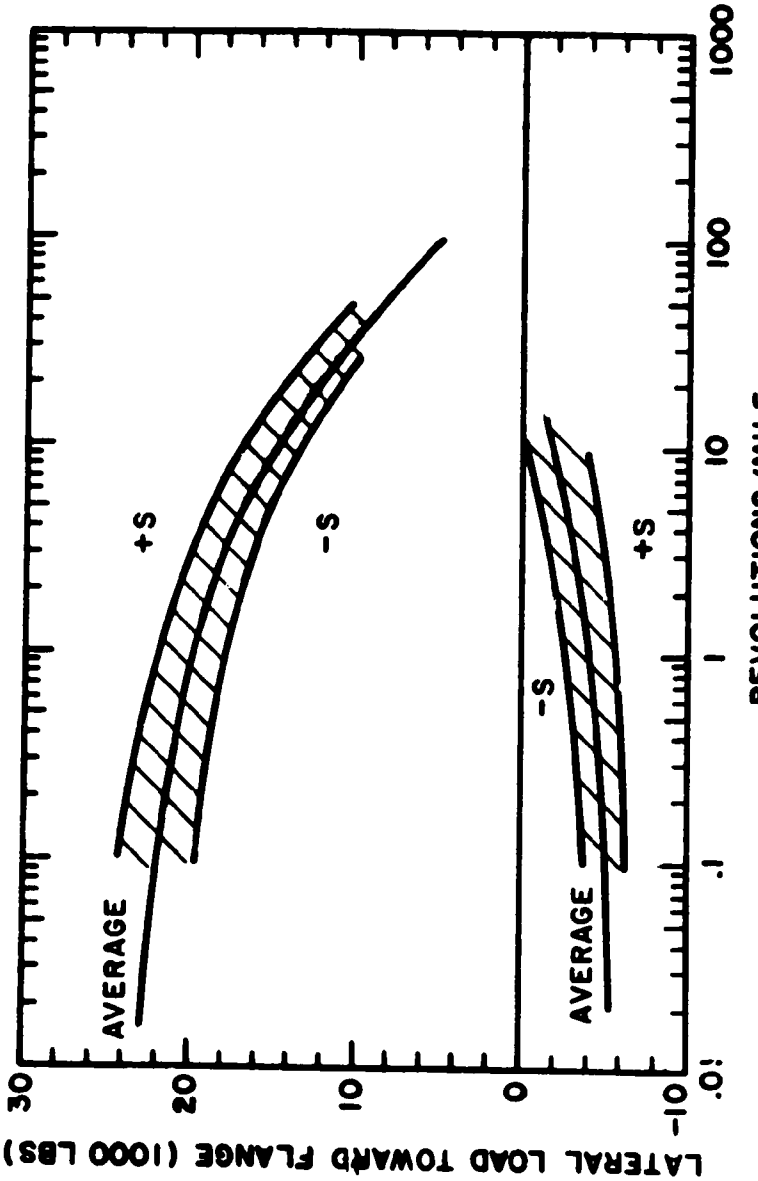

Fig. 4.26 AVERAGE LEAD AXLE LATERAL WHEEL LOAD SPECTRUM AT 35 MPH

Figure 4.27 shows the spectrum associated with the operation of the short wheelbase (20 ft-6 in. truck center distance) car.

Figure 4.28 compares load spectra from tangent track operation with the average data. Figure 4.29 compares data from operations over a 2° 58' curve with the average data. Note the increase in severity of the forces acting on the wheel at the high rail in comparison to the low rail spectrum. Figure 4.30 compares similar data for operation on a 10 degree curve.*

Figure 4.31 compares an average spectrum from data obtained with worn wheels with the average spectrum for wheels with the standard AAR contour. The tendency of a wheel/axle set with worn wheels to ride with one wheel against the rail results in an increase in the frequency of lower level loads acting toward the flange. There is a corresponding increase in the frequency of loads acting away from the flange on the opposite wheel. The worn wheel spectrum represents the average of both wheel loads.

Figure 4.32 compares the spectrum for a truck equipped with an auxiliary car-body roll control device with the average curve. The increased resistance to truck swiveling provided by this device leads to the increase in the level of the load spectrum.

---

*The load spectra in Figs. 4.29 and 4.30 are related to the lateral wheel load data in Figs. 4.16 and 4.17 in the following way. The "peak" load shown in Fig. 4.16 represents the maximum load acting for approxi. tely 1/2 wheel revolution. For the 2° 58' and 10° curves, which were approximately 1/3 and 1/4 miles long, respectively, the peak loads represent a rate of occurrence of from 1-2 revolutions per mile on the spectra. The "average" loads shown in Figs. 4.16 and 4.17 represent a rate of occurrence of from 100-300 revolutions per mile depending on the manner in which the maximum average (quasi-steady) lateral force is attained on the curve (see Fig. 2.5).

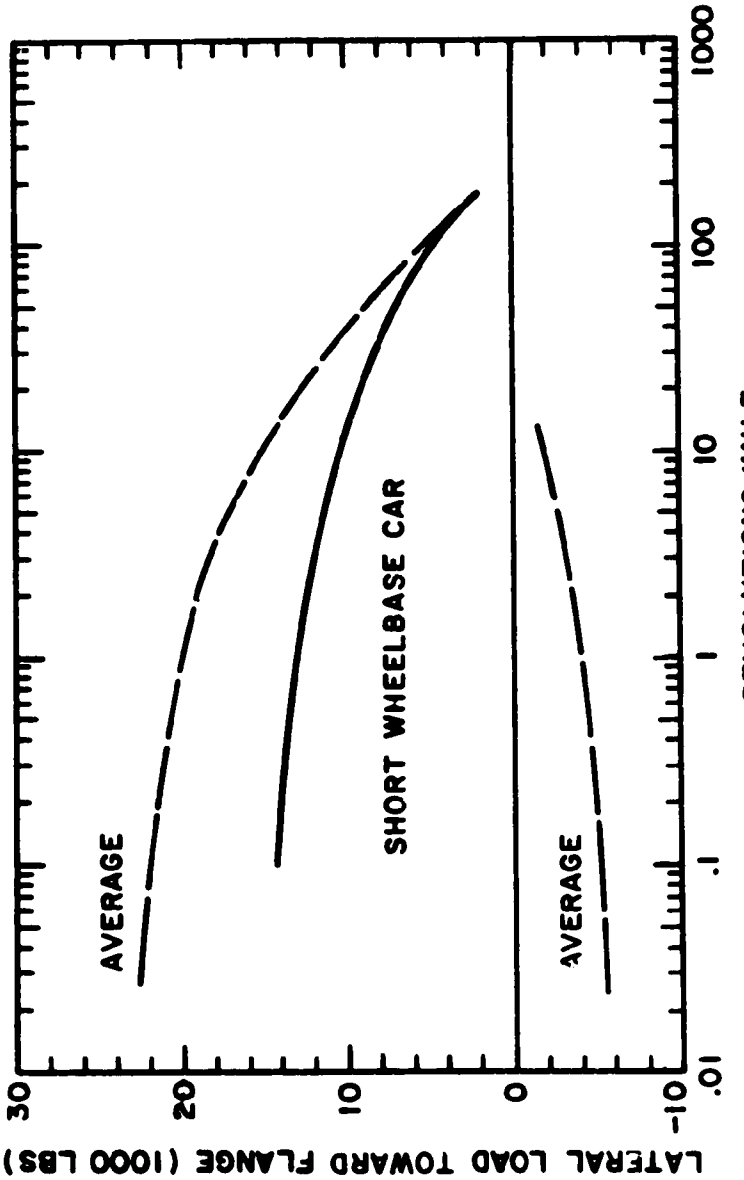

Fig. 4.27 COMPARISON OF AVERAGE LEAD AXLE LATERAL WHEEL LOAD SPECTRUM FOR SHORT WHEELBASE CAR (20 FT-6 INCH TRUCK CENTERS) WITH AVERAGE SPECTRUM AT 35 MPH

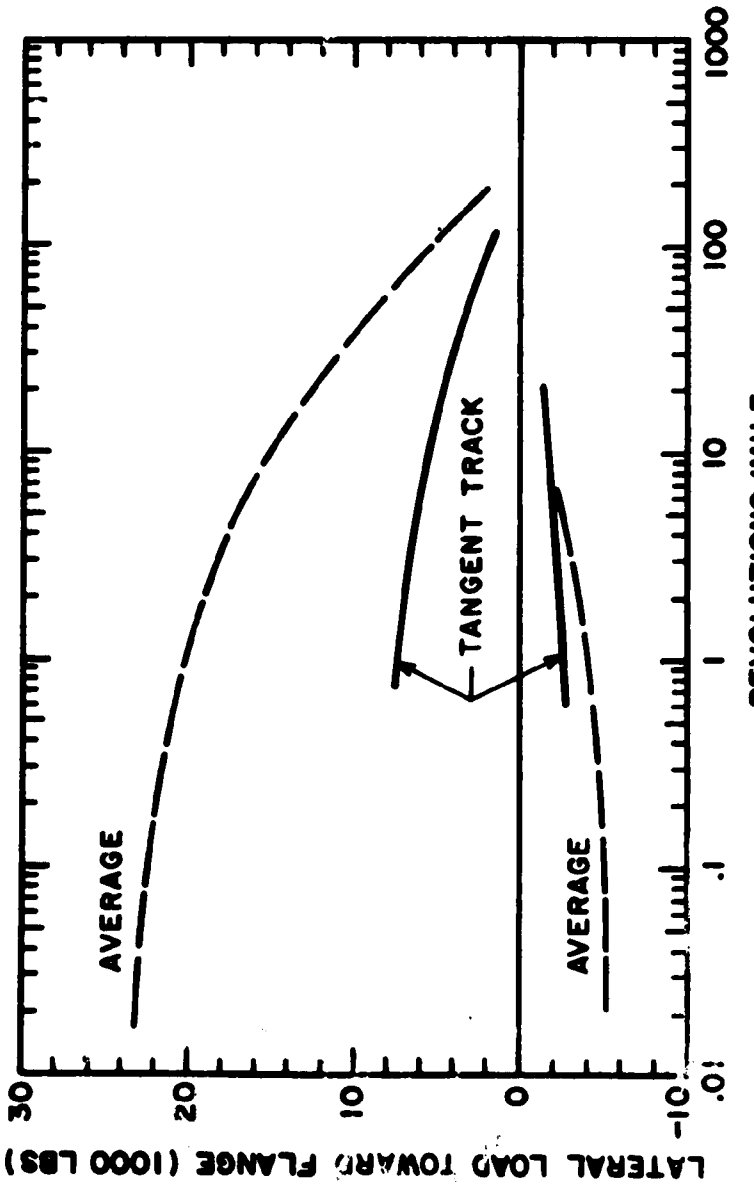

Fig. 4.28 COMPARISON OF TANGENT TRACK LEAD AXLE LATERAL WHEEL LOAD SPECTRUM WITH AVERAGE SPECTRUM AT 35 MPH

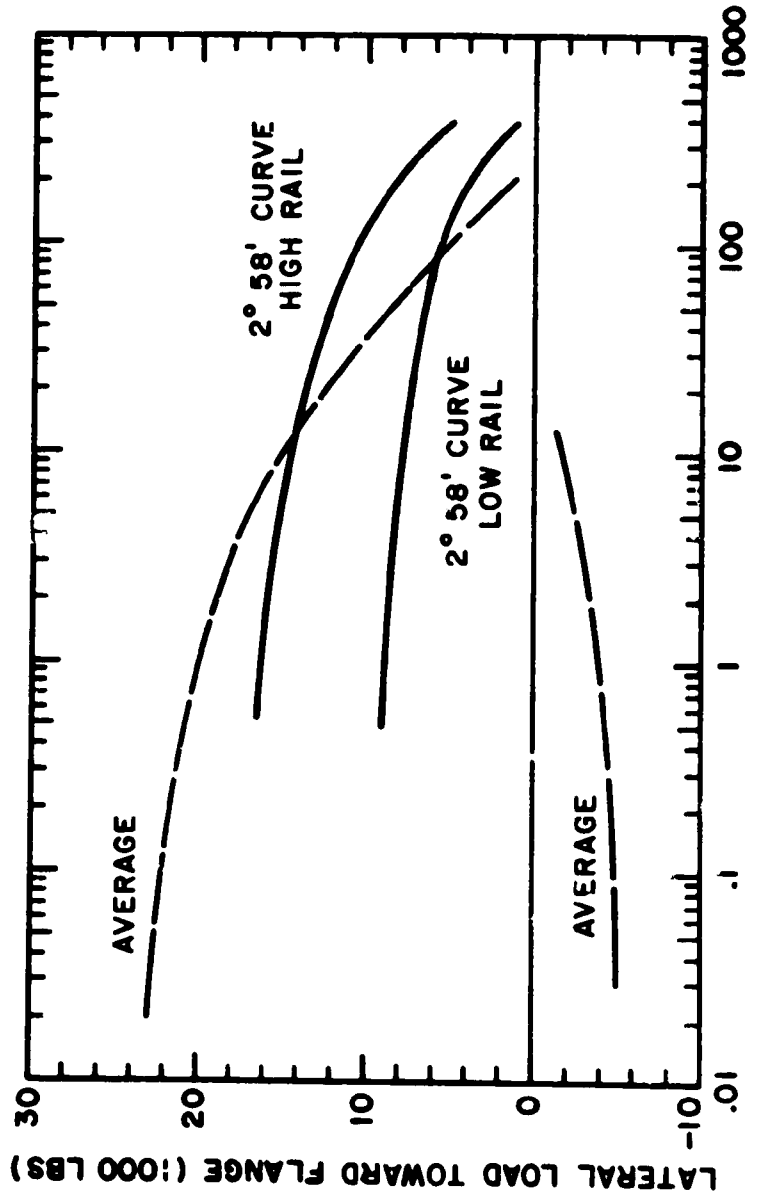

Fig. 4.29 COMPARISON OF $2^{\circ}58'$ CURVE LEAD AXLE LATERAL WHEEL LOAD SPECTRUM WITH AVERAGE SPECTRUM AT 35 MPH

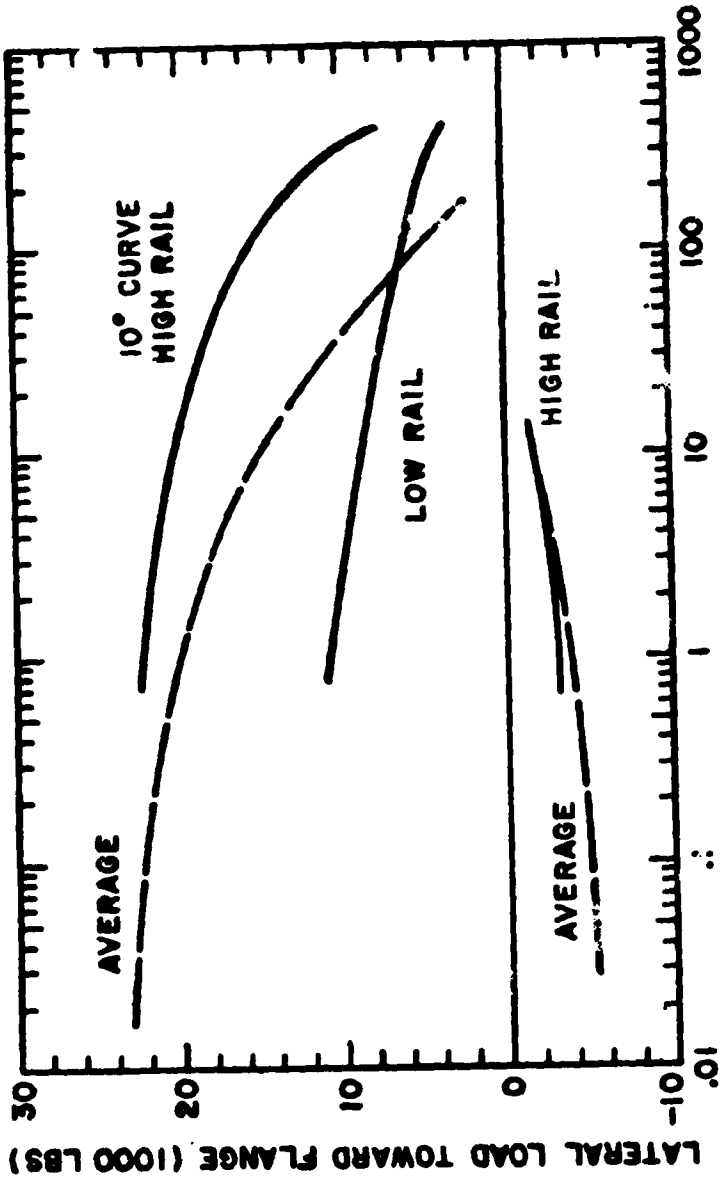

Fig. 4.30 COMPARISON OF 10° CURVE LEAD AXLE LATERAL WHEEL LOAD SPECTRUM WITH AVERAGE SPECTRUM AT 35 MPH

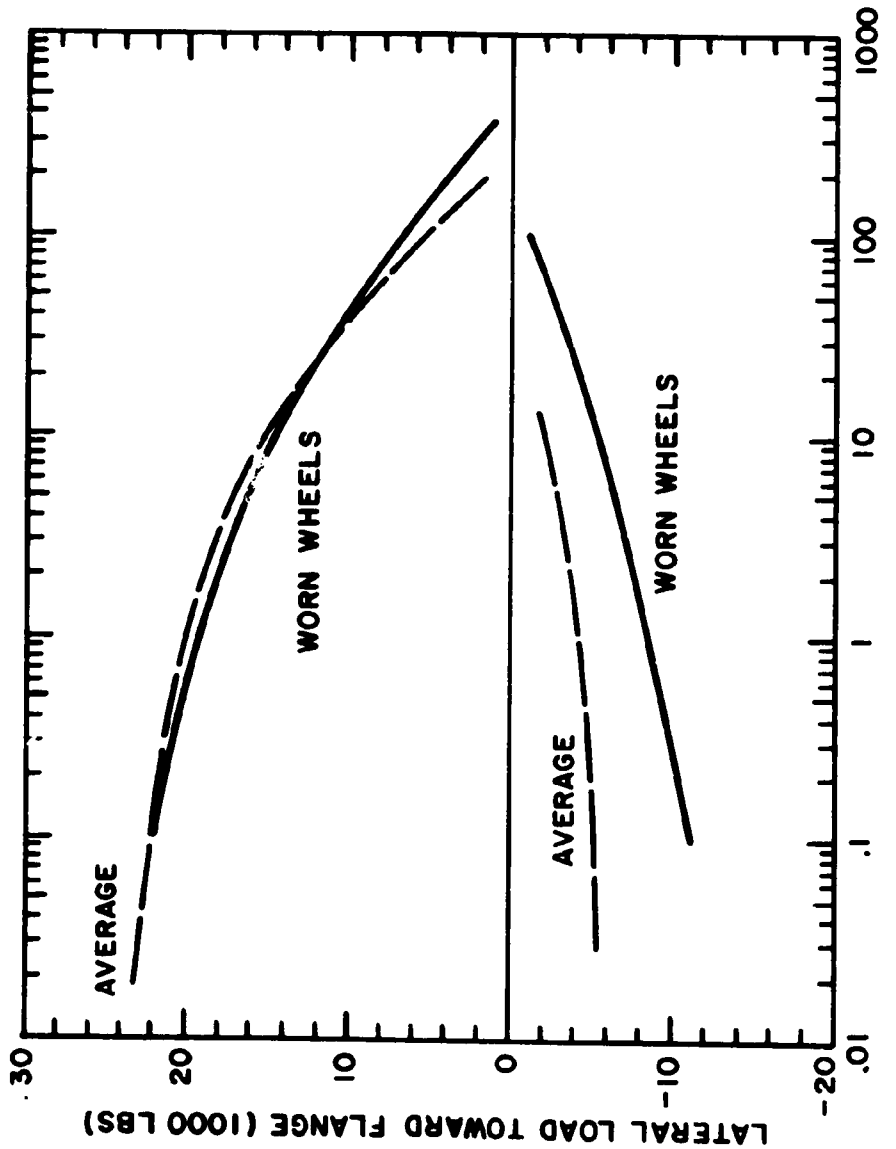

Fig. 4.31 COMPARISON OF "WORN WHEEL" LEAD AXLE LATERAL WHEEL LOAD SPECTRUM WITH AVERAGE SPECTRUM AT 35 MPH

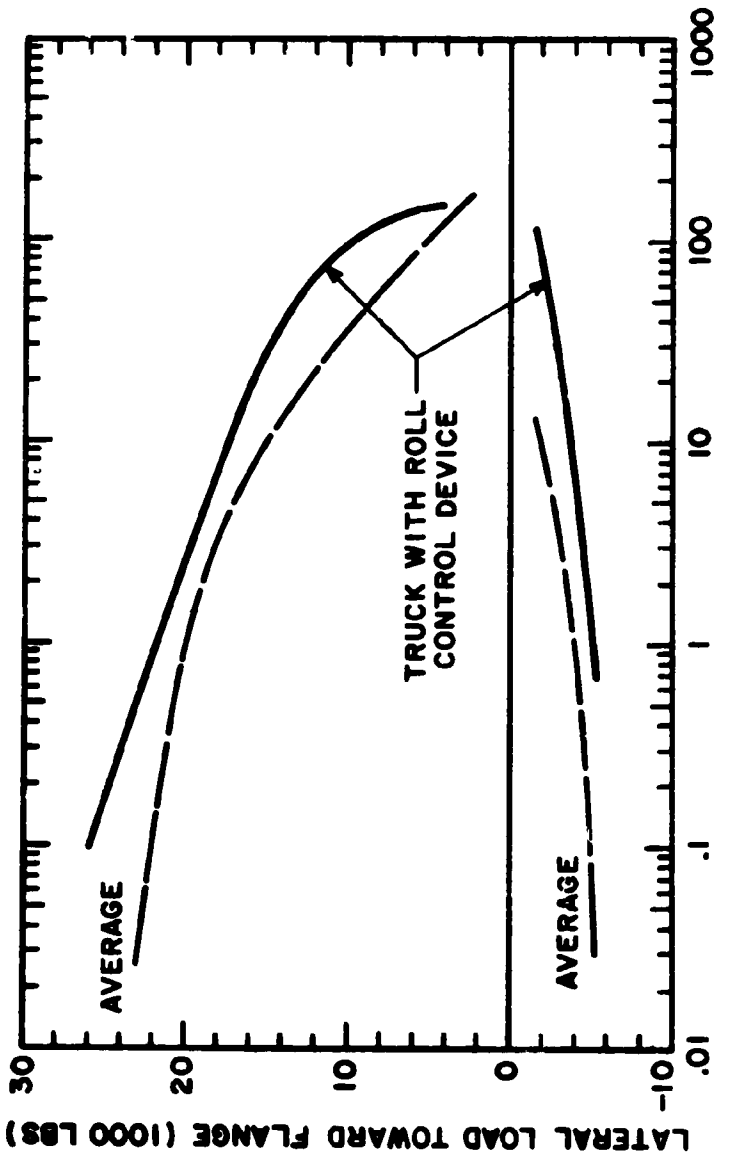

Fig. 4.32 COMPARISON OF LEAD AXLE LATERAL WHEEL LOAD SPECTRUM FOR TRUCK UTILIZING CAR BODY ROLL CONTROL DEVICE WITH AVERAGE SPECTRUM AT 35 MPH

4.3 Bolster Side Bearing Loads

As previously stated, the primary cyclic stress effects in the bolster are due to car body roll motions which cause a transverse movement (with respect to the car) of the line-of-action of the vertical load. When the movement of this load exceeds the diameter of the center plate, load is transferred to the side bearings. Load spectra curves have been developed for bolster side bearing loads. A side bearing load of approximately 120,000 lbs would imply the transfer of all of the static load from the center plate to the side bearing. Spectra shown in this section are based on the analysis of the load cell records at the side-frame-pedestal/roller-bearing-adapter interface because direct side-bearing load measurements were not made. The spectra are drawn for the average of the side bearing loads on both sides of the truck for the entire run over the test track. Figure 4.33 shows the average spectrum for nine cases and also indicates the spread of the data making up the average curve by plotting plus and minus one standard deviation about the average curve. Figure 4.34 compares spectra for operations over a 10 degree curve with jointed rail and tangent track operation with welded rail. These two spectra represent the extremes for influence of various track conditions. Figure 4.35 compares spectra from single tests over the entire test track at 10, 20, and 27.5 mph with the average curve (35 mph). The high low-cycle values for the 35 mph spectrm are due to outward lean during curve traversal.

Additional analysis showed that there is no significant difference in side bearing load spectra for operations over frozen roadbed or normal roadbed. The data also indicate that there is no significant difference between the side bearing load spectra for tests under modified spring suspension conditions, which were previously noted in Section 4.1.4, or standard conditions.

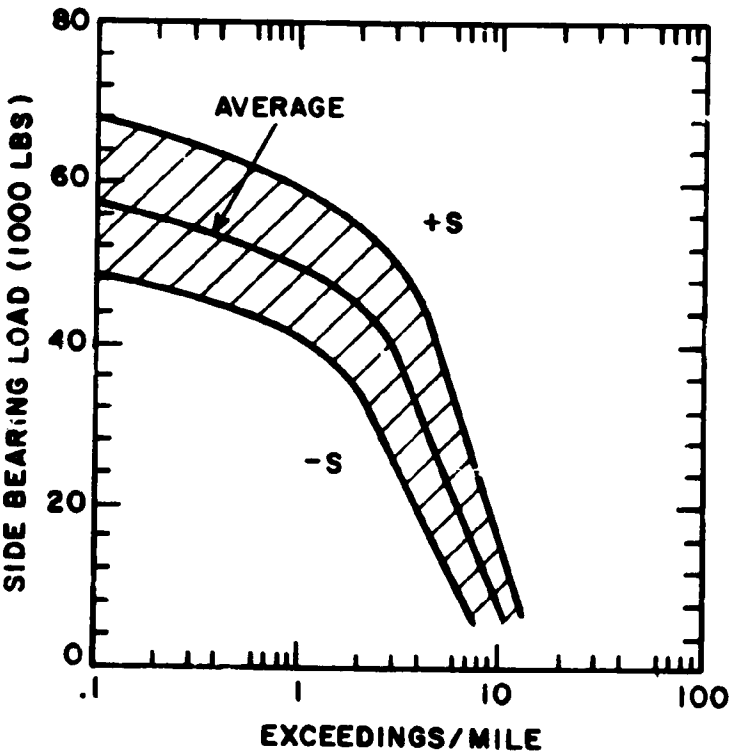

Fig. 4.33 AVERAGE TRUCK BOLSTER SIDE BEARING LOAD SPECTRUM AT 35 MPH

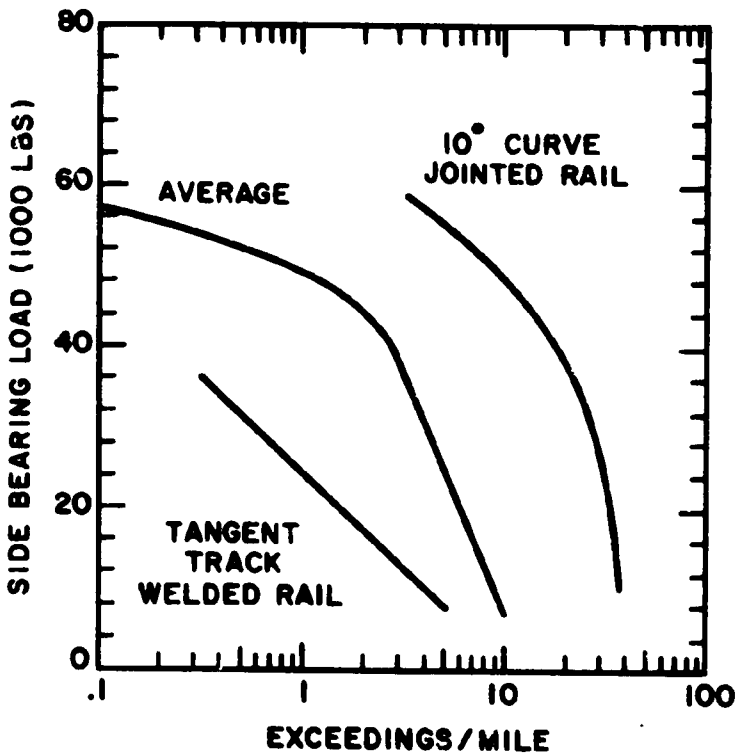

Fig. 4.34 COMPARISON OF SIDE BEARING LOAD SPECTRA FOR CURVED AND TANGENT TRACK WITH AVERAGE SPECTRUM AT 35 MPH

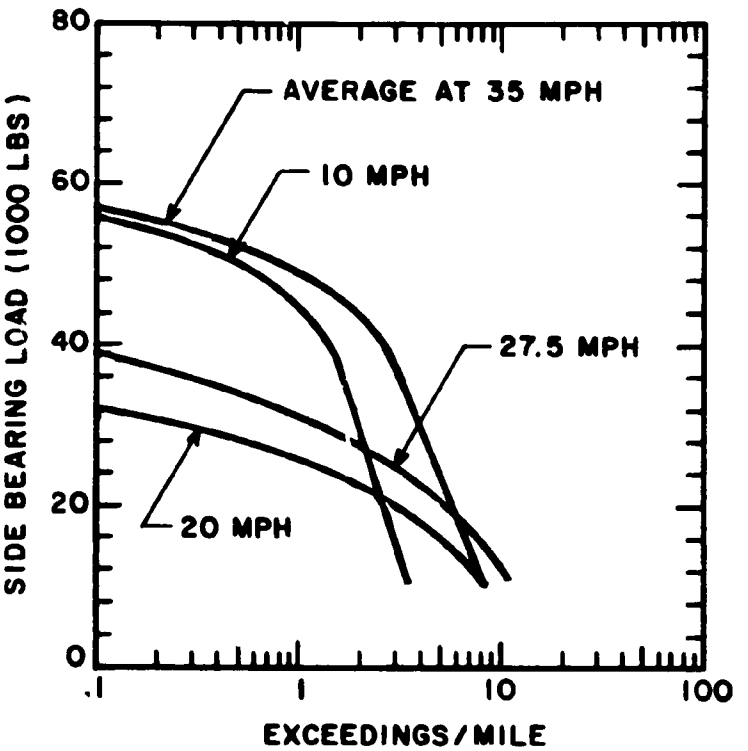

Fig. 4.35 COMPARISON OF SIDE BEARING LOAD SPECTRA FOR 10, 20, AND 27.5 MPH WITH AVERAGE SPECTRUM AT 35 MPH

4.4 Net Lateral Load

The difference in the two lateral wheel loads on an axle results in a net lateral force which is transferred to the truck structure. This force is primarily associated with the traversal of curved track, although there is a small random fluctuating component guiding the truck on tangent track. During curve traversal the highest net lateral forces usually occur on the lead axle and are directed toward the center of the curve.

The analysis of test data shows that the net lateral load is a function of the degree of curvature. Figure 4.36 representing 13 test runs shows the average net lateral load as a function of curvature for both the leading and trailing axles. The average peak net lateral load is also shown for the leading axle.

The net lateral load can be used to define a portion of the fluctuating load environment on several components. The load would be assumed to vary from zero to an extreme value once during the traversal of a curve. The application of this force to the definition of truck component loads is indicated as follows.

Bearings

A conservative approach is to assume that all of the net lateral load is transmitted through a single bearing.

Side Frame

The side frame lateral load is related to the net lateral load. Again it may be assumed that the entire load is taken through one of the pedestals. The reaction to the load is taken up by the bolster so that an opposite lateral load and moment would be applied to the side frame columns at the interface with the bolster (see Fig. 2.3).

Bolster

The net lateral load, as indicated above for the side frame, gives rise to the bolster twist load and may be used to define its magnitude in the same way as suggested for the side frame.

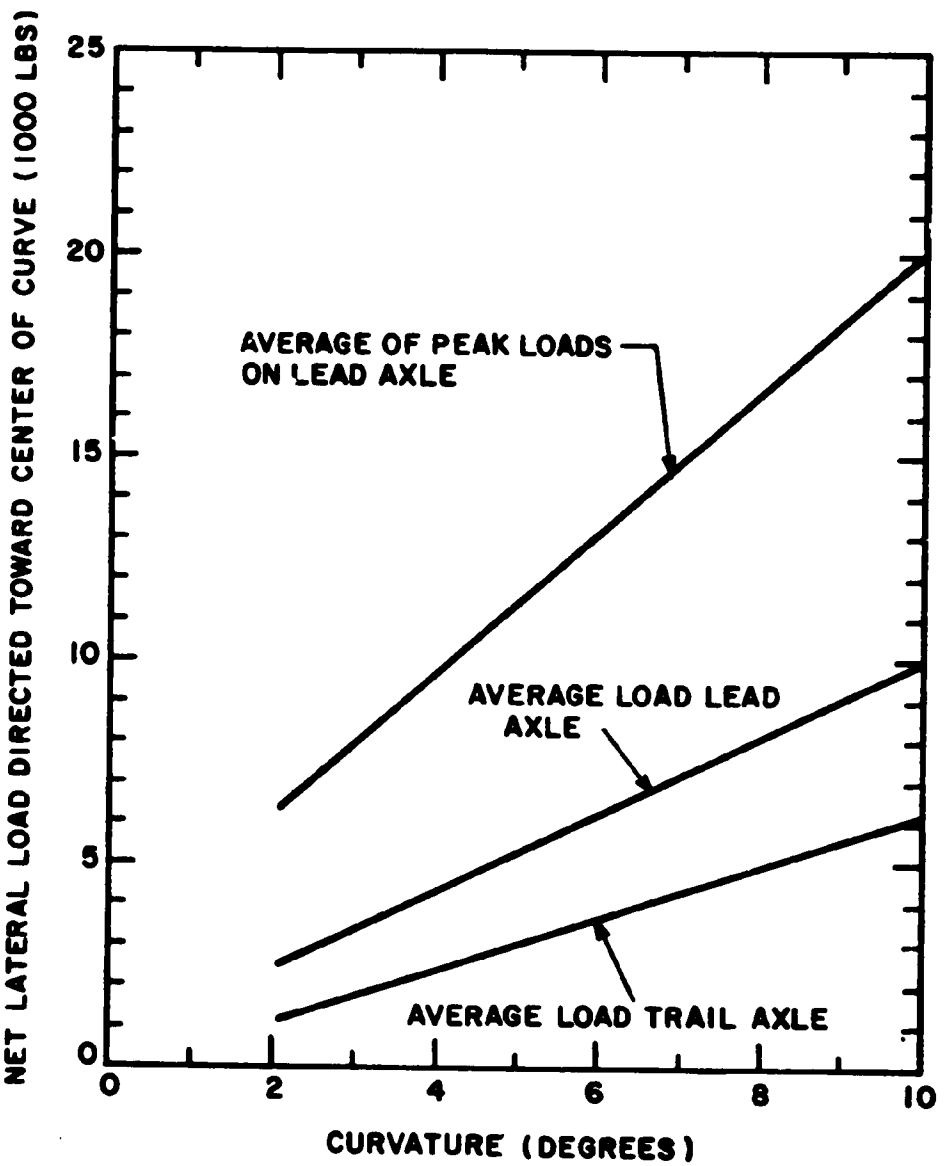

Fig. 4.36 NET LATERAL LOADS ON WHEEL/AXLE SETS AT 35 MPH

4.5 Limitations of Data

The data presented in the previous sections cover a wide range of service conditions. However, it was not possible to conduct tests under the scope of this program encompassing all operating conditions which may be significant in the description of the load environment pertinent to the accumulation of fatigue damage. What are thought to be the most important of these conditions are discussed in the following paragraphs.

4.5.1 Severe Rock-and-Roll Motions

At no time during the course of the tests did any of the test cars develop a severe rock-and-roll motion. This is evident from the moderate side bearing loads indicated by the data (e.g., approximately 70,000 lbs maximum; see Fig. 4.33). Side bearing loads in excess of 100,000 lbs are indicated (Refs. 11 and 12) for operation of high center-of-gravity cars at critical speeds over track where rail joints have been shimmed to produce an irregular rail profile. The rate at which cyclic load counts accumulate under these conditions is approximately 130 cycles/mile. This load environment would be several orders of magnitude more severe than that determined on this program. The extent to which it represents a realistic environment for the accumulation of a significant number of loading cycles is unknown. It would seem that only a relatively small portion of the total load environment would be due to such conditions because of the relatively low probability of operations under the coincident conditions of severe rail profile irregularities and movement at the critical speed. Nevertheless further investigation is warranted to determine the significance of these conditions in defining the load environment.

4.5.2 High Speed Operations -- Loaded Car

The limitation of most of the test runs to a maximum speed of 35 mph was previously noted. Some data are available from limited higher speed operations over the beginning portion of the test track where there are no sharp curves. One of the

characteristics of the vertical SF/BA load noted at speeds above approximately 50 mph is the tendency for the development of a "bounce" load at a frequency of 4 to 5 Hz. This is illustrated in Fig. 4.37 where simultaneous load records from the four SF/BA positions on the truck are shown. The frequency is somewhat higher than the fundamental 2 Hz frequency for car bounce and may represent a rigid body pitching mode of the car body vibration. If this cyclic load is a characteristic of higher speed operations with loaded cars and if the amplitude were to become somewhat greater than that illustrated in Fig. 4.37 there would be a significant increase in the severity of the load environment than indicated in the present SF/BA load spectra.

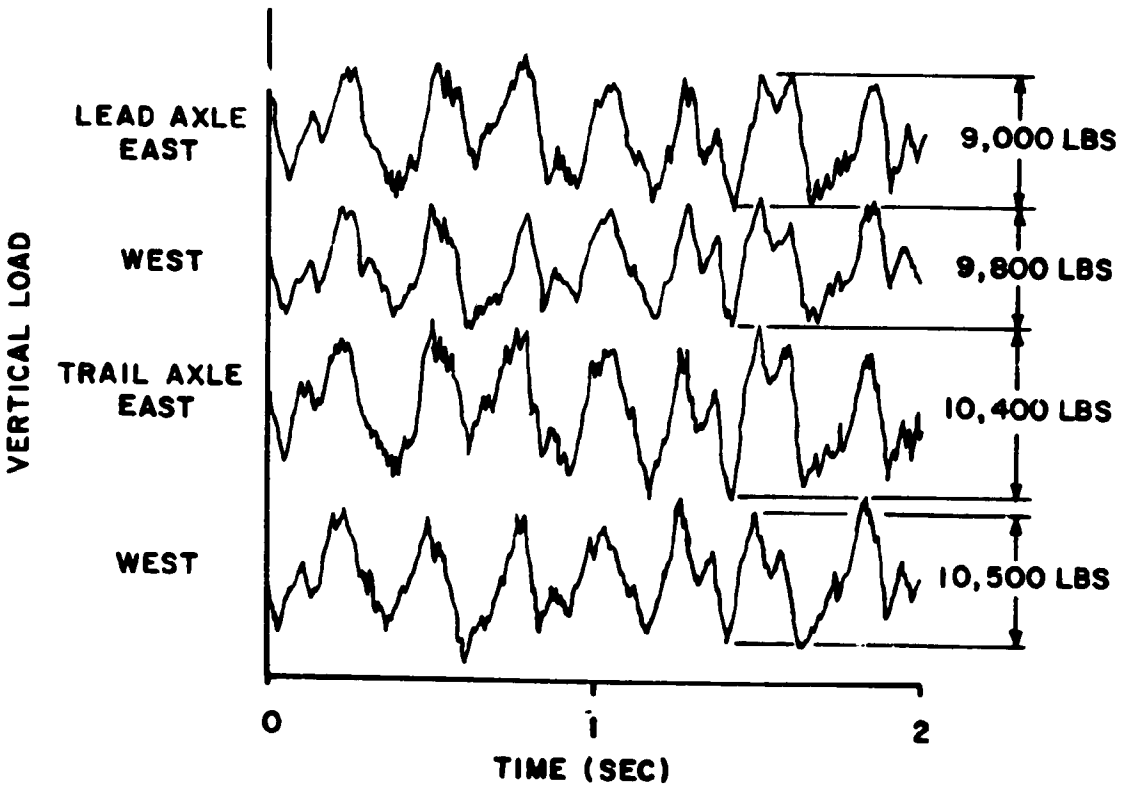

Fig. 4.37 VERTICAL LOAD RECORD AT FOUR SF/BA POSITIONS SHOWING "BOUNCE" LOAD OSCILLATION AT 53 MPH

4.5.3 High Speed Operations -- Empty Car

The development of severe truck oscillations involving primarily the in-phase side-to-side motions of the wheel/axle sets while operating at high speeds (above approximately 50 mph) and with an empty car has been widely noted (e.g., see Refs. 13 and 14). This type of oscillation, which has been referred to as "truck hunting," occurs at a frequency of approximately 3 Hz and could lead to severe lateral loads against the wheels. On the test runs conducted with an empty car on this program there was no evidence of this phenomena and, in fact, all of the loads measured for the empty car condition were substantially below the load levels associated with the loaded car. Whether or not the lateral wheel loads associated with truck hunting are as high as the lateral loads experienced on moderate to sharp curves with loaded cars can only be determined by performing load measurement tests.

4.5.4 Ineffective Side Bearing Clearances

The test data gathered under this program indicated relatively infrequent side bearing loads of significant magnitude (e.g., 50 percent of total bolster load once every 10 miles). When conventional side bearings are used a side bearing load does not develop unless there is a distinct car body roll motion because clearances are required between the side bearings and the body bolster. Several conditions may reduce the effectiveness of the side bearing clearances in limiting the side bearing load by tending to concentrate the weight of the car on diagonally opposite side bearings. The first is the operation of a car with high torsional stiffness over track with non-uniform geometric and compliance characteritiscs. The track responses may be such that the vertical axes of the trucks tend to lean in opposite directions. If the car cannot easily twist along a longitudinal axis to accommodate this response, the weight of the car will be concentrated on diagonally opposite side bearings. This condition can also occur when the transition from tangent track to super-elevated curved track takes place over a relatively short distance. This phenomena

will also take place if the car body itself is warped so that clearances on diagonally opposite side bearings are low or non-existent.

4.5.5 Large Longitudinal Train Forces

The tests on this program were performed on a special train consisting of five cars. As a result, the longitudinal train forces were relatively low. The large longitudinal train forces associated with long train operation could result in higher truck forces. Their most important influence would probably be to modify the lateral wheel load forces on curved track.

5.0 FATIGUE PERFORMANCE CRITERIA

The development of performance criteria for specifying the structural adequacy of freight car truck components with respect to fatigue damage is discussed in this section.

Fatigue performance criteria would: (a) describe the test procedures for determining fatigue strength including the maximum and minimum values of the alternating load, the relative number of cycles at various load ranges, and the manner in which the load is to be applied; and (b) designate fatigue-life factors-of-safety stating the minimum acceptable ratio of the fatigue strength of the part under test to the representation of the operating load environment.

5.1 Fatigue Strength Determination

The fatigue strength of a truck component can be evaluated by subjecting it to a fluctuating load until failure occurs. The preferred method for conducting such tests is to utilize randomly-sequenced variable-amplitude cyclic loads since this procedure is most representative of the manner in which loads are applied in service and also eliminates block-loading effects.* The amplitude of the cyclic loads would be selected to follow the load spectrum for the component being tested. For test purposes the load spectrum would be represented by a stepwise distribution of constant amplitude loads as shown in Fig. 5.1. The load would be defined by the peak alternating load level, the mean load, relationships of the lower alternating load levels to the peak alternating load, and the relative number of cycles at each load level. Low amplitude cycles which are below the level causing significant fatigue damage would be truncated. A fatigue test loading sequence illustrating these characteristics is shown in Fig. 5.2.

---

*Extensive research and test work has shown that the fatigue characteristics of structural elements are sensitive to the manner in which variable amplitude loads are applied. Empirical trends observed in variable-amplitude tests are reviewed in Ref. 15.

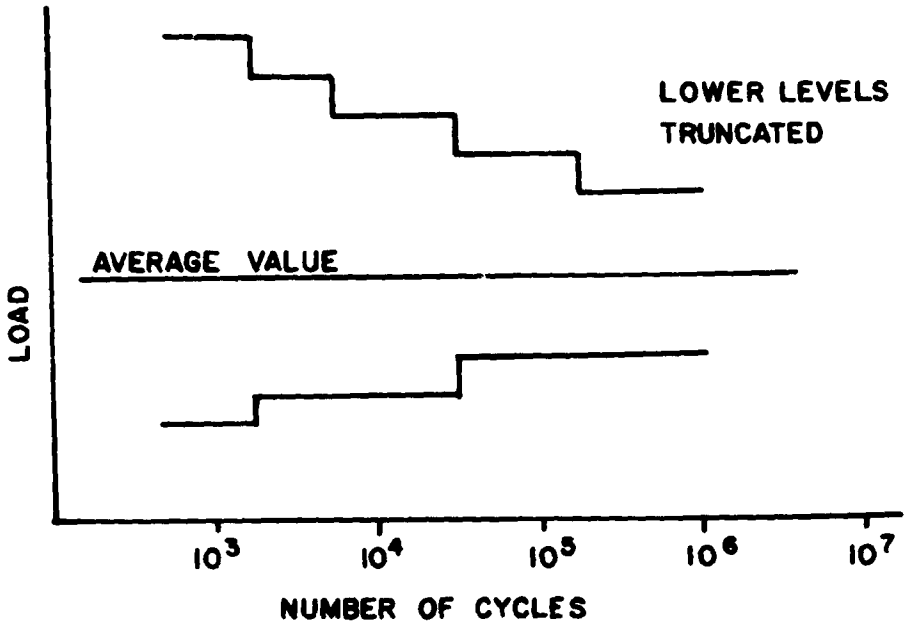

Fig. 5.1 STEP LOAD REPRESENTATION OF LOAD SPECTRA

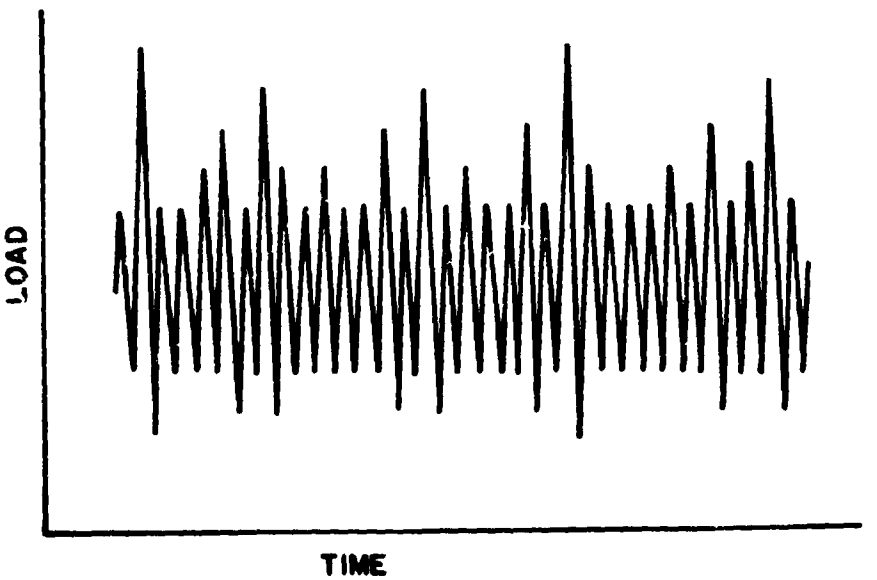

Fig. 5.2 LOAD HISTORY OF RANDOMLY-SEQUENCED STEP LOAD

Fatigue tests would be conducted by repeating the sequence of loads until failure* of the part occurs. Such tests would determine the fatigue strength of the part relative to the normal load environment.

Tests must also be conducted with amplified versions of the load spectrum in order to gain a complete understanding of the fatigue strength of the part. The amplified load spectrum would be formulated by multiplying the average value of the load and each of the alternating load levels by a constant factor. In this way, the relative relationship between the peak alternating load, the mean load and the intermediate levels of alternating load, would be maintained. In some cases the amplified load spectrum must be used for a fatigue evaluation because the normal spectrum of loads are below the fatigue limit. The danger of a fatigue failure of a component in service then comes from the statistical probability of the part being subjected to higher than average service loads (see Section 5.2.4).

5.2 Establishment of Factor-of-Safety

The factor-of-safety relating the required fatigue strength to the load environment would be based on a number of considerations including:

- the desired reliability of operation
- frequency and quality of inspections
- design philosophy: fail-safe or safe-life
- the statistical distribution of the load spectrum reflecting different conditions of truck operation

---

*The specific definition of failure of a part has been avoided in this discussion. Various definitions are possible ranging from the development of a detectable crack transverse to a tension field (similar to that used in the present side frame fatigue test specification) to the complete separation of the component resulting in its inability to carry any load.

- the statistical distribution of the experimentally determined fatigue strength of individual truck components
- the number of specimens used to evaluate fatigue strength

These are discussed in the subsections which follow.

5.2.1 Reliability Goals

The basis for the establishment of fatigue standards for freight car truck components and wheels would be the desired level of safe operations. Standards for individual components must be based on the reliability of the entire truck.

In selecting a reliability goal several factors have to be considered. The first of these is that reliability goals for individual components would have to be greater than for the system as a whole. For example, if the truck were idealized as consisting of two side frames and a bolster, and if the reliability of each of these components were 0.9999 over their lifetime, then the truck has an overall reliability of 0.9997.

A second factor is that reliability goals should be commensurate with the quality control exercised in manufacture. Fatigue characteristics are established by conducting tests on a small sample of the total population of manufactured items. These tests establish the probability of failure with respect to a given load environment. If the probability of shipping a defective part, one with a much lower fatigue strength, is greater than the probability of the fatigue failure of a normal part in service, then the use of a conservative fatigue strength for the normal part will not enhance system reliability.

5.2.2 Inspection Interval

The factor-of-safety that is chosen for the fatigue performance standard would be influenced by the frequency and quality* of service inspections. The phenomena involved are illustrated

*The term "quality" here refers to the threshold size of the crack which can be detected by the inspection equipment and the completeness with which the part can be examined for these cracks.

in Fig. 5.3, where the crack length and strength of a representative structural element are plotted as a function of time. The structural element is assumed subjected to a fluctuating load which is stationary in time. The figure indicates the growth of a typical flaw with time. Structures initially contain microscopic flaws, which are an inherent material property or the result of manufacturing processes. As the component is subjected to a time varying load, a typical flaw would increase in size. At time t_1 the crack length reaches the threshold of detectability and as the crack length increases its growth is accelerated. Finally it is unable to sustain the load and fracture occurs at t_3.

The decrease in strength of the element which accompanies crack growth is also plotted on Fig. 5.3. The ratio of the initial design strength, p_2, to the maximum expected service

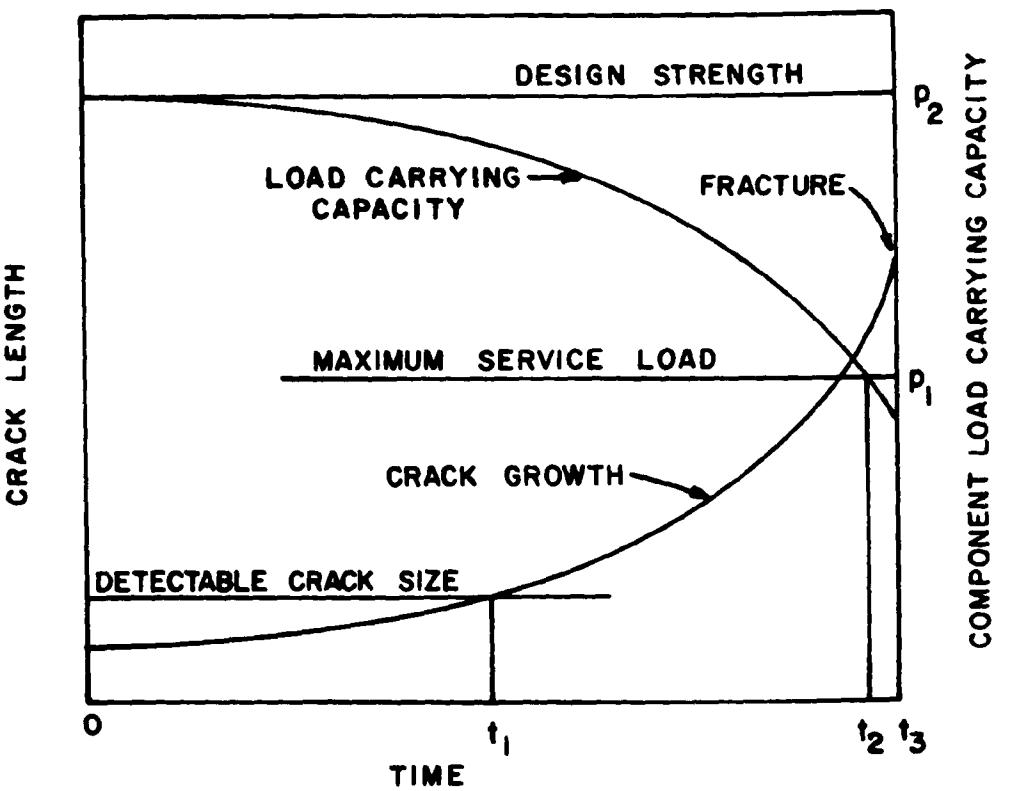

Fig. 5.3 FATIGUE CRACK GROWTH

load, p_1, represents the static design safety factor. A decrease in strength accompanies the crack growth as illustrated in the figure. At time t_2, the part is no longer able to sustain the maximum anticipated service load. Failure of the part would follow shortly thereafter.

The diagram shows that the frequency and quality of service inspections will influence the fatigue requirements of truck components. If a component is allowed to operate in a region of time greater than t_1, it is obvious that the minimum inspection interval should be less than t_2-t_1. The more frequently components are inspected and the smaller the size of the flaw which can be detected by this inspection, the closer the part can be operated to the limit of its fatigue strength. Also note that improved inspection techniques, which lower the threshold size of detectable flaws, would allow an increased interval in the period between inspections.

5.2.3 Fail-Safe or Safe-Life Design

Fatigue standards which are based on a specific reliability goal will be influenced by whether or not the structural design philosophy is fail-safe or safe-life. Fail-safe design relies on utilization of redundant structural members. The probability of a catastrophic failure is small because failure requires simultaneous defects in each member. Low probabilities of failure can be developed even though the separate members possess only moderate fatigue properties. Fail-safe structures are commonly allowed to operate in the region of detectable cracks, as illustrated in Fig. 5.3, the region greater than t_1, the assumption being that a defective part can be replaced at the time of inspection and the redundancy of the structure restored. There are only a few examples of fail-safe design principles in the freight car truck. One of these is the truck-bolster/body-bolster connection where the center plate rim and the center pin provide redundant structural elements in the connection between the two bolsters. Another example is the multiplicity of springs in the spring support system.

Safe-life design requires maintaining the integrity of each structural element, because failure of one component implies failure of the system. Structural components must be designed for an extremely low probability of failure during intervals between inspections. Conventional freight car truck construction is based primarily on safe-life principles. Failure of one of the major structural elements, such as the side frames, bolster, wheels, or axles, inevitably leads to derailment. Safe-life structures are generally restricted to operate in the region where no detectable cracks will occur, that is, in the region less than t_1 as shown in Fig. 5.3, and thus require very conservative fatigue properties.

The adoption of fail-safe design principles for future freight car truck development would be desirable where this is feasible. For the present, however, the safe-life philosophy implied by present design practices must be recognized, and the major emphasis of the establishment of fatigue criteria directed to this condition.

5.2.4 Statistical Considerations

The statistical characteristics of both the load environmental and fatigue test data play an important role in the establishment of a factor-of-safety. Figure 5.4 shows a plot comparing a load environment with fatigue test data. In this plot the variable-amplitude load sequence may be characterized by the peak load. The fluctuating load environment to which the component is exposed over its lifetime is represented by a specific number of cycles. Thus, the load environment can be characterized by a single point on the figure. A position at some other ordinate than the one indicated would imply that all loads in the spectrum had been increased or decreased proportionately.

Figure 5.4 also shows a plot of fatigue test data. These data would be obtained from tests utilizing the environmental load spectra at various levels of amplification. As indicated

in the figure, both the fatigue test data and the load environmental data would be most accurately described by a series of curves indicating the statistical distribution of the data.

Fatigue performance characteristics for freight car truck components would have to require very low probabilities of failure because of the serious consequence of a freight car truck failure and the safe life character of their design. This means that one is interested in the statistical data of both the load environment and the fatigue strength at very low probabilities of occurrence.

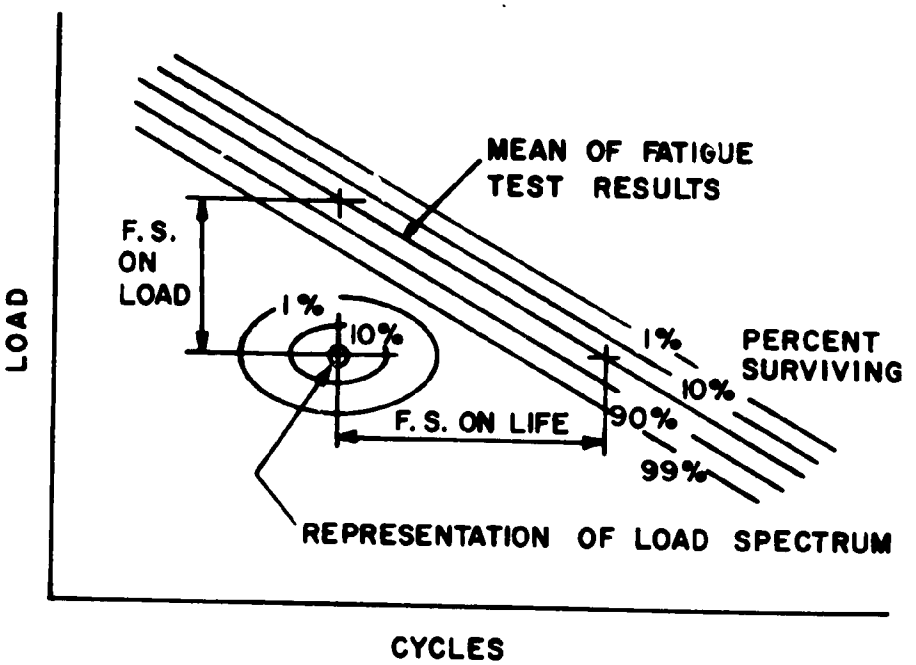

Fig. 5.4 COMPARISON OF FATIGUE TEST RESULTS WITH LOAD SPECTRUM

An appreciation for the failure rates of interest can be gained from derailment failure data. Federal Railroad Administration accident statistics show that in 1971, 942 of 5131 train derailments were attributed to the failure of truck components and wheels. In this period 29.2 billion freight car miles were operated. Considering each truck of the car as an independent system, this is a failure rate of 1.6×10^{-8} per truck mile. Fatigue failure, which is the cause of only a portion of these derailments, would have a lower failure rate.

It would be desirable to have fatigue strength and environmental load data down to low values of probability of occurrence, because then one could make direct calculations of the probability of failure. It is impractical, however, to get sufficient test data, with respect to both the load environment and fatigue strength, to be able to define the curves representing the extremes in the statistical distribution (e.g., 0.1 and 0.01 percent). The definition of these curves would require a large number of tests, which would be impractical to perform because of the cost of the components themselves and the expense of operating test equipment of the size and capacity needed to conduct fatigue studies. Therefore, it is necessary to base the fatigue design criteria on a more limited understanding of the distribution of test points and an arbitrary specification for the degree of separation of the load environment and fatigue curves.

The idealized distribution curves for environmental load and fatigue data shown in Fig. 5.4 illustrate the fact that not only is the degree of separation of the two sets of curves important, but that the degree of scatter in the data is significant as well. If, for example, there is a high degree of scatter in the fatigue life data, the probability of failure increases because there will be a larger overlap in the two distributions.

The log-normal distribution is commonly used as an overall fit to fatigue test data. Substantial deviations from this distribution have been noted at the extreme values in some larger samples of data (Ref. 16). It nevertheless represents the most generally acceptable distribution for the purpose of making statistical calculations involving the confidence in test data and probability of survival.*

The scatter of the fatigue strength characteristics is defined by the standard deviation, σ. Since it is impractical to test large numbers of any given test specimen to accurately determine the standard deviation, this parameter must be estimated. The concept of using "pooled data" has been found useful in this regard (Ref. 16). This involves combining data from a number of similar tests to gain a more reliable estimate of for a given class of structures and materials. This procedure could be followed once the fatigue testing of freight car truck components is carried out in a standardized manner.

An important consideration in the establishment of a scatter factor is the number of specimens to be used in the fatigue test group. The group of test specimens is regarded as a sample from the total population of the specific type and design of component. The larger the group of test specimens the more nearly the average fatigue properties of this group can be expected to represent the fatigue properties of the population at large. Therefore, the scatter factor can be inversely related to the size of the test group in specifying the fatigue life that must be demonstrated by the tests; see Albrecht (Ref. 17).

5.2.5 Defining the Factor of Safety

As shown in Fig. 5.4, a factor of safety can be established either with respect to the fatigue life or the load intensity. The usual practice is to specify a factor of safety on life,

*Other analytic models for the representation of fatigue test data are presented by Weibull (Ref. 18).

and this is generally referred to as a "scatter factor". The scatter factor is selected to account for variations in both the load environment and fatigue strength. Various scatter factors are specified by different regulating agencies.*

It is desirable to provide for tests utilizing an amplified version of the load spectrum for demonstrating the required safety factor. The amplified load spectrum would be formulated by multiplying the average value of the load and each of the alternating load levels by a constant factor. In this way, the relative relationship between the peak alternating load, the mean load, and the intermediate levels of alternating load would be maintained. The use of an amplified load spectrum is necessary when evaluating a component with a fatigue strength in the vicinity of the fatigue limit of the component. Under these conditions demonstration of a safety factor with respect to lifetime (number of cycles) would require long periods of testing. This procedure is currently reflected in the fatigue test specification for side frames, where the specimens must withstand a given number of cycles at a load substantially above the normal load environment.

---

*The Air Force requires demonstration of a scatter factor of 4 when testing a full-scale complete airframe (Ref. 19).

The Federal Aviation Administration outlines procedures for determining the fatigue strength of cirtical helicopter components (Ref. 20). Safety factors with respect to stress (comparable to load) are presented for demonstrating that stresses are below the fatigue limit. These factors depend on the number of specimens in the test group as indicated below:

Number of Specimens	Safety Factor with Respect to Maximum Oscillating Stress
4	1.1
3	1.25
2	1.5
1	2.0

Because of the slope of the load versus cycles curve (e.g., Fig. 5.4) the factor of safety with respect to load is lower than the equivalent factor of safety with respect to cycles (life).

5.3 Tentative Fatigue Performance Criteria

Based on the factors discussed in this report, an acceptable fatigue performance specification would include these elements:

1. The standard would be based on specific reliability goals.
2. The standard would be expressed as performance test requirements.
3. The operational load environment for each truck component would be represented by a load spectrum, based on test data depicting severe operating conditions.*
4. For test purposes, the test load spectrum would be represented by a stepwise distribution of constant amplitude loads.
5. Tests would be conducted by randomly sequencing the variable-amplitude loads in the test spectrum.
6. Specimens subjected to the test load spectra would be required to survive a number of loading cycles exceeding the number of cycles defined in the lifetime environment. The scatter factor by which the mean life of the group of test specimens must exceed the lifetime cycles depends on the number of specimens in a test group. Scatter factors based on 99 percent confidence in 0.9999 probability of survival with σ of 0.10 are listed below for various size groups of tests specimens:**

Number of Test Specimens	Scatter Factor
1	4.0
2	3.5
3	3.2
4	3.0

*The load spectra presented in this report probably should not be extrapolated below the .01 exceedings/mile or revolutions/mile rate of occurrence because of the limited number of miles worth of data on which the curves are based. It is anticipated that additional test data will be forthcoming to allow better definition of the spectra in the high-load low-rate-of-occurrence region.

**Based on an assumed log-normal distribution of fatigue test results.

The loading of a test specimen may be suspended prior to its failure, but the number of cycles at the time of test suspension shall be used in the establishment of the mean life of a group of specimens.

7. Tests can be conducted with a reduced number of cycles by utilizing an amplified load level subject to these restrictions:

   (a) Each load in the test spectrum must be proportionately increased (including the average component, if any).

   (b) Two groups of specimens shall be tested at two different amplified load levels.

   (c) The average lifetime, expressed in number of cycles, of the specimens tested at the lower amplified load level, must exceed the lifetime cycles in the original specification (see Fig. 5.5).

   (d) The expected lifetime of the component at the normal level of loading is determined from the elevated load test data by linear extrapolation on a plot of load level versus log-cycles, (see Fig. 5.5) from point representing average lifetimes of specimens at the two elevated load levels.

   (e) The expected lifetime, at the nominal load as determined above, is used to determine whether or not the scatter factor requirement has been met.

For each of the truck components a load spectrum may be prepared for the principal directions of loading. This will specify what the lifetime load environment is that must be used for the fatigue performance test.

The scatter factors presented in this criteria are based on assumptions including the shape of the distribution curve representing fatigue test results and its standard deviation. These assumptions should be continually reviewed as additional fatigue test data is obtained. The assumption of a log-normal distribution curve of fatigue test results, for example, can only be established by examining results from many fatigue tests.

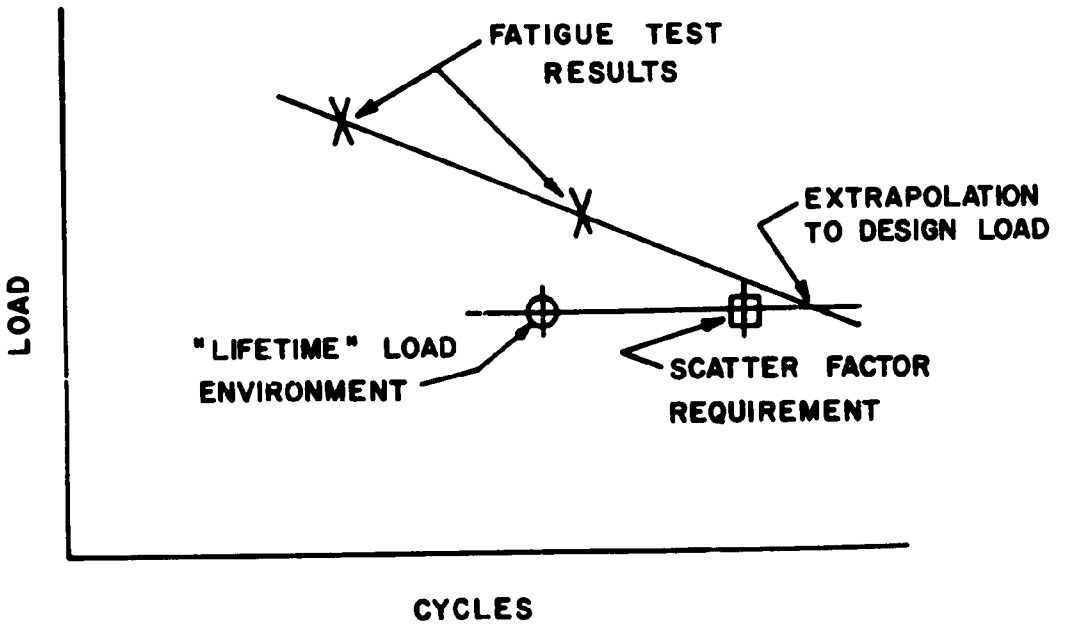

Fig. 5.5 EXTRAPOLATION OF AMPLIFIED LOAD LEVEL TESTS TO DESIGN LEVEL FOR REFERENCE TO SCATTER FACTOR REQUIREMENT

Since one is interested in very low probabilities of failure, the shape of the curve at extreme values is important. An assumed value of the standard deviation of fatigue test results has been used in the establishment of the requirements presented here. This value can be refined by the concept of "pooled data" (Ref. 16) which is used successfully in aircraft fatigue evaluation. Finally, as fatigue data become available and are evaluated, the scatter factors can be reviewed and modified, if appropriate.

6.0 CONCLUSIONS AND RECOMMENDATIONS

Fatigue standards for freight car truck components and wheels can be developed which reflect operational reliability goals. These standards would define a factor-of-safety between the load environment to which the truck components are subjected in service and the fatigue properties of the components themselves. They must be based on a broad understanding of the statistical nature of both the load environment and the fatigue strength properties of the truck components.

The load environmental studies which have been conducted as part of this project have provided useful data which clarify the nature of the fluctuating load environment. Both the magnitudes and statistical variations of the loads were noted within the scope of conditions examined in the tests. In addition, the parameters which have the most influence on the severity of the load environment were determined.

The fatigue strengths of representative components and the statistical variation of these strengths have not yet been adequately determined. The greatest need is for data establishing the range of fatigue strengths of components which are of the same design and which are subjected to the same levels of fluctuating load. These data would permit a more accurate definition of the margin between the load environment and the fatigue strength which is required to attain given reliability goals.

Although it would be possible to formulate specific fatigue performance standards for each of the truck components based on the load environmental data described in this report and on assumed fatigue strength distributions, it is recommended that the promulgation of such standards be delayed until additional data are available.

Additional load environmental tests need to be conducted which would determine load spectra under different conditions

than those covered in these tests. Conditions noted in Section 4.5 which may lead to severe loading environments include "rock-and roll" at critical speeds, high speeds with both loaded and empty cars, and operation with ineffective side bearing clearances. Data should also be gathered under a wider range of track conditions. In addition, improved truck load instrumentation systems should be developed to allow additional data to be obtained, such as the lateral load at the side-frame-pedestal/roller-bearing-adapter interface.

One of the basic assumptions of this program has been that for the purpose of determining fatigue damage the fluctuating loads to which a component is subjected during service operations can be represented by a load spectrum. The accuracy of this assumption should be examined by determining the fatigue strength of selected components after they have been in service for an extended period of time. The most desirable situation would be to determine the fatigue strength of a truck component which has been used in service, and compare the result with fatigue tests on parts of identical design which have been in service for an extended period of time. It might be difficult to find existing sets of truck components meeting these requirements. It would, however, be well to organize future tests of this type by testing newly manufactured components and then identifying similar components in high mileage service for testing after several years of operation. Comparison of the test results would indicate the rate in the degradation of the fatigue strength.

Conservative fatigue standards are required for freight car truck components because of the safe-life design philosophy that is generally followed in their design. The introduction of fail-safe design features would be a desirable means of increasing the safety and reliability of truck operation. Freight car truck designs need to be reviewed to determine if fail-safe principles can be introduced. Both technical and economic aspects need to be considered in a component-by-component review of the function and design of each part to determine the areas where changes are feasible.

The freight car truck wheel is a particularly difficult component for which to develop fatigue performance criteria. The dual nature of the lateral and vertical loads in producing stress fields within the wheel and the variability of their orientation due to its rotation are particularly difficult features to represent in a loading fixture. In addition, the role of the thermally-induced stresses caused by tread brake heating cannot be ignored. Thermally induced stresses may lead to plastic strain which will modify the residual stress field in the wheel making it more susceptible to fatigue damage. Further study of mechanisms of fatigue damage in the wheel would be helpful in the development of suitable procedures for conducting fatigue performance evaluations on this component.

Because of the wide variety of design details represented by different truck configurations and the wide range of operating conditions which exist in service, it is difficult to plan a test program which will examine the load environment under every set of circumstances. If records were available on truck components which have failed in service it might be possible to identify sets of circumstances where fatigue failure rates were significantly higher than average. Test programs could then be planned to examine these conditions in order to determine the circumstances which lead to higher failure rates. A service to provide this information should identify the specific design of the failed part, its age, the characteristics of the car in which it was installed, the track condition over which most of operations took place, etc.

In components which must function as safe-life structural elements, the detection of flaws while they are below the critical size is extremely important. The detection of such flaws in railroad freight car truck components is difficult because of the harsh environmental conditions under which many of these inspections must be made. The development and utilization of better inspection equipment and procedures for field use would enhance the system reliability of freight car truck operation.

The detection of flaws in newly manufactured parts is also important to ensure that components are not introduced into service with substantially lower fatigue strengths than the standard design. If the probability of shipping a defective part is greater than the probability of the fatigue failure of a normal part in service, then the use of a conservative fatigue strength for the normal part will not enhance system reliability. Once the fatigue strengths of standard designs are thoroughly understood, quality control procedures should be reviewed to determine the inspection requirements necessary to insure a desired level of system reliability.

In summary, as a result of the work performed on this project the following specific recommendations can be made:

- Conduct fatigue tests on freight car truck components and wheels to determine their fatigue strength and the spread of fatigue test results for components of the same design.
- Conduct additional load environmental tests particularly at higher speeds of operation than were used on this program.
- Develop truck load instrumentation systems which will allow a greater number of simultaneous load measurements.
- Review the safe-life design philosophy of the truck to determine if it is practical to introduce fail-safe features.
- Perform additional studies to determine the most practical procedure for conducting wheel fatigue performance tests.
- Develop and implement an information service that will report the specific characteristics of truck component fatigue failure and allow identification of parameters influencing high rates of fatigue failure.
- Continue research and development of field procedures for detecting cracks in truck components before they reach a critical size.

- Review manufacturing quality control procedures to determine their affect on truck system reliability, particularly with reference to the probability of introducing into service a component with a defect which substantially lowers its fatigue strength.

7.0 REFERENCES

1. Peterson, L.A.; Freeman, W.H.; Wandrisco, J.N.; Measurement and Analysis of Wheel-Rail Forces," ASME Technical Paper 71-WA/RT-4.

2. "Manual of Standards and Recommended Practices," Section A, Specification for Materials, Specification M-203 Association of American Railroads, Mechanical Division (1971).

3. "Manual of Standards and Recommended Practices," Section D, Trucks and Truck Details, Specifications for Approved Journal Roller Bearings Applicable to Interchange Freight Cars, Association of American Railroads, Mechanical Division (1971).

4. "Manual of Standards and Recommended Practices," Section A, Specification for Materials, Specification M-202, Association of American Railroads, Mechanical Division (1971).

5. "Manual of Standards and Recommended Practices," Section A, Specifications for Materials, Specification M-107 and M-108 and Section G, Wheels, Association of American Railroads, Mechanical Division (1972).

6. "Manual of Standards and Recommended Practices," Section A, Specifications for Materials, Specification M-101, and Section D, Truck and Truck Details, Association of American Railroads, Mechanical Division (1971).

7. Porter, S.R.M, "The Mechanics of a Locomotive on Curved Track," The Railway Engineer, (July-December 1934), (January 1935); The Railway Gazette (February-March 1935).

8. Minchin, R.S., "The Mechanics of Railway Vehicles on Curved Track," J. Inst. Engineers, Australia, Vol. 28 (July-August 1956).

9. Cain, B.S., Vibration of Rail and Road Vehicles, Pitman Publishing Co. (1940).

10. Bruner, J.P.; Benjamin, G.N.; Bench; "Analysis of Residual, Thermal, and Loading Stresses in a B33 Wheel and Their Relationship to Fatigue Damage," ASME Journal of Engineering for Industry, May 1967, pp 249-258.

11. Martin, A.E.; Smith, L.W., "Determination of Car Body Center Plate Fatigue Design Criteria by Full-Scale Car Testing," ASME Technical Paper 74-RT-8.

12. Monselle, D., "Truck-Bolster Dynamic Loadings Measured Under Harmonic Roll Conditions, ASME Technical Paper 71-WA/RT-6.

13. Reynolds, D.J., "Hunting in Freight Cars," ASME Technical Paper 74-RT-2.

14. "Truck Hunting Accelerates Wear," Railway Locomotives and Cars, (May 1973).

15. Schijve, J., "The Accumulation of Fatigue Damage in Aircraft Materials and Structures," AGARD Report 157 (January 1972).

16. Abelkis, P.R., "Fatigue Strength Design and Analysis of Aircraft Structures, Part I - Scatter Factors and Design Charts," AFFDL-TR 66-197 (June 1967).

17. Albrecht, A.L., "Statistical Evaluation of a Limited Number of Fatigue Test Specimens Including a Factor of Safety Approach," American Society for Testing and Materials, ASTM Special Technical Publication 338, 1962, pp 150-166.

18. Weibull, W., Fatigue Testing and Analysis of Results, Pergamon Press, N.Y., (1961).

19. Military Specification, MIL-A-008867A, (USAF) (March 31, 1971).

20. Civil Aeronautics Manual 6, Rotorcraft Airworthiness; Normal Category, Federal Aviation Agency (October 1, 1959).

APPENDIX A

DERIVATION OF VERTICAL AND LATERAL WHEEL LOADS FROM LOAD CELL AND AXLE BENDING MOMENT DATA

The B&LE test truck used for the measurement of lateral and vertical forces at the wheel/rail interface is described in this appendix. For obvious reasons these measurements must be made by an indirect procedure. The transducers used to make these measurements consist of four specially-designed roller bearing adapter load cells, which are used for the measurement of vertical load transmitted to each of the bearings, and two bending-moment strain gage bridges mounted on each of the two axles of the truck. Each of the axle-mounted strain gage bridges consists of two gages mounted at diametrically opposite positions. These gages provide a sine curve output as the axle rotates through 360°. This output is a direct measure of the bending moment in a vertical plane only when the two gages are in this plane (twice per revolution). The vertical bending could be sampled more often by the installation of additional pairs of strain gages at other angular positions, but only one pair is used in the present system.

Vertical and lateral loads at the wheel/rail interface can be determined once appropriate axle bending moments are known. The maximum moments are introduced as known values in free-body equations of the wheel/axle set. The free body diagram is shown in Fig. A.1 for which the equilibrium conditions are:

$$M_L = L_L c + B_L (a + d) - V_L d \tag{1}$$

$$M_R = L_L c + B_L \left[a + (f - e)\right] - V_L (f - e) \tag{2}$$

$$M_R = L_R c + B_R (b + e) - V_R e \tag{3}$$

$$M_L = L_R c + B_R \left[b + (f - d)\right] - V_R (f - d) \tag{4}$$

where M_L, M_R, B_L, and B_R are known measured quantities and a, b, c, d, e and f are physical dimensions.

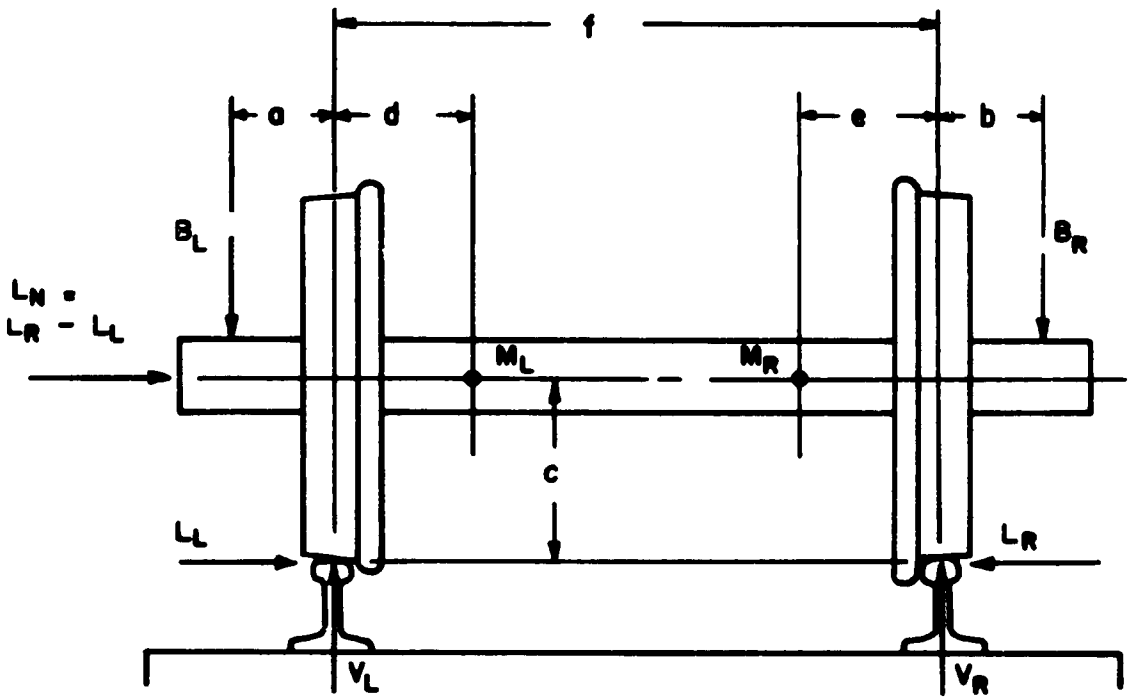

Fig. A.1 FREE BODY DIAGRAM OF AXLE

These equations can be solved simultaneously, in pairs, to give expressions for calculating the desired V_L, V_R, L_L, and L_R values. The equations so derived are:

$$V_L = \frac{M_L - M_R}{(f - d - e)} + B_L \tag{5}$$

$$V_R = \frac{M_R - M_L}{(f - d - e)} + B_R \tag{6}$$

$$L_L = \frac{M_L - M_R}{(f - d - e)}\left[\frac{f - e}{c}\right] + \frac{M_R}{c} - B_L\left(\frac{a}{c}\right) \tag{7}$$

$$L_R = \frac{M_R - M_L}{(f - d - e)}\left[\frac{f - d}{c}\right] + \frac{M_L}{c} - B_R\left(\frac{b}{c}\right) \tag{8}$$

The net lateral force applied at the axle, L_N, is obtained from a summation of forces in the horizontal direction

$$L_N = L_R - L_L$$

The desired lateral and vertical force values are obtained by substituting the known dimensions and measured quantities for the appropriate terms. A resultant computed value having a negative sign indicates that the force vector is in the opposite direction to that shown in Fig. A.1.

Although the physical dimensions, a, b, c, d, e, and f, represent known constants, it is recognized that the specific locations of force applications, such as the vertical rail-wheel locations, actually do shift small distances as the car rolls on the rails and that the force vectors, in general, are not always oriented or acting in as simple a manner as illustrated in the diagram. However, the magnitude of error introduced by treating the moment arms as constants, appears to be well within acceptable limits.

In practice, these equations are solved twice per wheel revolution by A to D conversion of the analog data, and real-time processing of the data to find the time of maximum axle bending moment and the resulting vertical (V) and lateral (L) forces.

APPENDIX B

DEVELOPMENT OF LOAD SPECTRA

The load spectra for vertical loads at the SF/BA interface, which are presented in Section 4.1, were developed by determining peak loads between crossings of the mean level falling in several load ranges. Figure B.1 shows the points which were used to construct the average spectrum presented in Fig. 4.1. In most cases, 8 such data points were determined for each test run, 4 on the portion of the spectrum above the static load, and 4 below the static load. These data points were also determined for the signals from each of the 4 load cells recorded during each test. (However, in some cases, data from a load cell had to be discarded because of instrumentation difficulties.) The data points were established at $\pm$ 1500, $\pm$ 4500, and $\pm$ 7500 lbs load exceedance levels from the static load and also at the load levels occurring at a frequency of .244 exceedings/mile. The $\pm$ 1500 and $\pm$ 4500 lbs load exceedances were established by processing samples of the data on a computer for selected curve and tangent track segments totaling about 0.6 miles. The sampling rate was 100 samples per second and the data was not filtered. The other 4 points were determined from an examination of a Brush chart display of the data for 4.1 miles of each test run. Processing the data in this way effectively filtered it at 35 Hz. The $\pm$ 7500 lbs exceedance rates were established by counting the peak loads above (and below) these values over the entire 4.1 miles. The highest load in this 4.1 miles record determined the point plotted at the .244 exceedances/mile position. The 2 points at the lowest rate of exceedances, + 18,300 lbs at .0072 exceedances/mile and -14,700 lbs at .0072 exceedances/mile were obtained by considering the complete ensemble of data, namely the 68 load cell records, on which the data shown on Fig. 4.1 are based. The two points are the second largest $\pm$ peak values and the rate of exceedances (1 peak/139 miles) represents 2 exceedances in 279 miles.

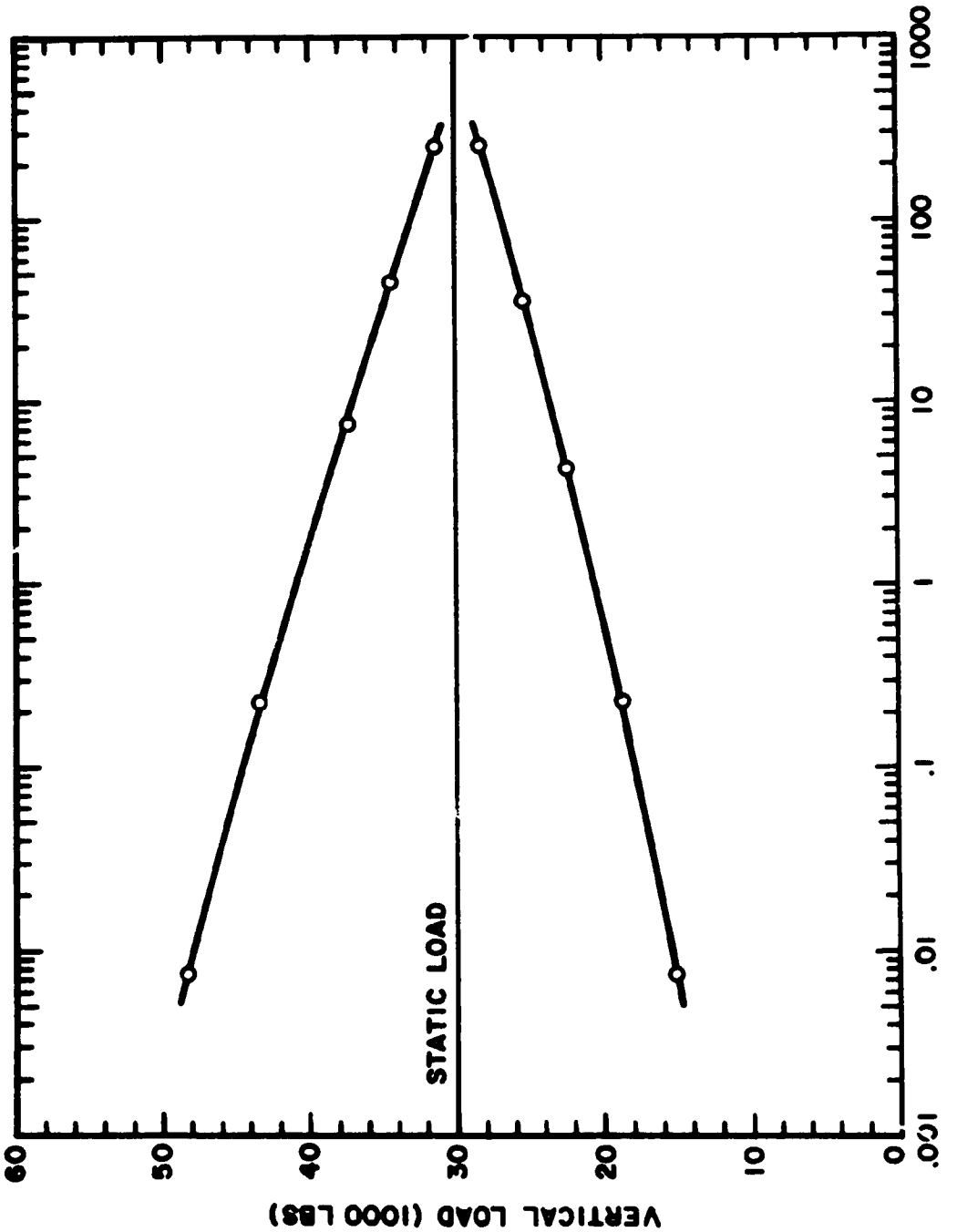

Fig. B.1 AVERAGE VERTICAL SF/BA LOAD SPECTRUM AT 35 MPH

A slightly different procedure was utilized to construct the load spectra curves for lateral wheel load presented in Section 4.2.3. Since the lateral wheel load data is highly dependent on the degree of track curvature, the lateral wheel load data were developed for specific curved and tangent segments of the test track. Also, one is concerned with the duration of the load measured in terms of the number of wheel revolutions. Cyclic strain in the wheel plate is due primarily to the revolution of the wheel, the fluctuations in the magnitude of the lateral load being a second order effect. Lateral wheel load data were obtained from a computer analysis of data digitized at 100 samples per second, unfiltered. It was classified in load ranges at 3600 lb intervals (e.g. $\pm$ 1800 lbs, 1800-5400 lbs, 5400-9000 lbs, etc.). For each segment the number of revolutions of the wheel associated with the length of time the load was in each of these load ranges was determined and totaled to develop the load spectra curve. These curves were developed for each test run. The data registered at the 1, 10, 100 and 400 revolutions/mile rates were recorded from these individual curves and averaged for constructing the summary curve. Figure B.2 shows the points which were used to construct the load spectrum curve for the 10 degree curved track segment shown in Fig. 4.30. The average curves, representing data of the entire test run, were determined by constructing the weighted average of the curves (based on track segment length) for each of the specific track segments.

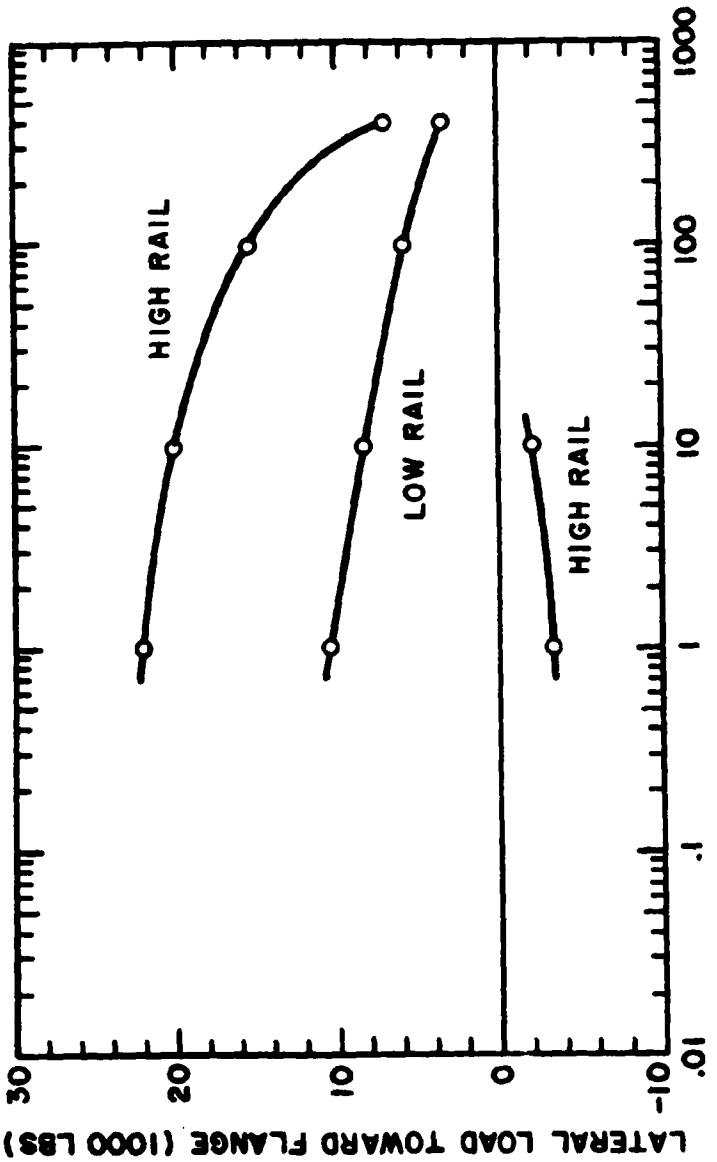

Fig. B.2 LEAD AXLE LATERAL WHEEL LOAD SPECTRUM FOR 10° CURVE AT 35 MPH

APPENDIX C
WHEEL TREAD CONTOURS FOR WORN WHEEL TESTS

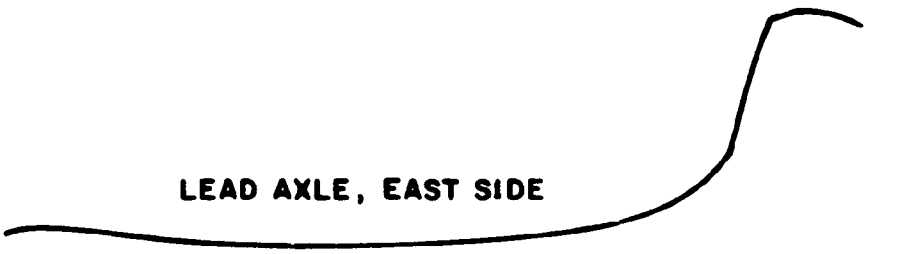

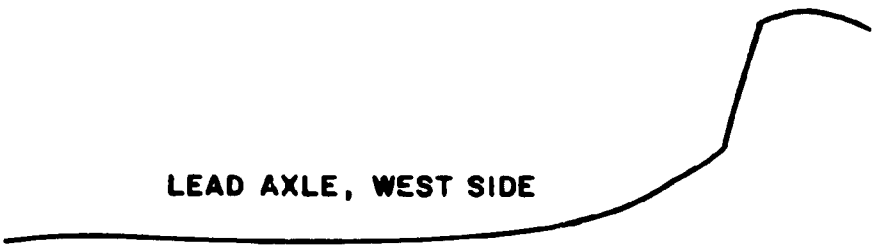

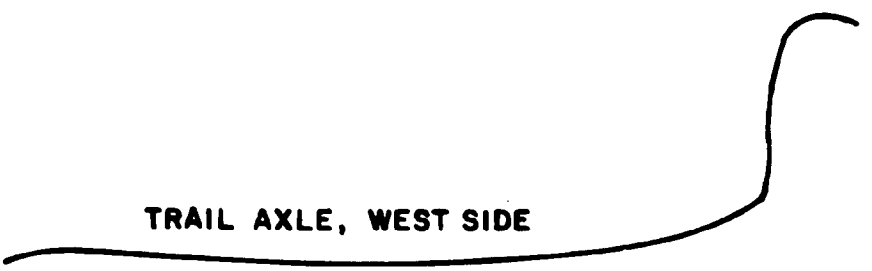

APPENDIX D

REPORT OF INVENTIONS

After a diligent review of the work performed under this contract, no new innovation, discovery, improvement or invention was made.